SECURITY CLASSIFICATION OF THIS PAGE (WHEN DATA ENTERED)

REPORT DOCUMENTATION PAGE		READ INSTRUCTIONS BEFORE COMPLETING FORM
1. REPORT NUMBER DAAK10-80-C-0049	2. GOV'T ACCESSION NUMBER AD-A094284	3. RECIPIENT'S CATALOG NUMBER
4. TITLE (AND SUBTITLE) JAN POINT DETONATING/DELAY FUZE		5. TYPE OF REPORT/PERIOD COVERED Final Technical Report 28 Feb. 80 - 30 Nov. 80
		6. PERFORMING ORG. REPORT NUMBER
7. AUTHOR(S) Wade Williams Alan Wendler		8. CONTRACT OR GRANT NUMBER(S) DAAK10-80-C-0049 new
9. PERFORMING ORGANIZATIONS NAME/ADDRESS Honeywell DSD 600 Second Street N.E. Hopkins, MN 55343		10. PROGRAM ELEMENT, PROJECT, TASK AREA & WORK UNIT NUMBERS
11. CONTROLLING OFFICE NAME/ADDRESS U.S. Army Research & Development Command Dover, New Jersey 07801		12. REPORT DATE November 30, 1980
		13. NUMBER OF PAGES 115
14. MONITORING AGENCY NAME/ADDRESS (IF [illegible] CONT. OFF.)		15. SECURITY CLASSIFICATION (OF THIS REPORT) Unclassified
		15a. DECLASSIFICATION DOWNGRADING SCHEDULE

AD A094284

LEVEL II

16. DISTRIBUTION STATEMENT (OF THIS REPORT)

DISTRIBUTION STATEMENT A
Approved for public release;
Distribution Unlimited

DTIC ELECTE JAN 29 1981 S D

17. DISTRIBUTION STATEMENT (OF THE ABSTRACT ENTERED IN BLOCK 20, IF DIFFERENT FROM REPORT)

18. SUPPLEMENTARY NOTES

19. KEY WORDS (CONTINUE ON REVERSE SIDE IF NECESSARY AND IDENTIFY BY BLOCK NUMBER)

Revolution Sensor/Counter
Auto Impact Delay
Explosive Barrier Module
Electronic Fuze

20. ABSTRACT (CONTINUE ON REVERSE SIDE IF NECESSARY AND IDENTIFY BY BLOCK NUMBER)

Demonstration of Technical Performance of Subsystem Modules
For An Electronic Joint Army/Navy Point Detonating/Delay Fuze.

393171

DD FORM 1 JAN 73 1473 EDITION OF 1 NOV 55 IS OBSOLETE

SECURITY CLASSIFICATION OF THIS PAGE (WHEN DATA ENTERED)

DDC FILE COPY

HQ-189 REV 11/74

(9) Final Report. 28 Feb-30 Nov 80

(6) Electronic Joint Army/Navy
Point Detonating/Delay Fuze.

(11) October 1980

(15) DAAK10-80-C-0049

(12) 17.6

(10) Wade / Williams
Alan / Wendler

249

Abstract

Honeywell expended a level of effort of 1779 hours of professional, technical, and support labor toward the demonstration of technical performance and physical capability of the subsystem modules required for an Electronic Joint Army/Navy P.D./Delay Fuze. The primary objective of this program was to develop an electronic system which can meet both the Army and Navy large caliber fuze requirements and be cost competitive with existing mechanical fuzes. Specific tasks included: requirements definition, systems analysis, subsystem development, subsystem testing, reliability and safety analysis, and documentation.

The Electronic Joint Army/Navy PD/Delay Fuze will sense three environments and it will have the hand selectable option of functioning on super quick or void sensing with delay. The JAN fuze will evaluate the setback pulse, spin rate, and the number of projectile revolutions before enabling fuze arming.

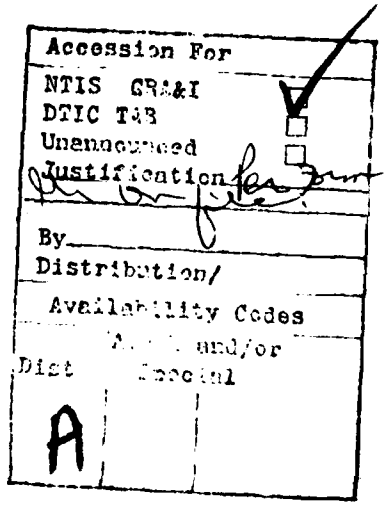

Table of Contents

Table of Contents
(Cont.)

I. Introduction

This report will describe work done and achievements made towards the completion of the program objectives. The Requirements Definition, Subsystem Development, Theoretical Analysis, System Integration, and the Reliability Analysis are discussed with an explanation of Fuze operation included in the System Integration section. The conclusion includes a summary of the effort done and recommendations for further work.

The project engineer was Ed Stryker. Other technical personnel participating in the project included:

Wade Williams:	Lead Engineer
Alan Wendler:	Electronic Design Engineer
Tom Cossette:	Penetrator Design Engineer
Dan Vavrick:	EPIC-2 Simulation

II. Requirement Definition

The requirements for the JAN PD/Delay Fuze are outlined in Table I. The Navy and Army Fuze requirements are similar except for weight, setback arming level, spin arming level and arming distance as shown by Table II.

The different weight requirements require separate Navy and Army penetrators, while the different setback spin and arming distance requirements can be met during assembly with minimal part substitution and a jumper select option.

Table I

JAN Requirements

The following charts show the requirements for the JAN PD/Delay Fuze. The Service label means that the Army and the Navy have different requirements, which up to the present time cannot be harmonized, and therefore both the Army and Navy requirements must separately be met.

Physical Requirements

		Army	Navy	JAN
1.	Contour	MIL-STD-333A	MIL-STD-333A	MIL-STD-333A
2.	Weight	1.55±.051 lbs.	2.10±.055 lbs.	Service
3.	Settability	Hand	Hand	Hand

Environmental Requirements

The JAN fuze shall meet the following tests of MIL-STD-331A:

	Test No.	Title
4.	101.2	Jolt
5.	102.1	Jumble
6.	103.1	Forty-foot Drop
7.	105.1	Temperature and Humidity
8.	107.1	Salt Fog
9.	108.	Waterproofness
10.	111.1	1.5 Meter Drop
11.	113.1	Thermal Shock
12.	119.	Transportation Vibration-Temperature

In addition the JAN and/or the Army and Navy fuzes shall meet the following environmental requirements:

		Army	Navy	JAN
13.	Setback Force (g's)	28,000	26,000	30,000
14.	Shock Start (kg/ms)	———	50/.12	50/.12
15.	Maximum Spin (rpm)	28,000	26,000	30,000
16.	Maximum Spin Eccentricity (in)	.060	.040	.060
17.	Rain Insensitivity at 2,700 fps (in/hr)	25 (4mm drop)	7 (2mm drop)	25 (4mm drop)
Ramming Shock				
18.	Velocity Change (ft/sec)	20	8	20
19.	Acceleration/Time (g's/ms)	5000/1	100/3	500/3 & 5000/1

Table I (Continued)

		Army	Navy	JAN
	Safety Requirements			
20.	Arming Distance (Min/Max Rev)	22/33	37/52	Service
21.	No/All Arm Setback (g's/g's)	400/600	900/1400	Service
22.	No/All Arm Spin (spin/spin)	1100/1700	3000/4500	Service
23.	Meets MIL-STD-1316B except for	Yes	Yes	Yes
24.	Fail safe objective	No	No	Yes
25.	Anti-malassembly feature	No	Yes	Service
26.	Safing and Arming X-raying MIL-STD-331A	No	Yes	Service
27.	Test No. 115.1 Static Detonator Safety	Yes	Yes	Yes
28.	Test No. 208.1 Impact Safe Distance	Yes	Yes	Yes
	Functional Requirements			
29.	Maximum Time of Super-Quick Function (ms)	.200	.200	.125
30.	Time of Delay Function (ms)	25	10	Auto-delay or Select-able 10 and 25
31.	Perpendicular Penetration at Velocity of 2000 fps	12" Brick	1/4 Steel	12" Brick & 1/4" Steel
32.	Super Quick Perpendicular Sensitivity	2" Plywood at 670 fps	2" Plywood at 900 fps	2" Plywood at 670 fps
33.	Graze Function	15^{o}	20^{o}	Service
34.	Super Quick Reliability	97%	97%	98%
35.	Delay Reliability	95%	95%	96%

Table II

Non-Standard JAN Requirements

	Army	Navy	Units
Weight	1.55 ± .051	2.10 ± .055	lbs
No/All Arm Setback	400/600	900/1400	g's
No/All Arm Spin	1100/1700	3000/4500	rpm
Arming Distance	22/33	37/52	revolutions

III. Subsystems

The major effort of this program was expended in the development of six subsystems and excellent results were achieved in most areas.

A. Penetrators

The basic design parameters of the JAN fuze as specified in the contract are contour, total weight and penetrability. Since penetration is primarily determined by the wall thickness of the penetrator nose, a major design objective is to thicken the nose wall as much as possible without exceeding the weight constraints of the fuze. Both Army and Navy fuze versions (Figures 1 & 2) utilize a plastic sleeve around the electronics module which, in effect, removes weight from the neck of the fuze and concentrates it in the nose. This sleeve also creates a modular assembly which enables the electronics package to be built and tested as an integral unit before being permanently installed into the penetrator housing. In order to maximize component commonality both fuzes have been designed with identical interior cavities.

To meet the required lot, penetration, and contour specifications, the Navy penetrator has been designed with a nose wall thickness of .400 inch. A .140 inch nose wall is considered sufficient to satisfy Army requirements.

As an aid for estimating effective projectile penetration, Honeywell has developed a computer simulation called EPIC-2 and this computer simulation was run for both the Army and Navy penetrators. The program assumed that the penetrators were made of 4140 steel and that the target was made of 1010 steel.

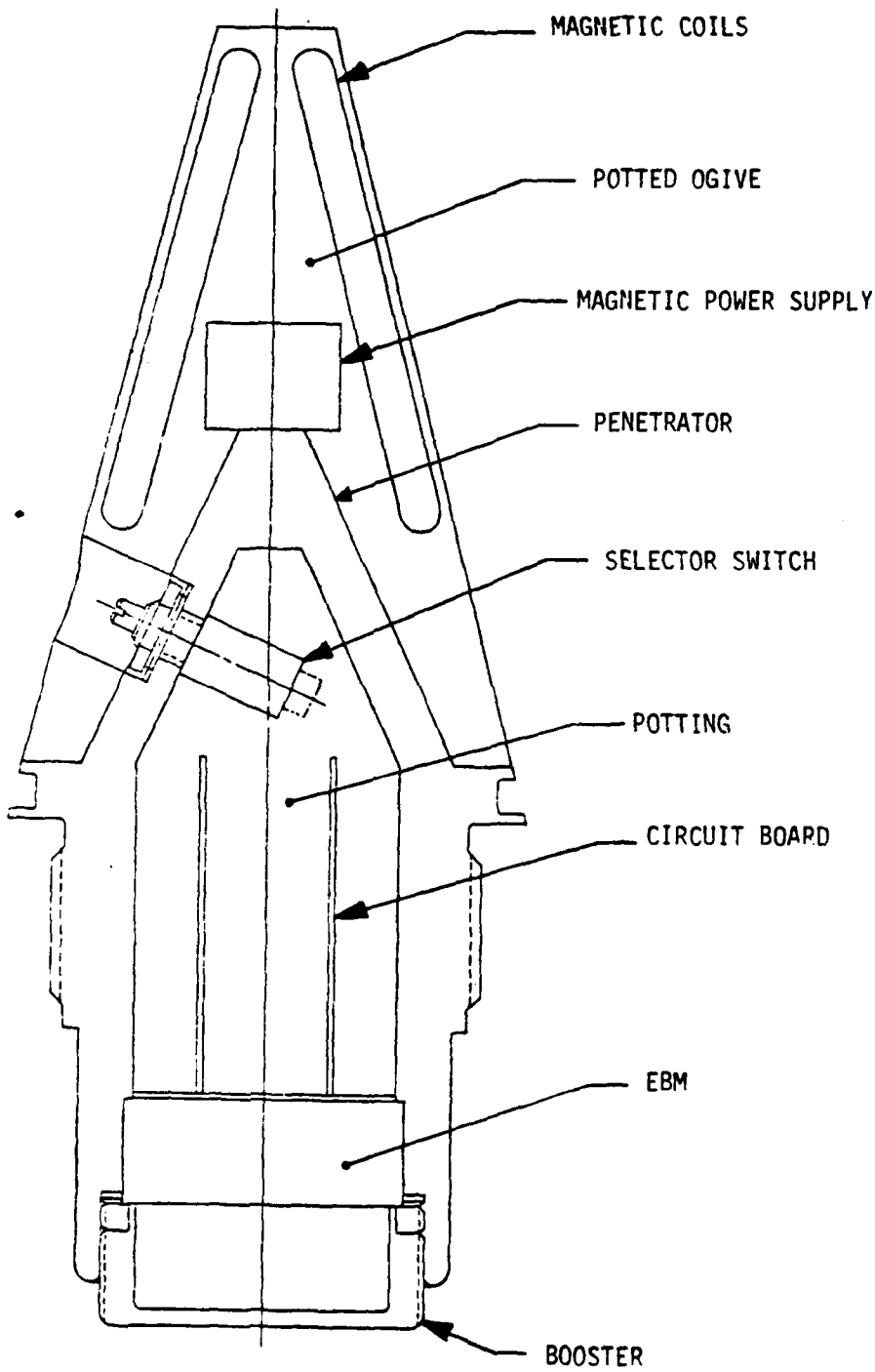

FIGURE 1

ARMY PENETRATOR FUZE

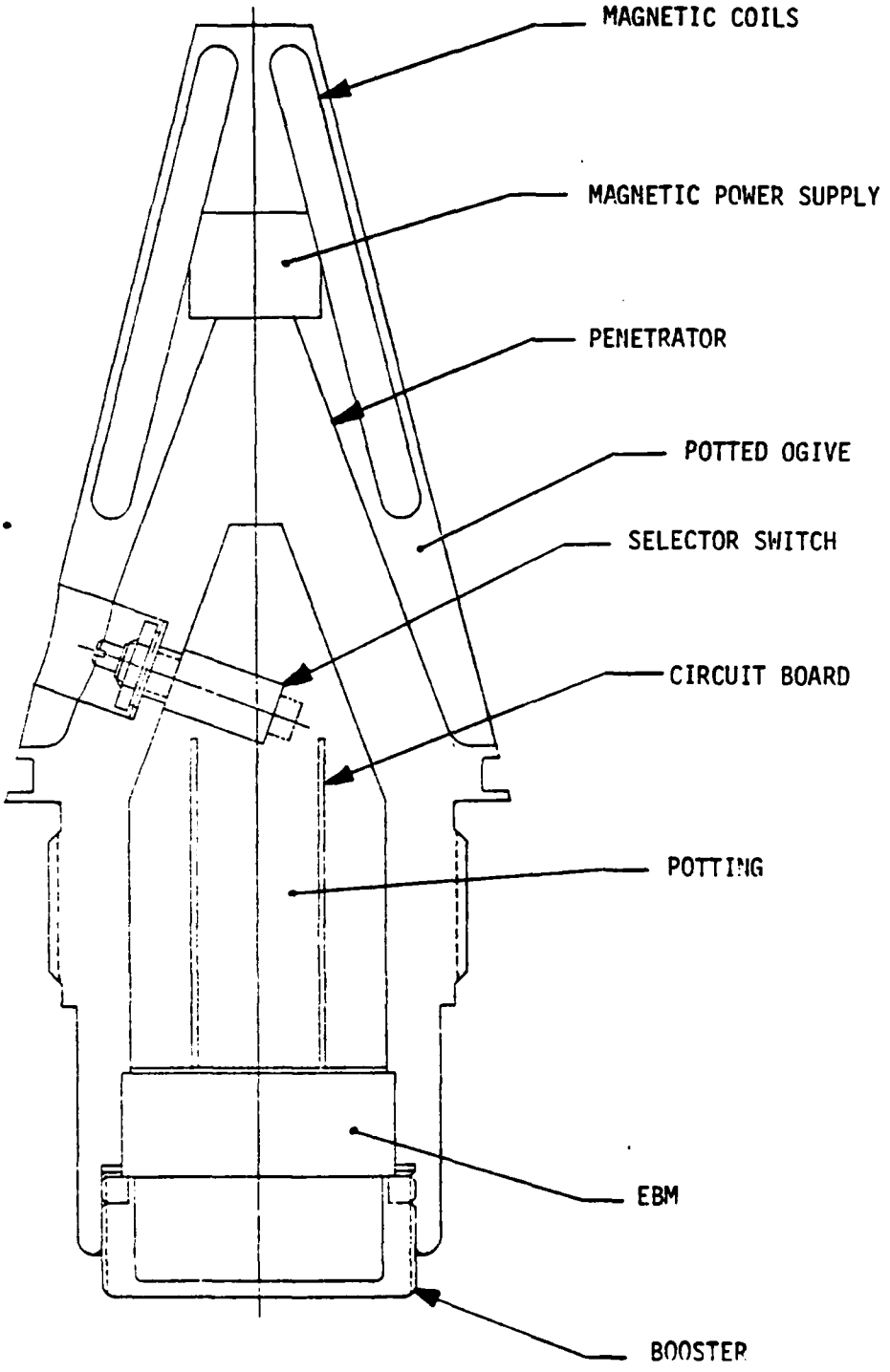

FIGURE 2

NAVY PENTRATOR FUZE

Both target and penetrator were assumed to have elastic strain hardening and the target was assumed to have shear failure at static ultimate 31%. The reader may refer to reference 1 for specifics about the computer program and reference 2 for target Hugoniot data.

1) Johnson, G.R., "EPIC-2, A Computer Program for Elastic-Plastic Impact Computations in 2 Dimensions Plus Spin," ARBRL-CR-00373, Honeywell Inc., Hopkins, Minnesota, June 1978.

2) Kohn, B.J., "Compilation of Hugoniot Equations of State", WL-TR-69-38, Weapons Lab, Kirtland Air Force Base, New Mexico.

The computer run simulating the impact of the Army penetrator to 4 inches of concrete showed noticeable housing deformation at 24μsec., Figure 3. (The design specification for the Army fuze calls for penetration of 12 inches of brick at 2000 ft./sec., but we could find no computer compatible description for brick, so the concrete substitute was used.) The deformation observed does not prove that the Army penetrator will fail the 12 inch brick requirements, but it does suggest that a review of the Army penetrator geometry and material is in order.

The computer run simulating the impact of the Navy penetrator to 1/2 inch of 1010 steel, Figure 4, showed the penetrator penetrated the steel plate. This output indicates that the Navy penetrator is ready for gun fire testing.

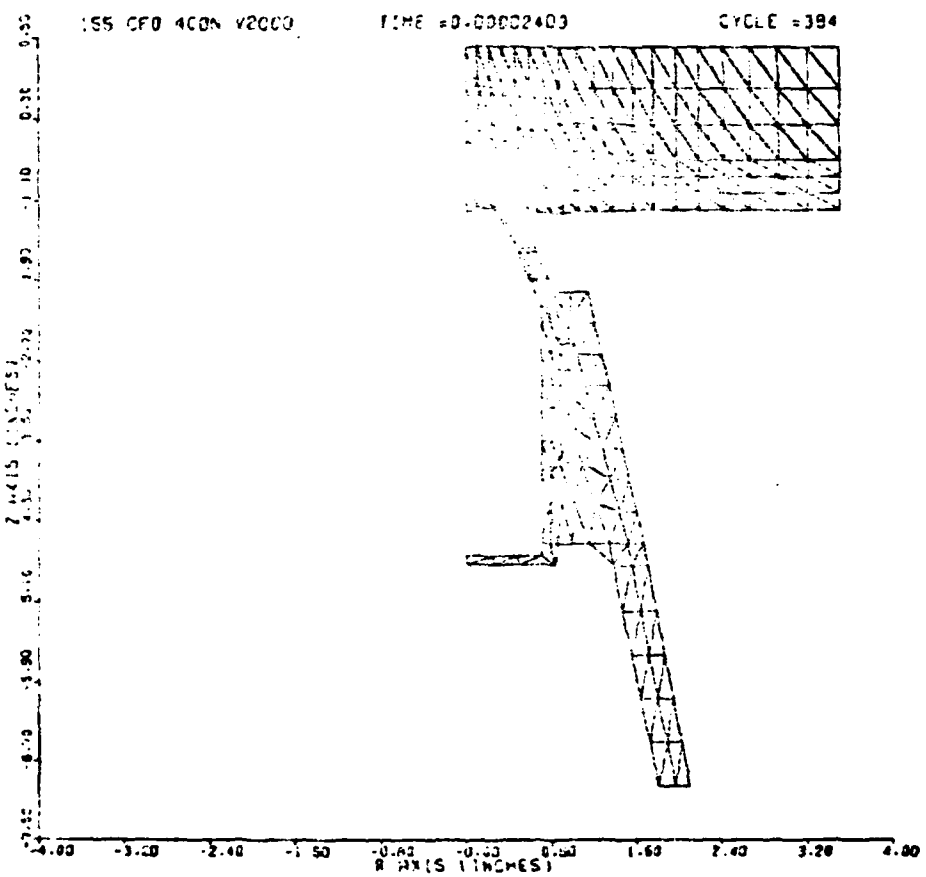

FIGURE 3 - ARMY PENETRATOR VS. CONCRETE

FIGURE 4

EPIC COMPUTER OUTPUTS

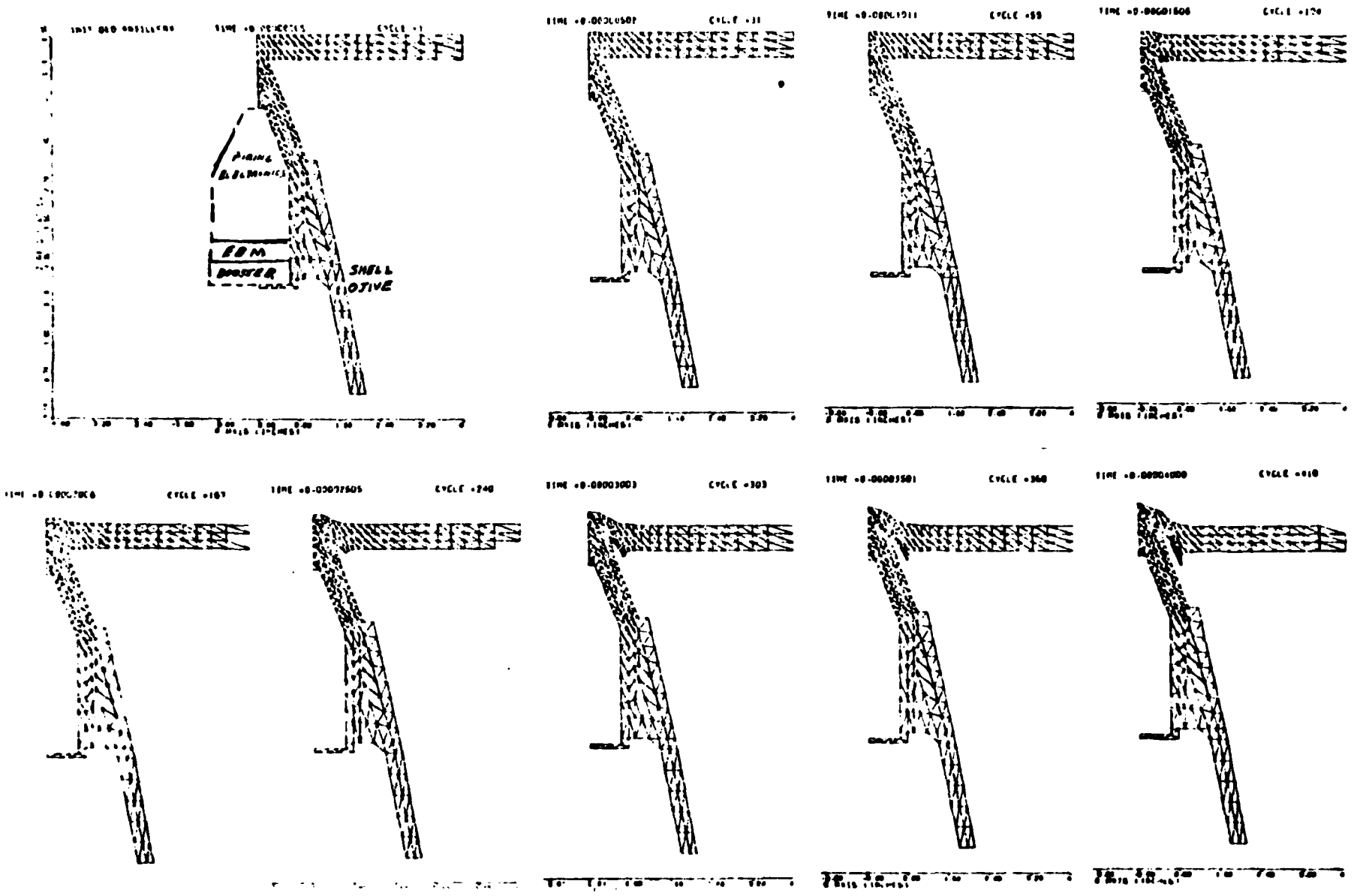

B. Revolution Sensor

1. Theory

Counting the number of revolutions that a projectile makes is a reliable method of determining when the projectile has travelled the safe separation distance and thereby enabling the projectile to arm. Detecting projectile revolution can be done by sensing the reversal of polarity of the earth's magnetic field, which occurs once for each revolution, and using this phenomena to increment a counter. The revolution sensor includes the actual sensor and the associated amplifier needed to output a signal whose frequency is proportional to the spin rate.

2. Spin Fixture

A spin fixture was assembled to spin the sensor candidates for testing, see Figure 5 and Figure 6. A sensor and associated electronics can be mounted in the ogive connected to a variable speed motor via a four foot aluminum shaft, used to minimize motor interference. Three carbon brush contacts and a chassis ground enable up to four electrical connections to be made between the spinning ogive and the monitoring equipment. A precise motor speed control was used to regulate spin rate up to 3000 rpm, in either a C.W. or C.C.W. direction.

3. Sensors

The three sensors evaluated in this program consisted of two types of air core coils (new coils and old coils) and a magnetoresistive bridge (M.R.B.).

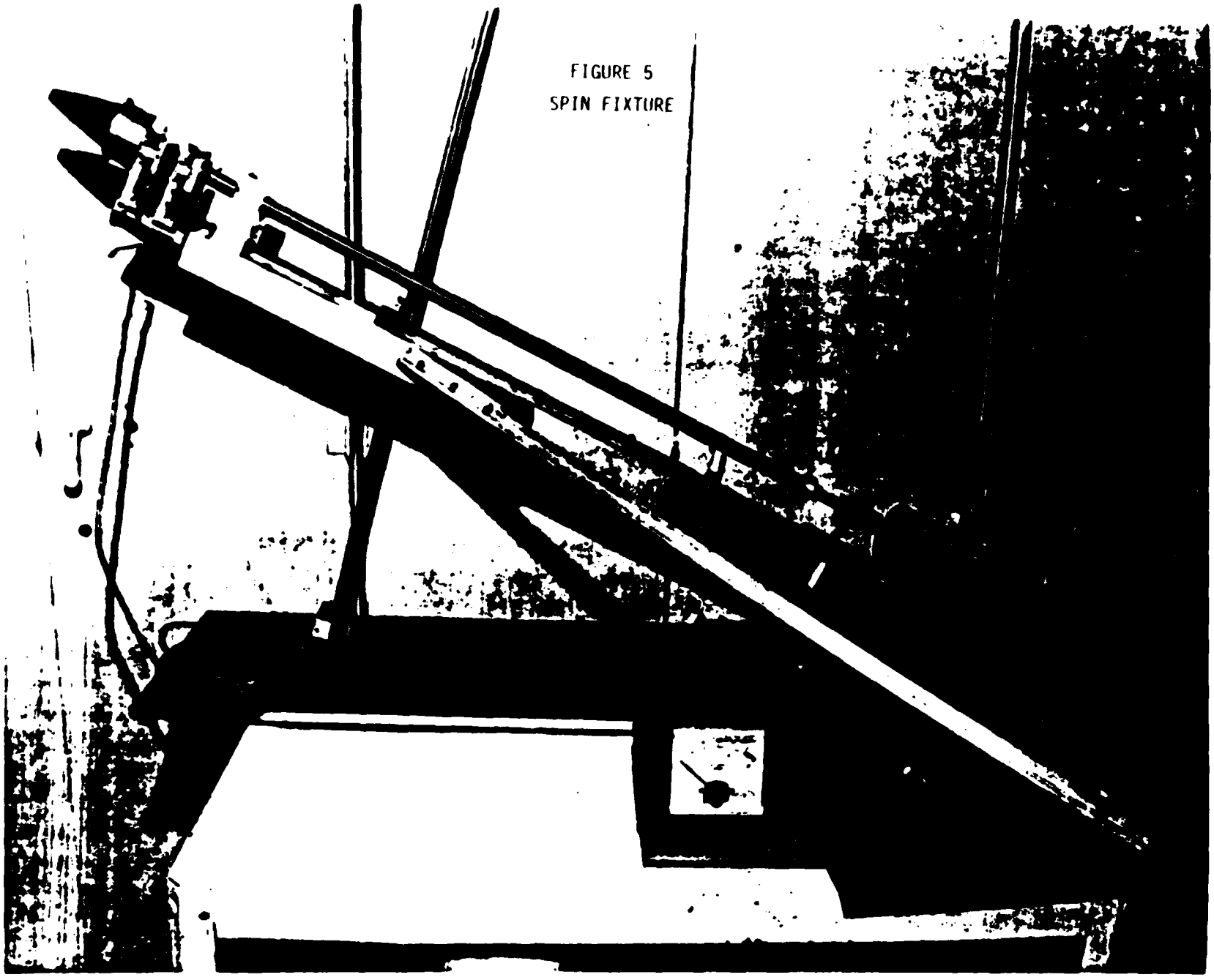

FIGURE 5
SPIN FIXTURE

FIGURE 6
SPIN FIXTURE OGIVE

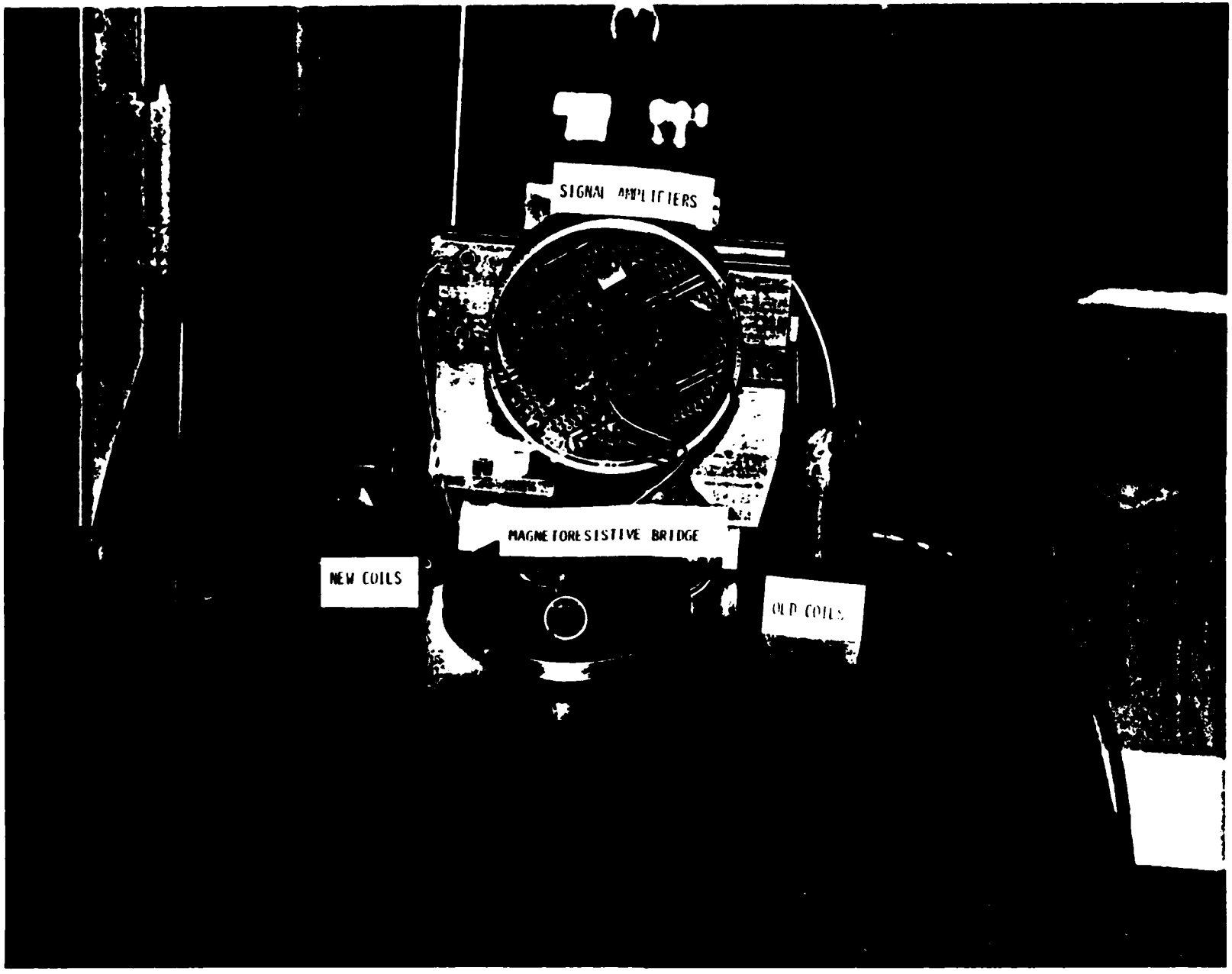

The new coils, as described in the proposal, consist of two 1000 turns of #44 wire wound in a "horse-collar" shape approximately 2" high with a 1 1/2" base. The coils are wired in series and mounted approximately parallel to each other.

The old coils are from an earlier program and consist of two 250 turns of #26 wire wound in a 2 1/2" x 1" oval. They are wired in series and mounted approximately parallel to each other.

The magnetoresistive bridge magnetometer is a new device manufactured by Honeywell SSEC. The major advantage of this sensor is its small size and process compatibility with large scale integrated circuit technology. The M.R.B. and signal processing electronics could be fabricated on a common silicon substrate resulting in a high volume, low cost potential inherent in using large scale integrated circuits.

The disadvantage of the M.R.B. over the coils is that it requires a bias current of approximately 100 micro Amps, so it is not well suited for extremely low power systems.

Appendix A includes a discussion of the Magnetoresistive Bridge Sensor.

4. Amplifier

The primary requirement for the Revolution Sensor Amplifier is that it be very low power with high voltage gain. Several high impedance programmable CMOS operational amplifiers were evaluated in addition to several MOS FET amplifiers.

The testing revealed that the Low Power OP Amps were better suited than the FET amplifiers for use in the JAN system.

A three stage differential input amplifier was built using Intersil ICL7611BCPA OP Amps for sensor evaluation, see Figure 7. This 55 db amplifier was run from a 10V supply and required approximately 30 micro Amps. Once sensor sensitivity tests were completed the amplifier was modified to a 2 stage amplifier and the gain was greatly increased causing the amplifier to easily saturate, outputting a square wave used to clock the counter. This circuit, Figure 8, requires only 15-20 micro Amps to operate and a sample output is shown in Figure 9.

5. Tests

Several test series were conducted to evaluate the sensor candidates. The first set of tests measured sensor output as a function of compass direction. The results of this test, see Figures 10, 11, and 12, show that the old coils have the highest relative output and that the MRB is the most linear of all three sensors. Since the critical factor in the operation of this type of revolution sensor is the position of the sensor relative to the earth's magnetic field, the compass direction data was manipulated to reflect degrees from the magnetic field as shown by Figures 13 and 14. The graphs indicate that the sensors were sensitive to $\pm$ 10^{o} from the earth's lines of flux.

The second series of tests involved sensor output vs spin rate and the data is presented in Table III. This test was done first with the spin fixture pointing south at 30^{o} elevation and then west at 0^{o}. The data indicates that the M.R.B. is the most sensitive sensor at low rpm and it has the most linear response as a

JAN MAGNETORESISTIVE BRIDGE REVOLUTION COUNTER AMPLIFIER

FIGURE 7

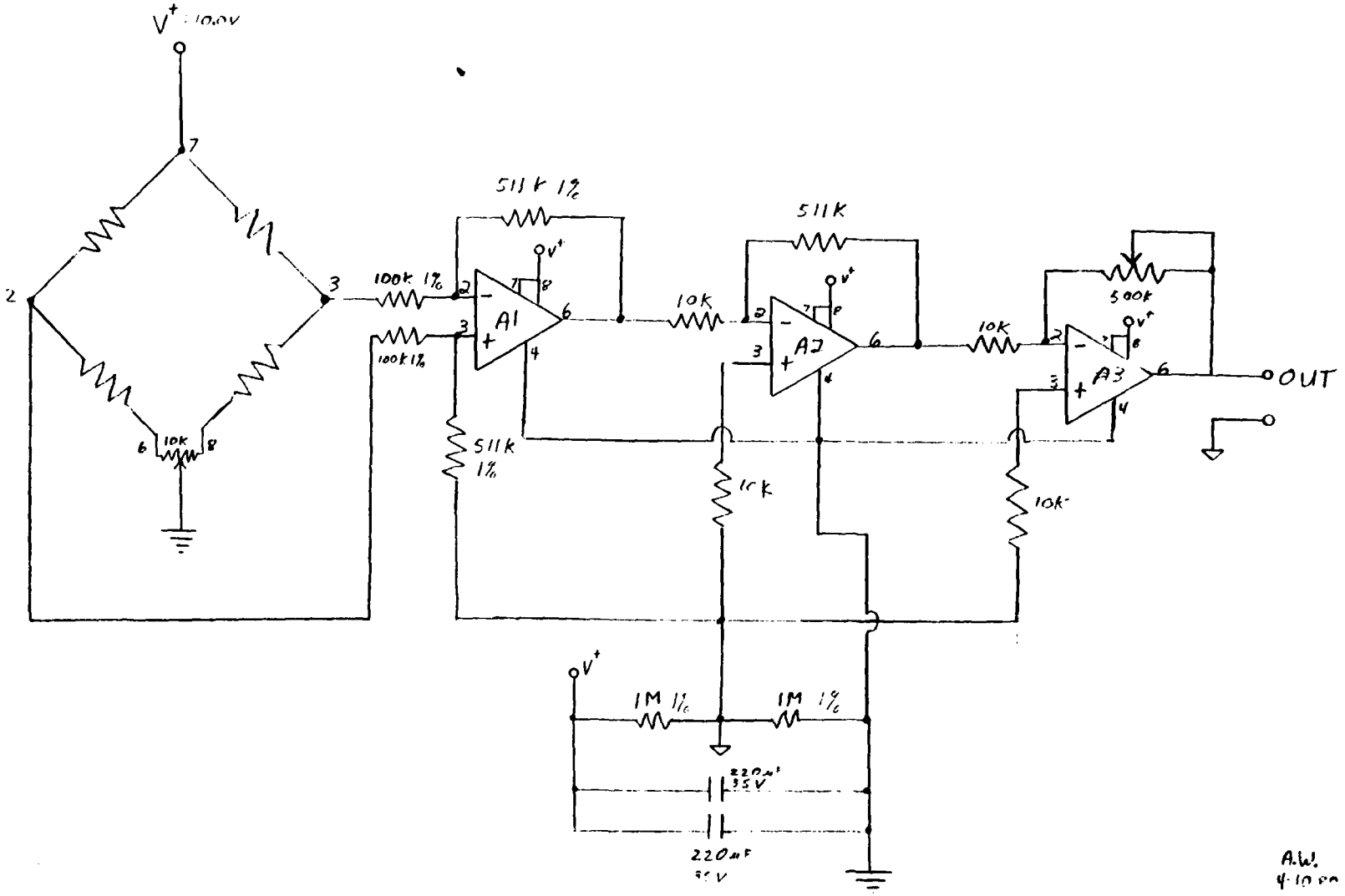

A.W.
4-10-80

01 AMPS

3-Intersil ICL7611K CPA
Low Power

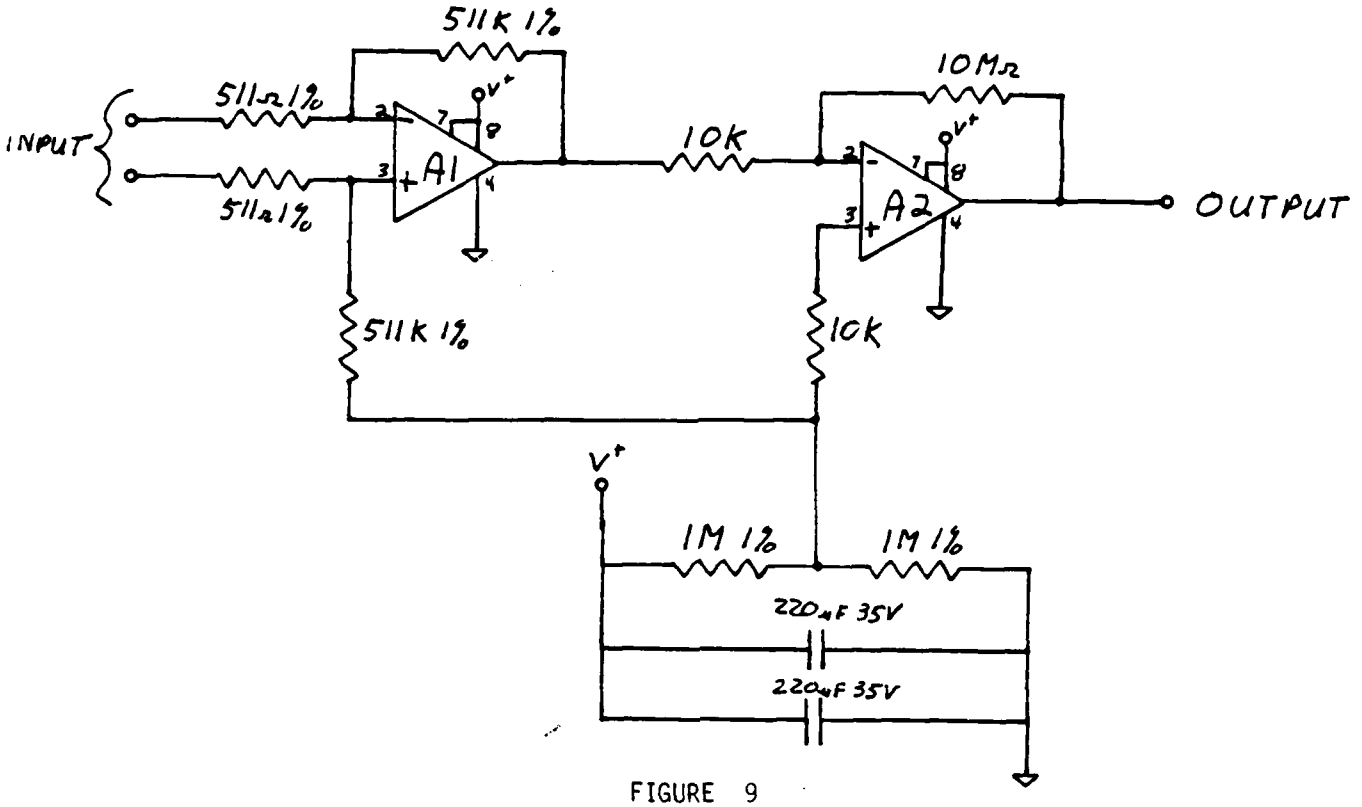

FIGURE 9

REVOLUTION COUNTER AMPLIFIER

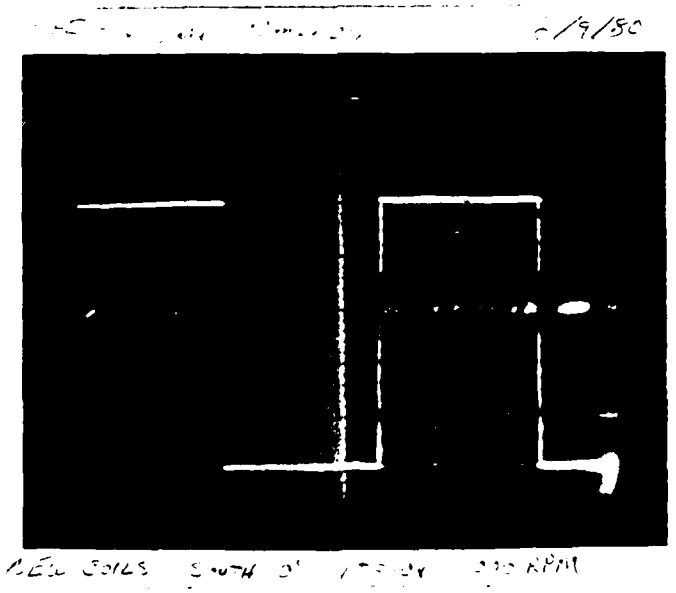

FIGURE 8

SAMPLE AMPLIFIER OUTPUT

FIGURE 10

V_o vs θ

Magnetoresistive Bridge

$V^+ = 10.0V$

direction = CCW

speed = 1000 r.p.m.

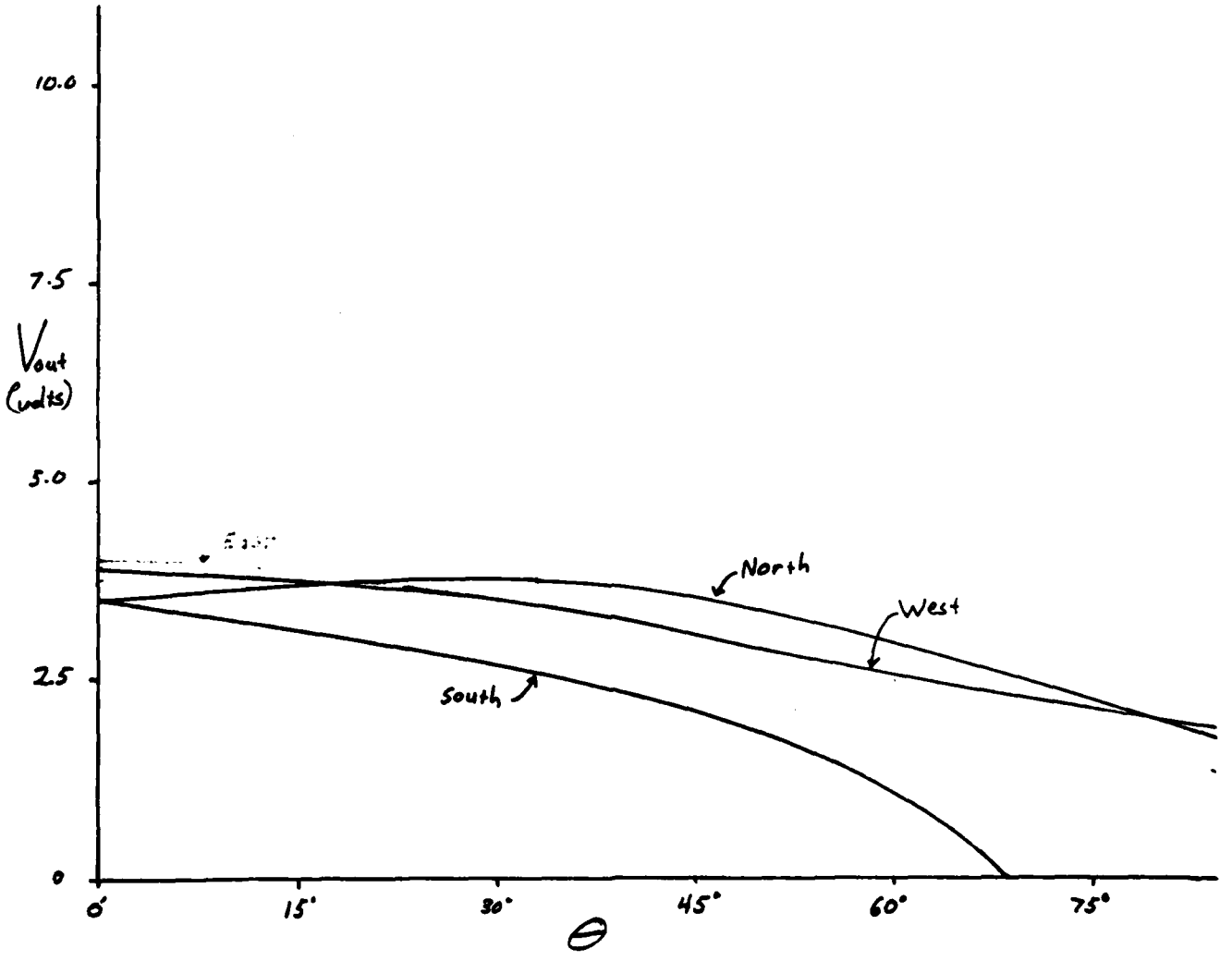

FIGURE 11

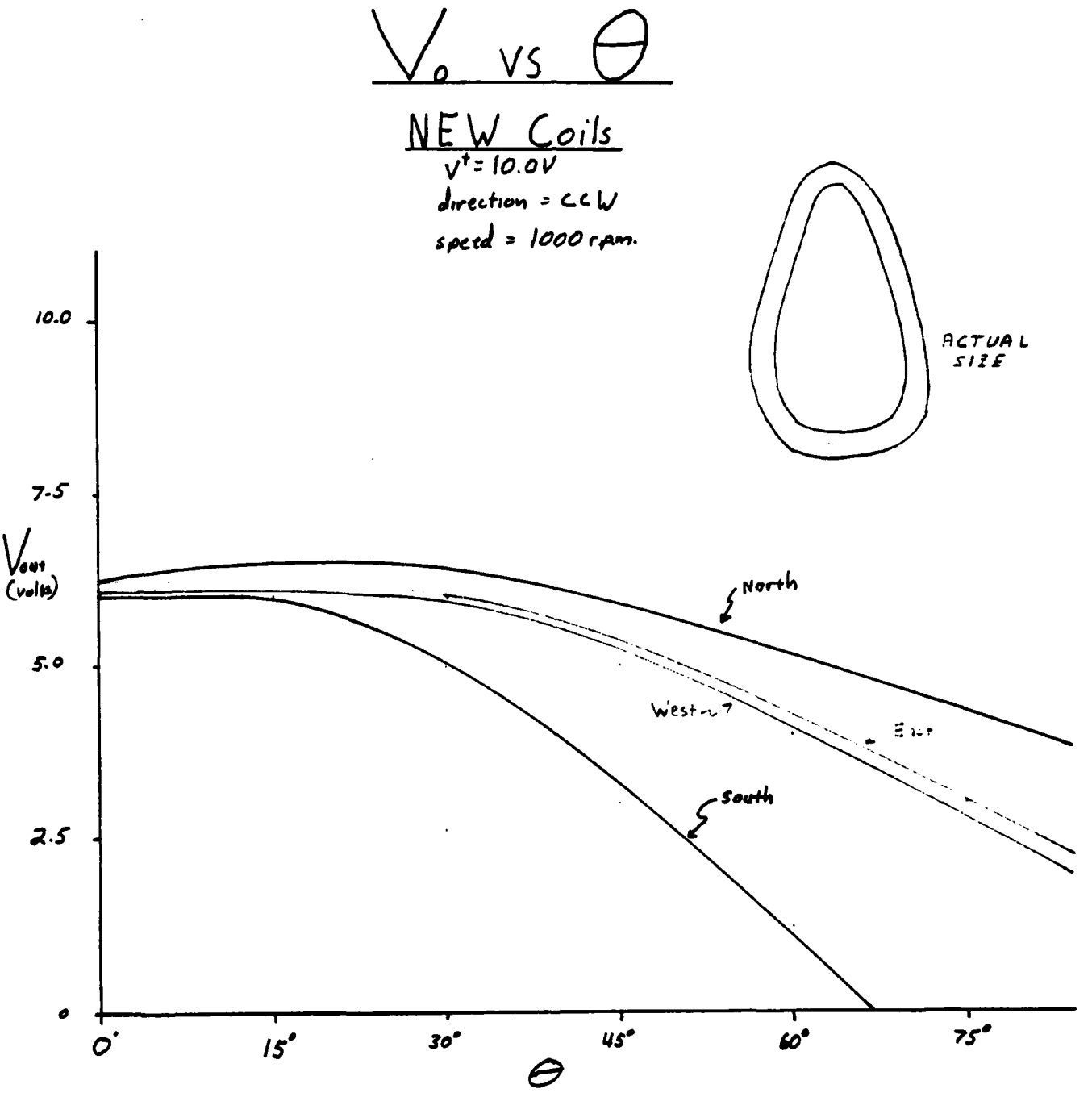
V_o vs θ
NEW Coils
V^t = 10.0V
direction = CCW
speed = 1000 rpm.
ACTUAL SIZE
10.0
7.5
5.0
2.5
0
V_{out} (volts)
North
West
East
South
0°
15°
30°
45°
60°
75°
θ

FIGURE 12

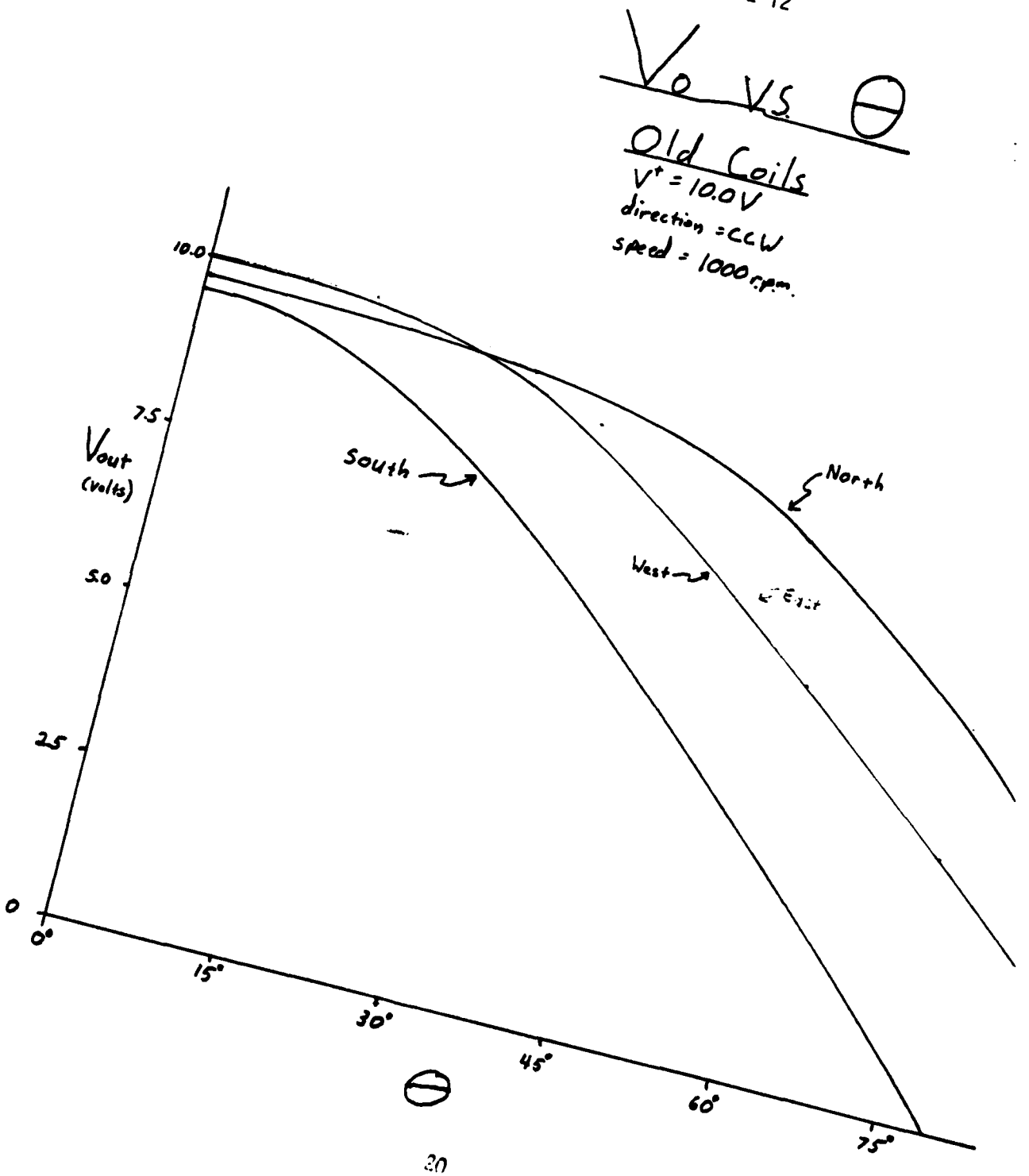
V_o vs. θ
Old Coils
V^t = 10.0V
direction = CCW
speed = 1000 rpm.
10.0
7.5
5.0
2.5
0
V_{out} (volts)
South
North
West
East
0°
15°
30°
45°
60°
75°
θ

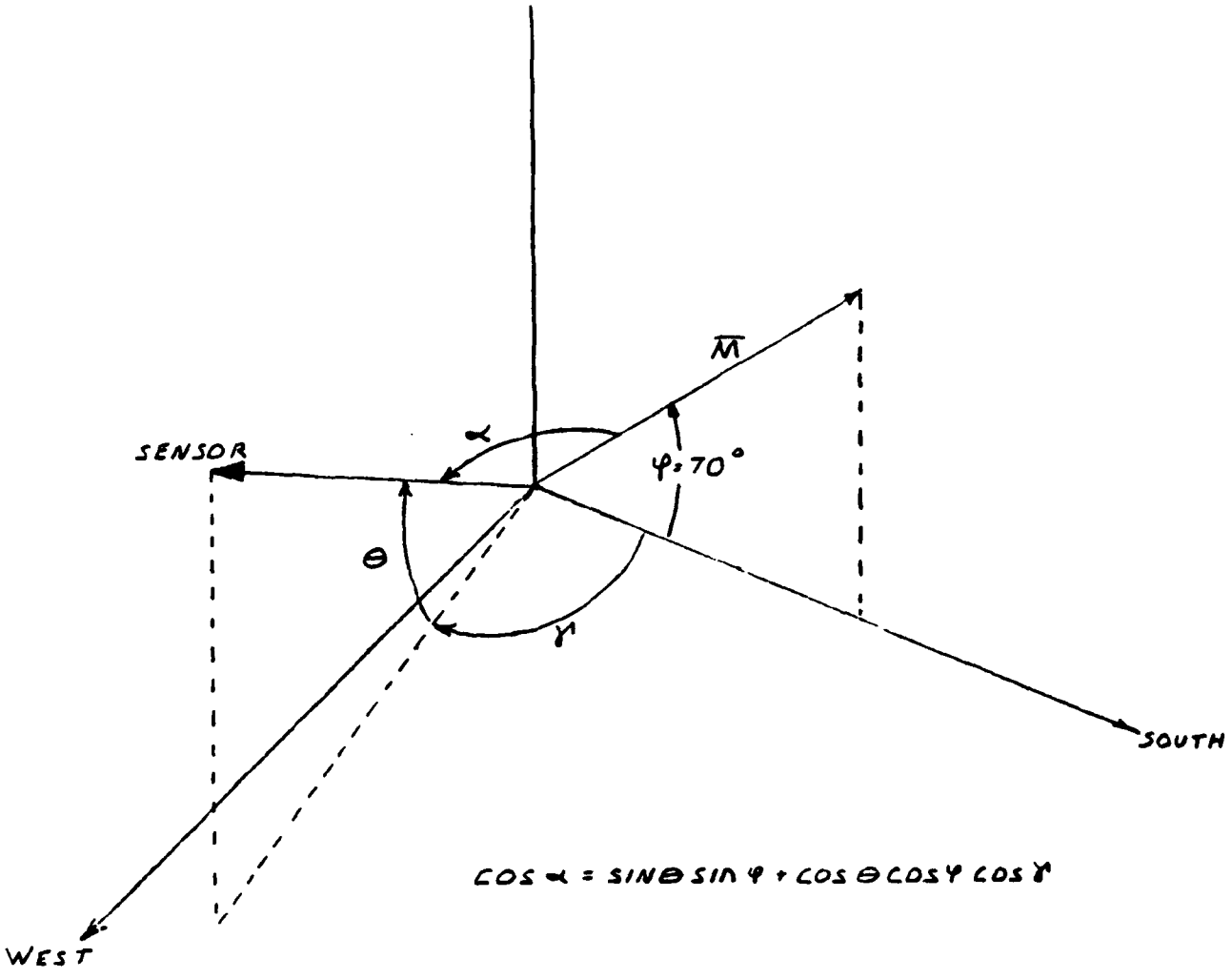

RELATING THE DATA TO THE MAGNETIC FIELD

Figure 13

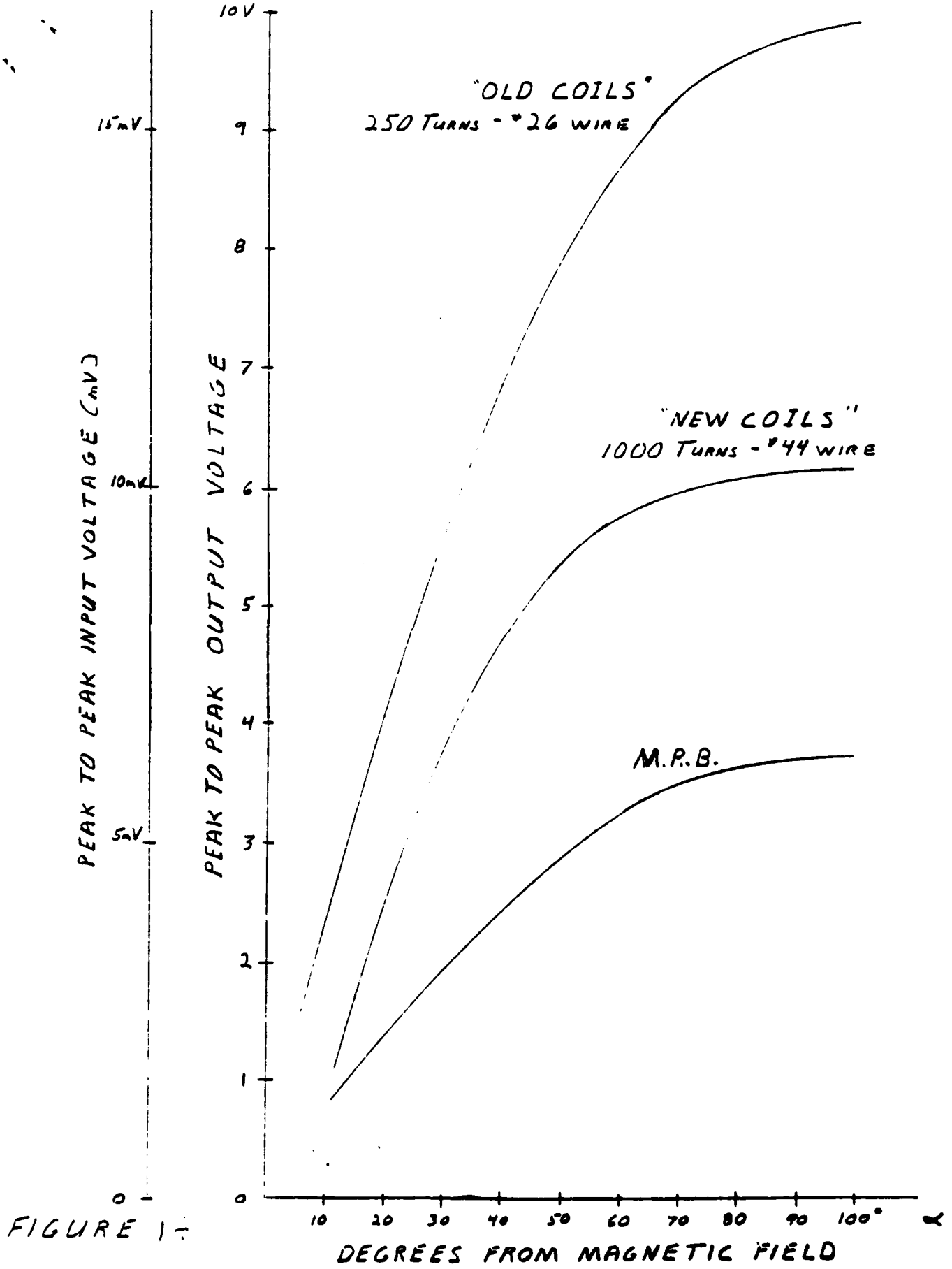
PEAK TO PEAK INPUT VOLTAGE (mV)
15mV
10mV
5mV
0
PEAK TO PEAK OUTPUT VOLTAGE
10V
9
8
7
6
5
4
3
2
1
0
"OLD COILS"
250 TURNS - #26 WIRE
"NEW COILS"
1000 TURNS - #44 WIRE
M.P.B.
10
20
30
40
50
60
70
80
90
100°
DEGREES FROM MAGNETIC FIELD

FIGURE 1

Table III

Sensor Output V.S. Spin Rate (RPM)

	South at 30°			West at 0°		
RPM	MRB	Old Coils	New Coils	MRB	Old Coils	New Coils
200	0.5	0.2	0.2	0.6	0.3	0.2
400	1.0	1.0	0.6	1.2	1.3	0.7
600	1.5	2.2	1.2	1.8	2.7	1.7
800	2.0	4.0	2.3	2.4	4.6	3.6
1000	2.5	6.0	3.5	3.0	7.5	4.5
1200	3.0	8.5	5.0	3.6	10.0	7.0
1400	3.5	10.0	7.2	4.2	10.0	9.0
1600	4.0	10.0	9.5	5.0	10.0	10.0
1800	4.5	10.0	10.0	5.5	10.0	10.0
2000	5.0	10.0	10.0	6.0	10.0	10.0

(V_{in} = 10.0 Volts)

function of spin rate. Since the all-arm Army spin rate for JAN is 1700 rpm, the coils are better suited for the revolution sensor since their output is higher than the MRB at spin rates greater than 600 rpm.

The revolution sensor amplifier was modified to easily saturate, Figure 8, and sensitivity window testing was done. Since the earth's magnetic lines of flux, at Hopkins, MN., are incoming approximately south at 70^{o}, the test was done with the spin fixture pointing south. The sensitivity window, defined as that region where a non-saturating output was observed, was recorded and those results are presented in Table IV. It was found that the circuit had a window of 69^{o} - 71^{o} ($\pm$ 1^{o} sensitivity) when the new coils were tested with an applied voltage greater than 6.5 volts. With only 4 volts, the circuit was sensitive to within $\pm$ 3^{o} of the earth's lines of flux, so the revolution counter will probably run at 4 to 6.5 V. The magnetoresistive bridge was not as sensitive as either coil, so this fact, in addition to the M.R.B.'s relatively large quiescent current (approximately 150 micro Amps), caused it to be rejected as the revolution sensor. The old coils were also rejected since they are larger and not as sensitive as the new coils.

C. Spin Rate Sensor

The proposed JAN spin rate sensor consisted of two piezoelectric (P.Z.) crystals with weights attached, mounted an equal distance from the spin axis. The crystals would be wired in parallel so only a centrifugal force, caused by the projectile spinning, would yield a net voltage ($\sim$0.5V) from the two P.Z. crystals. See Figure 15 & 16 for setup and Appendix B for a theoretical analysis of the system. Earlier tests, as noted in the proposal, had an output range of 1-

TABLE IV

SENSITIVITY WINDOW V.S. INPUT VOLTAGE
FOR M.R.B., OLD COILS, NEW COILS

VOLTAGE IN	M.R.B. WINDOW	OLD COIL WINDOW	NEW COIL WINDOW
10.0	67^0 - 72^0	69^0 - 71^0	69^0 - 71^0
9.5	67^0 - 72^0	69^0 - 71^0	69^0 - 71^0
9.0	67^0 - 72^0	69^0 - 71^0	69^0 - 71^0
8.5	67^0 - 72^0	69^0 - 71^0	69^0 - 71^0
8.0	67^0 - 72^0	69^0 - 71^0	69^0 - 71^0
7.5	67^0 - 72^0	69^0 - 71^0	69^0 - 71^0
7.0	67^0 - 72^0	69^0 - 71^0	69^0 - 71^0
6.5	67^0 - 72^0	68^0 - 72^0	69^0 - 71^0
6.0	67^0 - 72^0	67^0 - 73^0	68^0 - 72^0
5.5	67^0 - 72^0	66^0 - 75^0	68^0 - 72^0
5.0	66^0 - 73^0	64^0 - 76^0	67^0 - 73^0
4.5	66^0 - 73^0	63^0 - 77^0	67^0 - 73^0
4.0	66^0 - 73^0	63^0 - 77^0	67^0 - 73^0

NOTE: All tests done with fixture pointing south
spin rate = 1000 rpm

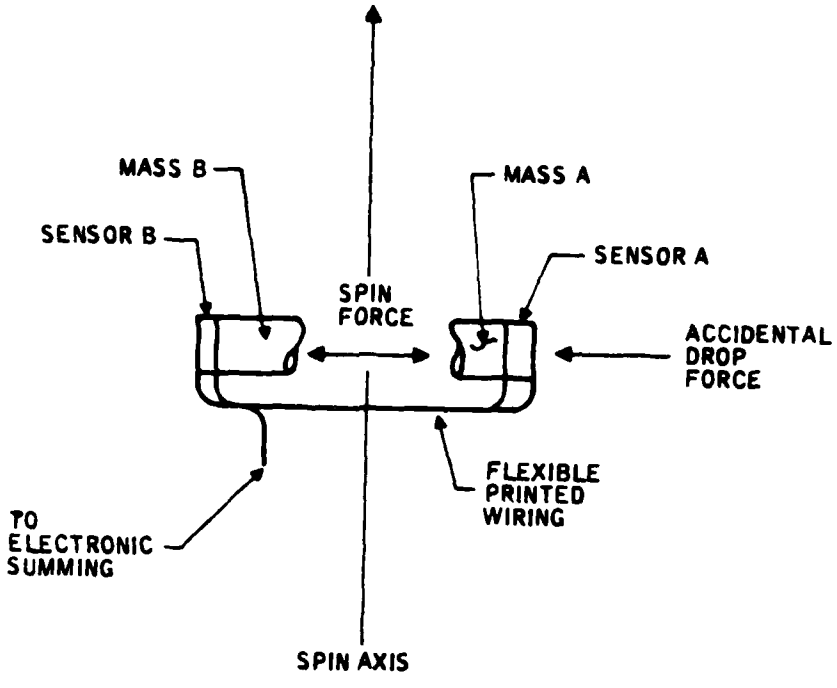

Figure 15 Spin Sensor Arrangement

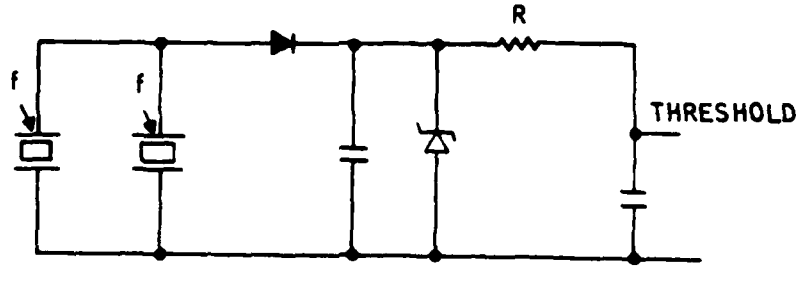

Figure 16 Electrical Circuit for Spin Sensor

10V versus a load capacitance of .01 F to 500pf at 6500 RPM. For the Army All Arm level of 1700 RPM $\frac{V(1700)}{V(6500)} = \frac{1700}{6500}^2 = .068$ the voltage range vs. capacitance becomes .07V to .7V for C = .01 F to 500pf. (The load capacitance is needed both to slow the rise time and to store the signal). During this program, we repeated the earlier test in a centrifuge and the spin fixture, but we were unable to distinguish any signature out of the vibration and background noise. (It is believed the earlier tests used a spin radius longer than the allowable JAN radius).

An alternate approach of detecting spin rate as a function of the revolutions sensor frequency was developed and successfully demonstrated. Figure 17 shows the circuit used. In order to get a signal out of the AND gate, the rate of revolution must be faster than the time set by the one-shot. Figure 18 shows the test circuit output vs. frequency.

D. Setback Sensor

The setback sensor consists of a piezoelectric crystal, a flexible printed circuit, a mass, and a discriminator. Upon setback, the mass compresses the P.Z. crystal which outputs a voltage pulse to the electronic discriminator. The discriminator consists of a peak clipper diode, passive integrator, comparator, and a latch. The integrator time constant, clipper diode, and comparator threshold regulate the criteria for an acceptable setback pulse and the latch will set to remember a good pulse. (See Figure 19 for circuit and experimental data). The Army setback pulse amplitude requirement is 400 g's no arm and 600 g's all arm, which corresponds to a no arm and all arm voltage of 3.2V and 4.7V, respectively. The setback pulse duration was not defined, so a pulse greater than 5

MONITORING SPIN RATE FROM THE REVOLUTIONS SENSOR

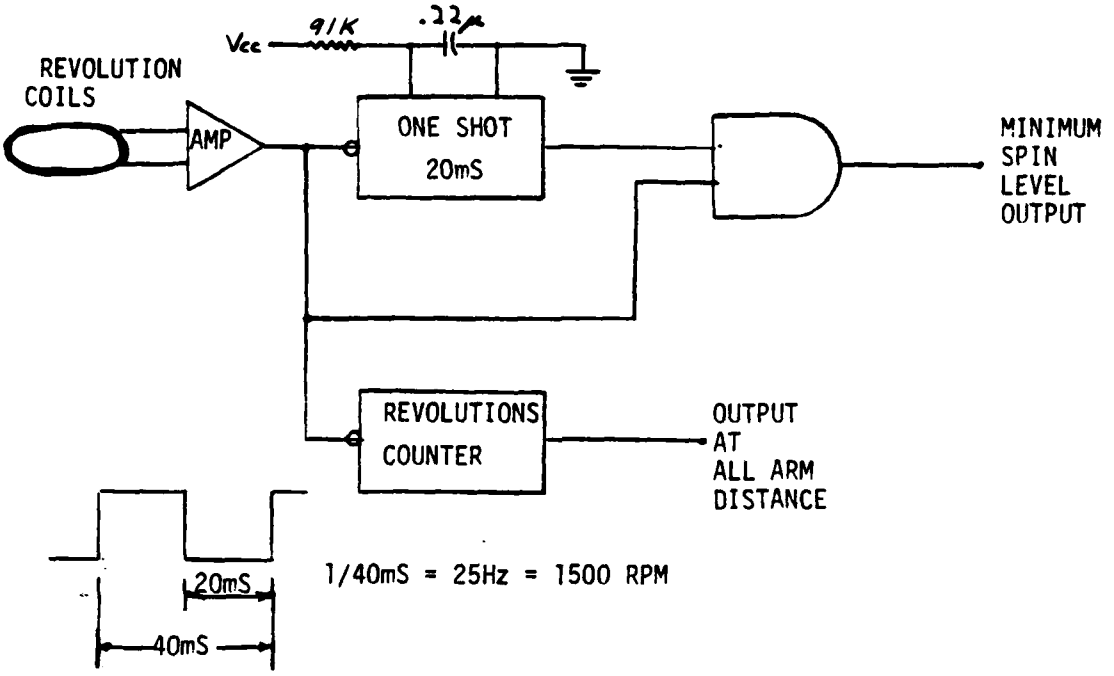

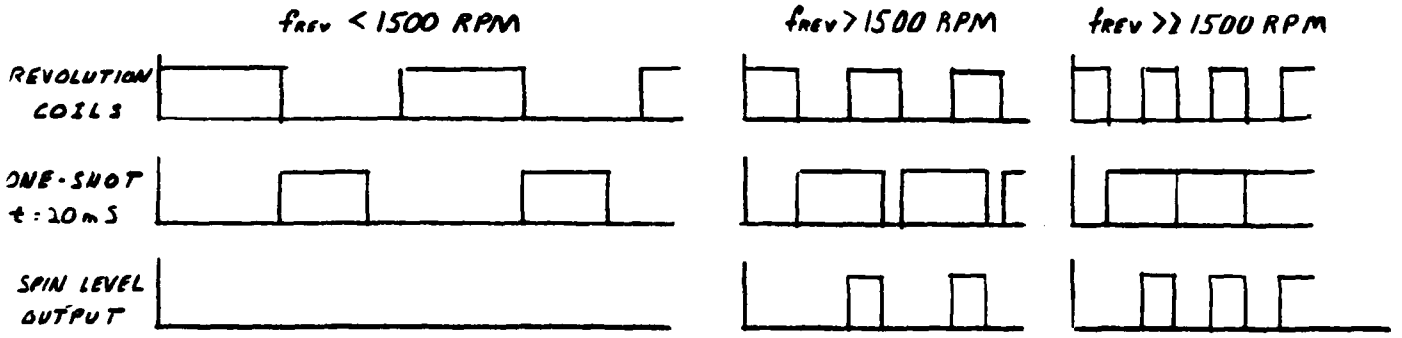

FIGURE 17

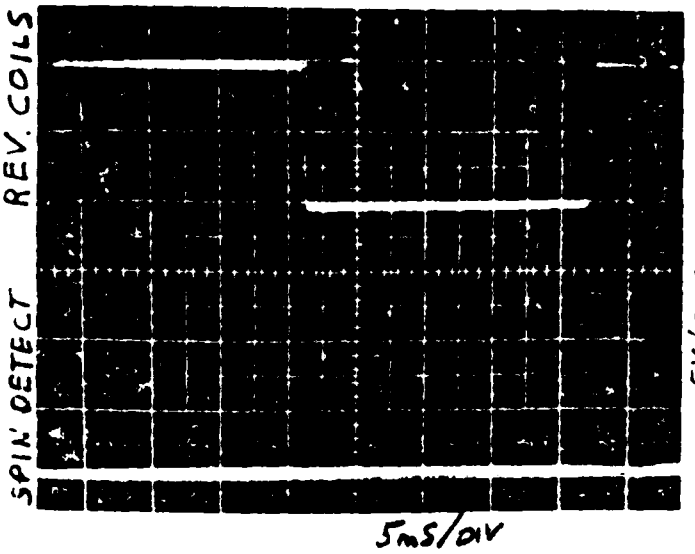

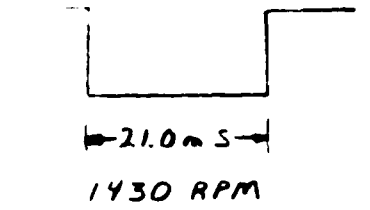

NO OUTPUT BELOW MIN SPIN RATE

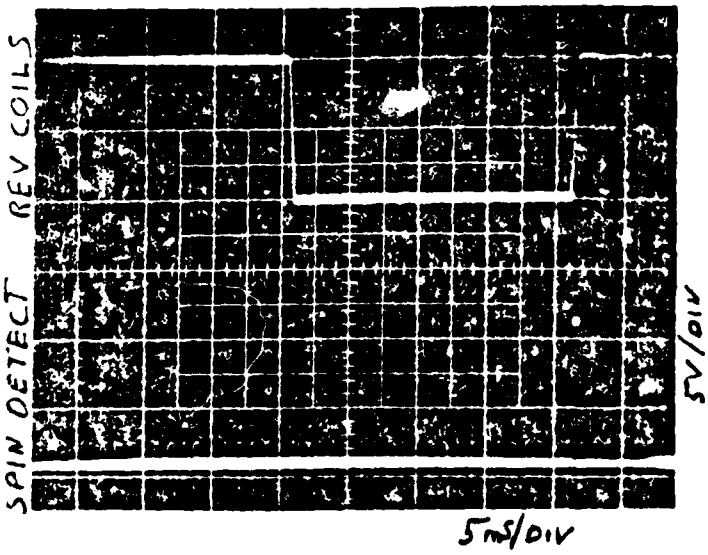

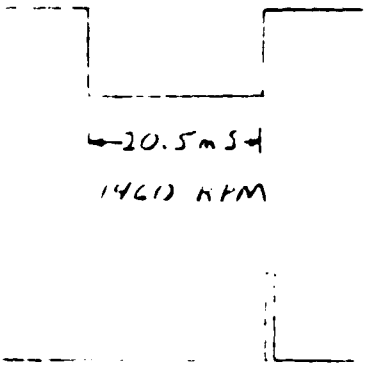

OUTPUT AT EVERY POSITIVE TRANSITION.

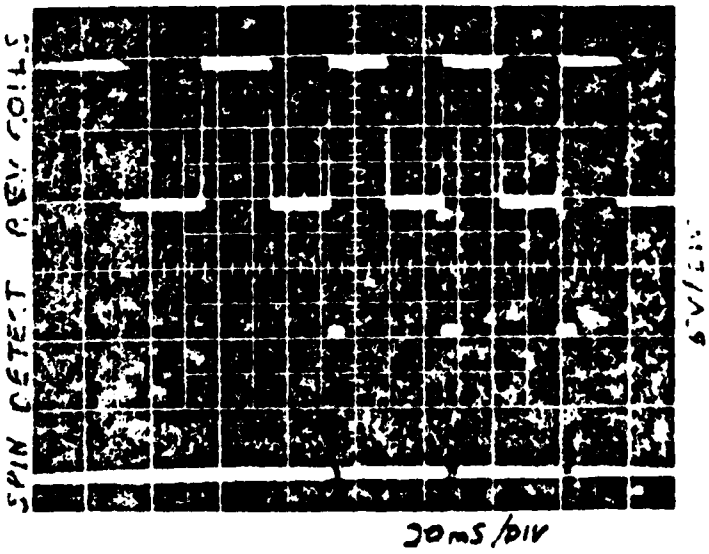

1430 RPM

AT START UP: NO OUTPUT
UNTIL SIGNAL TIMED 1145.0 RPM

FIGURE 12

FIGURE 19

JAN SETBACK DISCRIMINATOR

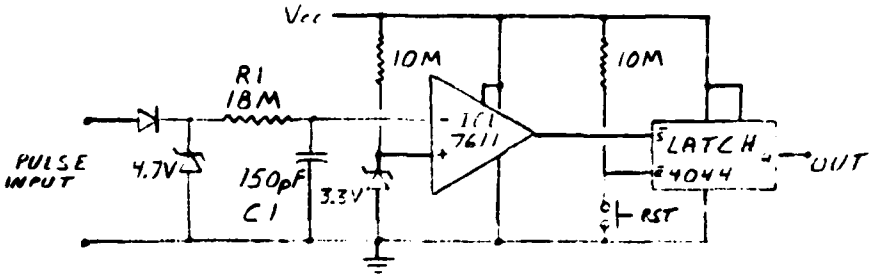

msec. was considered all arm while a pulse less than 0.5 msec. was considered no arm.

Testing of the setback sensor involved testing of the piezoelectric assembly on two shock machines and also testing of the electronic discriminator. The results from shock tests using a piezoelectric crystal (.132" x .2" dia.) as a sensing element and a similarly sized weight ran into several problems. The small shock machine in the lab was only able to reach 550 g's for 0.7mS (minimum JAN setback is 600 g's for about 5mS). The results for various g's and durations are shown in Figure 20. The problem of connecting from the crystal to the instrumentation panel seems to have introduced excessive capacitance loading to the system. The solid line on the graph represents the expected output from the crystal with a 150pF load (the crystal's capacitance is only 86pF). Attempts to use the large shock tower, which can reach 30,000 g's, added even more cabling problems, as shown on Figure 20. In both cases the longer pulse widths dropped off significantly from the shorter pulse results.

These problems do not disqualify the sensor, which seems to be working well despite the problems, but do imply that future tests should be conducted only in a more integrated system, such as a P.Z. crystal and discriminator mounted on the shock machine with a battery and a L.E.D. to indicate accepted pulses.

E. Impact Sensor

No development or testing was done with the impact sensor during this program. It is believed that the impact sensor will consist of a piezoelectric sensor, connected by a flexible printed circuit, epoxied in the electronics cavity. The

FIGURE 20

SETBACK PIEZOELECTRIC CRYSTAL OUTPUT VS SHOCK

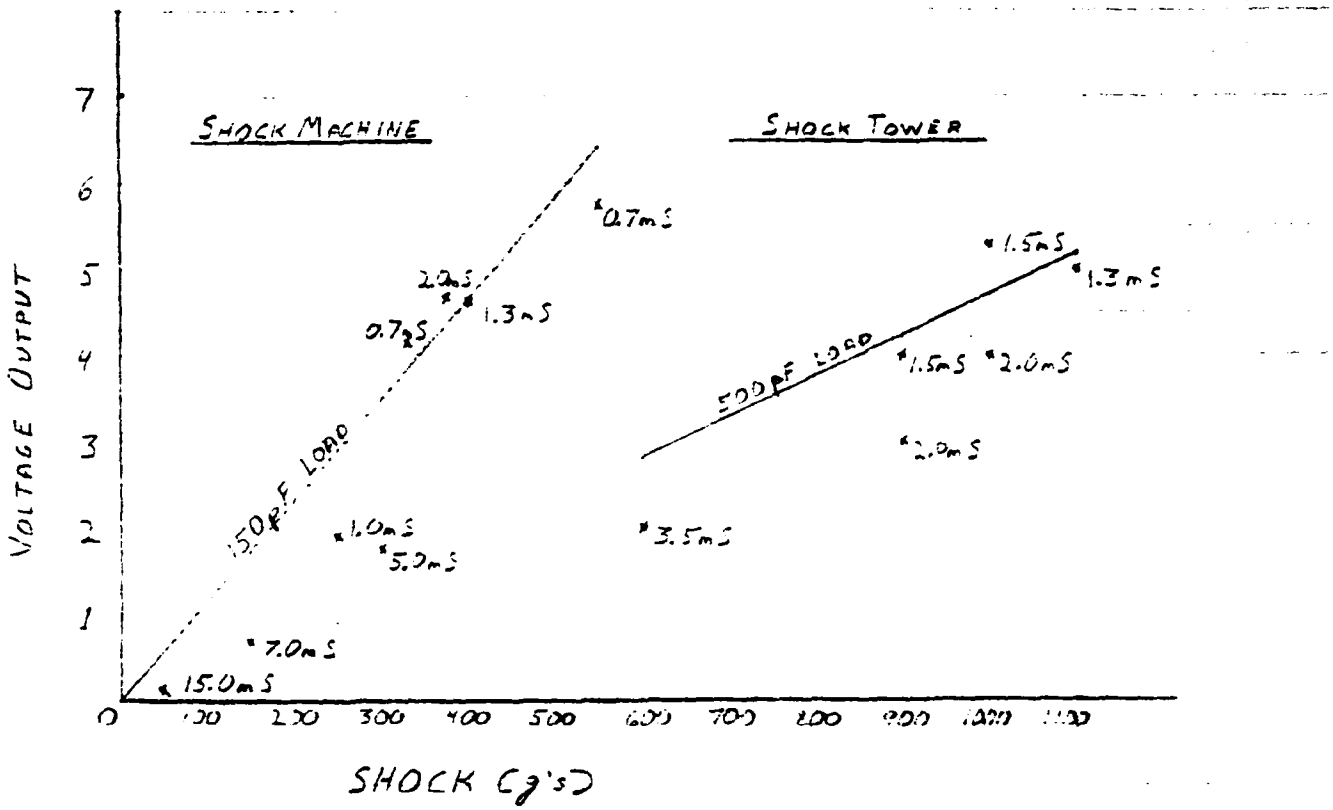

(TIMES INDICATE SHOCK PULSE WIDTHS)

P.Z. sensor will output a pulse train during impact, which will be detected by the SQ/Delay circuit, as described in the System Integration Section of this report.

F. P.D./Delay Circuit

The Point Detonation/Delay Circuit, Figure 21, was built and successfully tested. The P.D. or delay function is set by a selector switch and we located a company, Greyhill, that makes a miniature version of its MIL-S3786 rotary switch titled as "the world's smallest rotary switch." (This is the switch used in the fuze body layouts.)

The PD/Delay subsystem, after being enabled by the S&A circuit, waits for a signal from the piezoelectric impact sensor, which, in the superquick mode, will fire the detonator. In the Auto Delay mode, the delay gate inhibits the detonator fire signal until the impact (shock) signals stop, which indicates the nose of the shell has penetrated the target, and after a short delay ($\sim$ 3 msec) the detonator is initiated.

G. Power Supply

Requirements

Based on the current circuit configuration the power requirements of the system should be:

PD/DELAY SYBSYSTEM LOGIC DIAGRAM

FIGURE 21

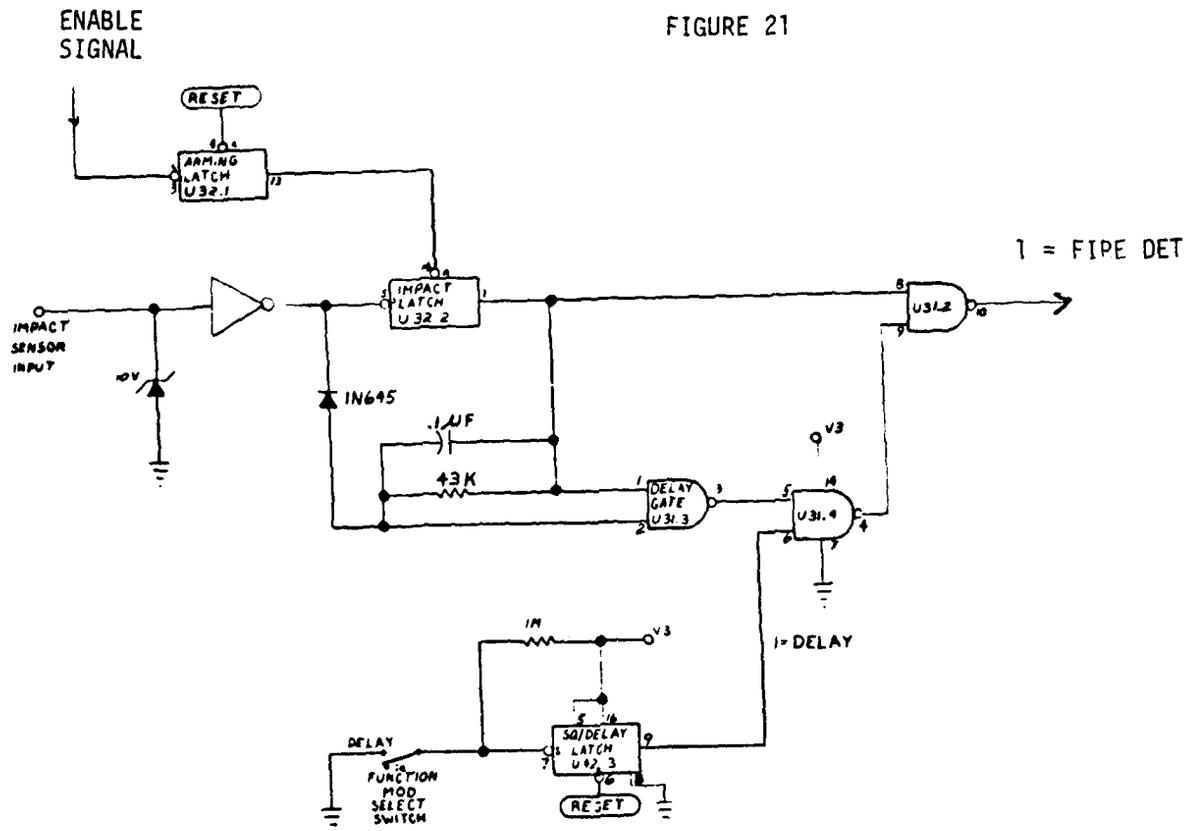

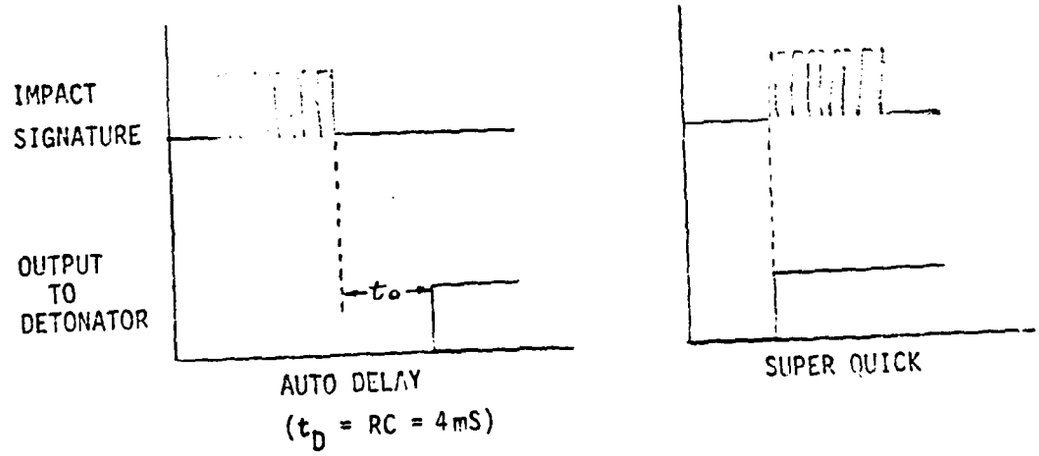

Circuit	V_{cc} (Volts)	I (μA)	t (sec)	e (ergs)
Setback Sensor	5	10	0.5	500
Revolution Counter & Spin Sensor	5	20.5	1.5	1500
Impact/Delay	5	0.25	12.0	$\frac{1500}{3500}$ ergs
Bolts (3) & Detonator	-	-	-	4000 ergs

The power supply will have to charge two capacitor banks for the logic and fire circuits. The logic supply is broken down into three isolated sections, each supplying one circuit area. The size of the supply will depend on the regulation method used. The fire circuits will consist of four isolated capacitors each with 1000 ergs stored on it. Their size will be a function of the initial voltage required by the logic circuits ($C = 2\ E/V^2$, $E = 4000 \times 10^{-7}$ Joules).

To maintain acceptable working voltages to the logic circuits, two approaches are available: regulated and unregulated.

REGULATED (5V)

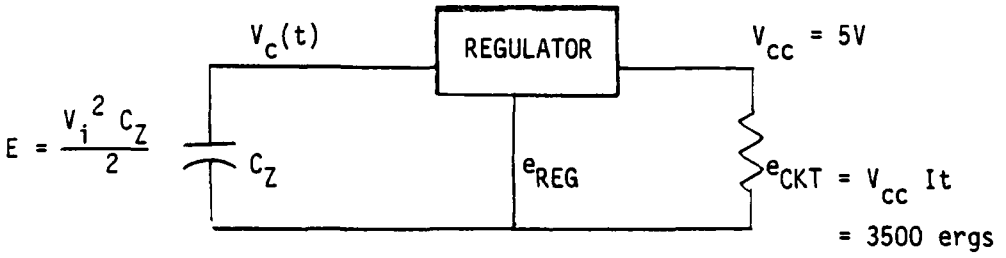

$$V_c(t) = V_i\ e^{-t/r}$$

$$C_Z = C_{CKT} + C_{REG} = \frac{e_{CRT} + e_{REG}}{(V_{cc} (V_i - V_c)}$$

Assuming an average regulator current of $1\mu A$ over a maximum flight time of 120 sec: $e_{REG} = (5)\ (1\mu A)\ (120\ s) = 6K$ ergs. For varying initial levels of $V_c(t)$ the total energy requirements would be:

V_i(volts)	C_{CKT} (μF)	E_{CKT} (ergs)	C_{REG} (μF)	E_{REG} (ergs)	E_{LOGIC} (ergs)
50	1.6	20K	2.7	34K	54K
35	2.3	14K	4	25K	39K
10	14.0	7K	24	12K	19K (min)

V_i(volts)	E_{DETS} (ergs)	C_{DETS} (μF)	$E_T = E_{LOGIC} + E_{DETS}$ (ergs)	$C_T = C_L + C_D$ (μF)
50	4K	0.32	58K	4.62
35	4K	0.68	43K	6.98
10	4K	8.0	23K	46.0

UNREGULATED (V_i decaying to 5V)

$$E = \frac{V_i^2\ C_{CKT}}{2}$$

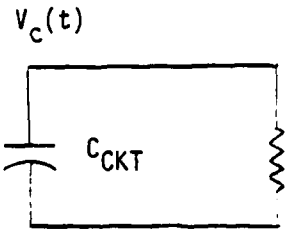

$$C_{CKT} = \frac{e_{CKT}}{5(5V)\ \ln\ (V_i/5V)}$$

$e_{CKT} = 3500$ ergs

The maximum operating voltage for CMOS logic is 18V. For varying initial levels of $V_c(t)$ the total energy requirements would be:

V_i(volts)	$C_{CKT}(\mu F)$	E_{CKT}(ergs)	E_{DETS}(ergs)	$C_{DETS}(\mu F)$	C_T	E_T
18	11	18K	4K	2.5	13.5	22K
15	13	15K	4K	3.6	16.6	19K
12.5	15.3	12K	4K	5.1	20.4	16K
10	20	10K	4K	8.0	28.0	14K
8.25	28	9.4K	4K	12	40.0	13.4K

Reviewing the tables it is clear that the unregulated system requires less energy (ergs) and also requires a power supply capable of charging a relatively large capacitor bank.

Design

The two candidates for the environmental power supply were: 1) a magnetic supply that breaks a magnetic circuit at setback to generate a current in a coil that charges the capacitor bank and 2) a piezoelectric crystal that is powdered at set back to release its charge (Q) which changes the capacitor bank (Q = CV).

The drawback to a piezoelectric supply is that since the charge (Q) available from a given crystal is constant the energy derived from crushing it will decrease directly as a function of C

$$E = \frac{1}{2} CV^2 \qquad Q = CV$$

$$= \frac{1}{2} C \left(\frac{Q}{C}\right)^2$$

$$= \frac{1}{2} \cdot \frac{Q^2}{C}$$

This means that with a standard C-16 piezoelectric disc 0.4 inches in diameter, it should be possible to get 20,000 ergs on a 0.1μF capacitor (200V). The same crystal will only supply 400 ergs to a 5μF capacitor bank (4V). Coupled with the fact that in a minimum setback firing reliably crushing the crystal would be very difficult. The piezo supply was dropped from contention.

The magnetic supply proved more acceptable to our power requirements. Based on ARRADCOM computer simulation (Appendix C) the expected output from a supply using 1000 turns of #38 gauge wire with a 1,000 g sheer plate at a setback force of 1500 g's would be:

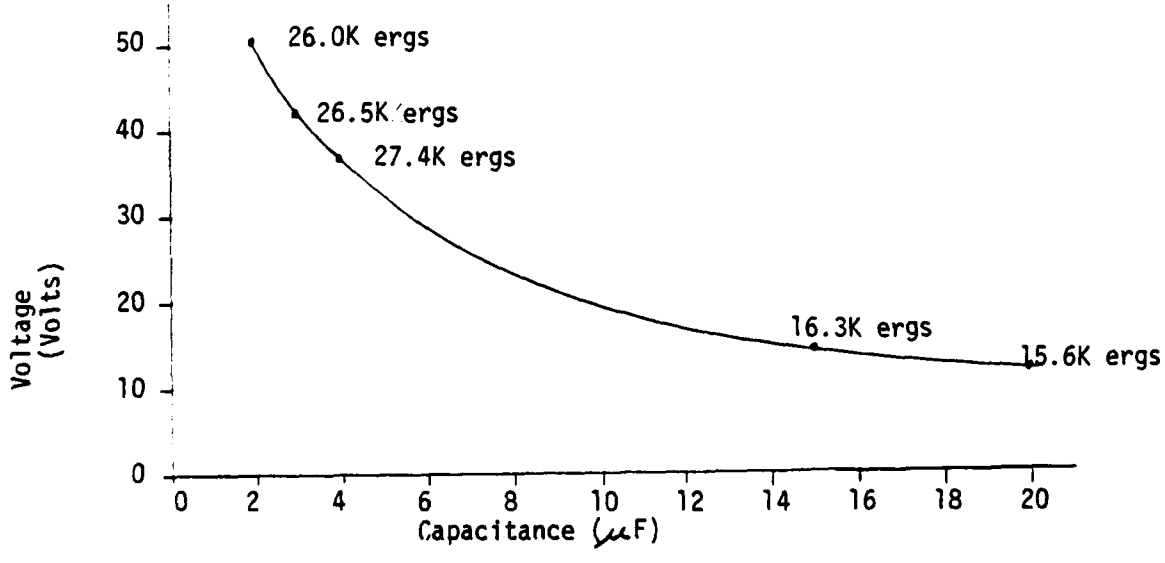

The final data point 12.5V on 20μF of capacitance compared to the projected unregulated system requirement of 12.5V on 20.4μF (16K ergs) indicates that the magnetic supply is a viable power source for the JAN fuze.

H. Explosive Barrier Module (EBM)

The EBM is assumed to be successful so no work was done on it in this program. The EBM major requirements are:

- Each of three interlocking bolts shall be locked in the unarmed position during handling, shipping, storage, jolt, jumble, 40 foot drop, spin to 20,000 rpm, and setback to 30,000 g.

- The bolts shall be interlocked such that bolt No. 1 must be moved first, bolt No. 2 moved second and bolt No. 3 moved last.

- Bolt No. 3 carries the M55 detonator and positions it in the armed position.

- The bolts must be locked in the armed position through the trajectory environment.

- Each bolt is positioned by explosive energy drivers requiring an initiation energy of 500 ergs.

- The fourth explosive energy device, when the EBM is armed, is positioned in line with the M55 and is used to detonate the M55 which initiates the explosive train and the main charge.

- o Bolt No. 3 is red; bolts No. 1 and 2 are green to provide visual armed indicators shown in Figure 22.

The explosive barrier module is being designed with independent electrical connections to each explosive energy device to prevent cross talk. The physical size is compatible with the Electronic JAN PD fuze. The four explosive energy driver bridgewires are applied by thin-film vacuum deposition processes for low cost. The bridge is then coated with the driver charge of lead styphanate. No lead azide is used. Honeywell is presently under contract to demonstrate the feasibility of the EBM.

IV. System Integration

This section will describe how all subsystems and concepts will be integrated to form a working JAN fuze. The packaging will be illustrated and then a discussion of the system electronics will be given.

A. Packaging

Figure 23 shows the JAN fuze configuration. The revolution sensing coils and magnetic power supply will be mounted outside the penetrator and encapsulated, forming the potted ogive. The penetrator cavity will primarily contain the setback sensor, impact sensor, power supply capacitors, and custom I.C. The selector switch, piezoelectric setback crystal, and piezoelectric impact sensor will be connected by flexible printed circuit boards to ease assembly. The Explosive Barrier Module and Booster will mount towards the bottom of the fuze.

FIGURE 22

EXPLOSIVE BARRIER MODULE (EBM)

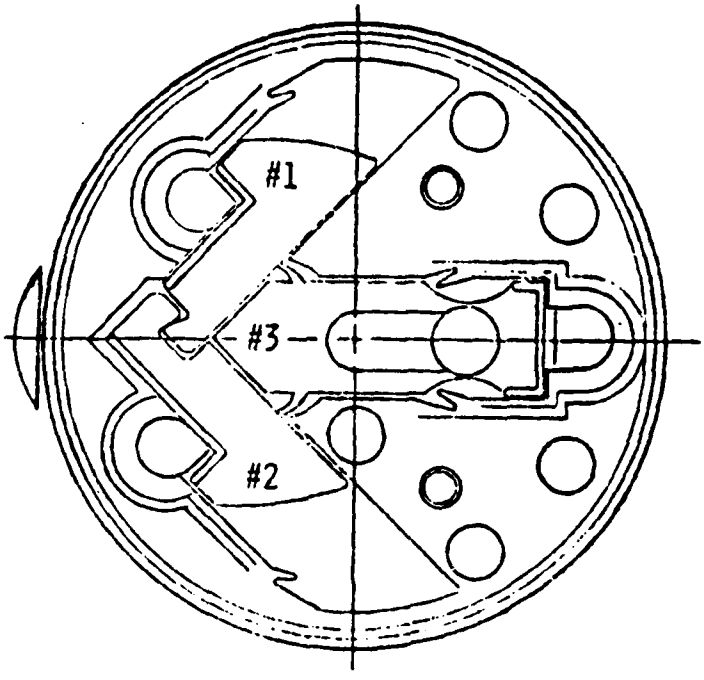

VISUAL CONDITION → GREEN

UNARMED

EBM FUNCTION	ENVIRONMENT
BOLT #1	SETBACK
BOLT #2	RATE OF SPIN
BOLT #3	SAFE SEPARATION
DET	IMPACT/AUTO DELAY

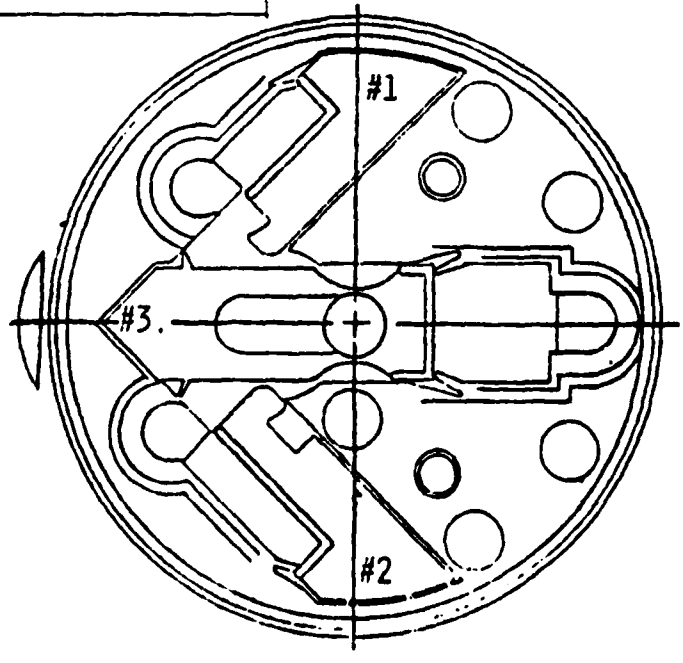

VISUAL CONDITION → RED

ARMED

FIGURE 23

JAN ELECTRONIC P.D. FUZE

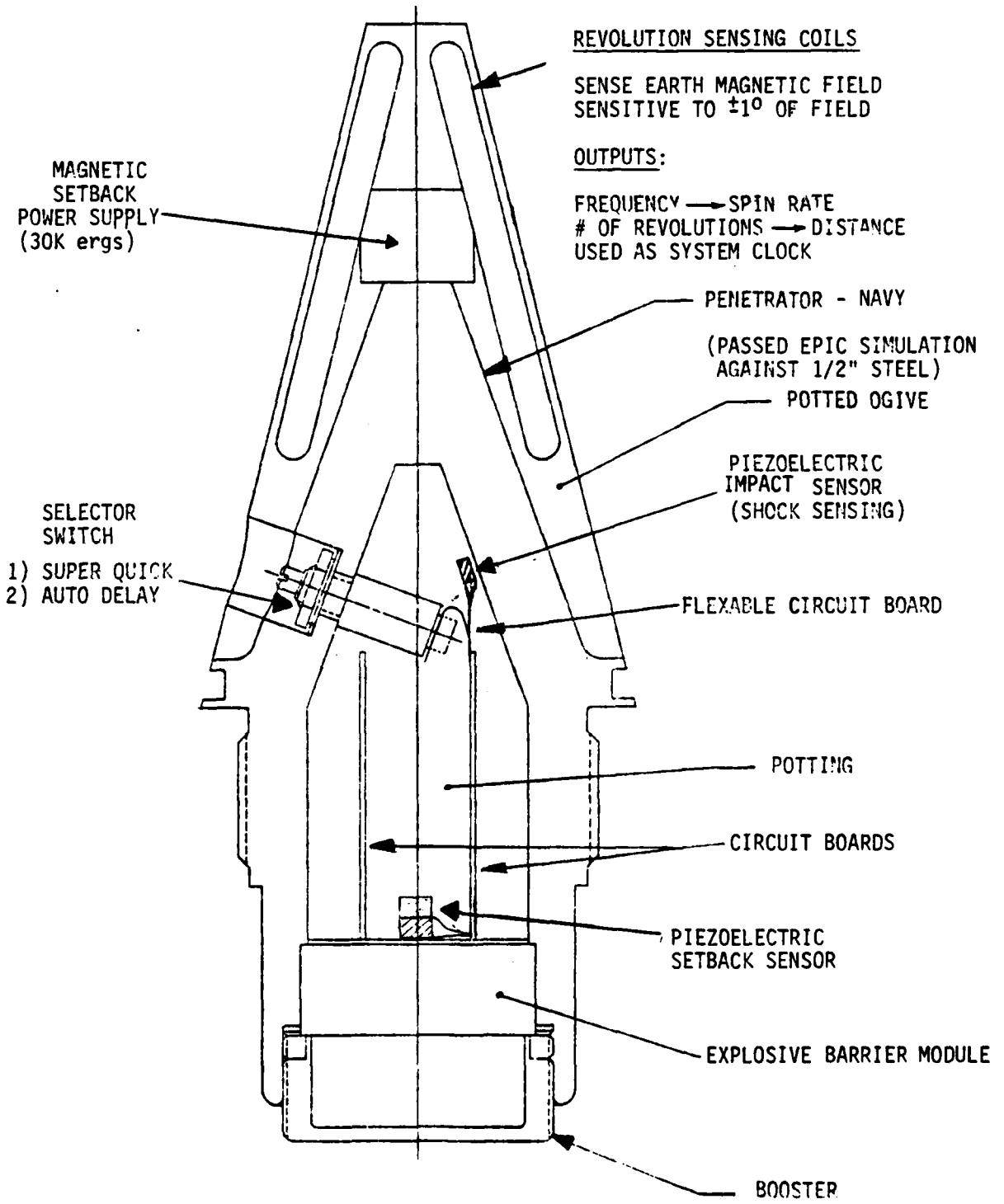

Two models were built to show the proposed packaging and they are shown in Figure 24 and Figure 25.

B. Circuit Operation

A breadboard display circuit, Figure 26, was built and successfully tested. This circuit can be modified to a tactical circuit by removing the display circuit and adding a firing circuit which will contain the dets. and separate firing capacitors.

Upon setback, the environmental power supply will be activated causing the power supply/reset circuit to charge several supply capacitors and output a power on reset to initialize all logic. The subsystems will process sensor outputs and transmit information about acceptable environments to the system logic, which will function the EBM and final detonator. The EBM must receive all three signals in proper sequence, or it will not arm the fuze.

Four isolated supplies are created and used so certain subsystems are turned off after functioning, thereby minimizing system energy requirements. Supply V1 is used to operate the setback detection circuit for 0.5 seconds, which will have caused EBM bolt 1 to move within this time, assuming an acceptable pulse was detected. Supply V2 will operate the revolution counter amplifier, revolution counter, and spin rate detector for 1.5 seconds, which is sufficient time to detect an acceptable spin rate, causing EBM bolt 2 to move, and to count the correct number of revolutions, causing EBM bolt 3 to move and the fuze to arm. Supply V3 is used to operate the Super Quick/Auto Delay circuit for 120 seconds, which waits for impact and will output a fire signal to the detonator at initial

JAN Model-figure 25

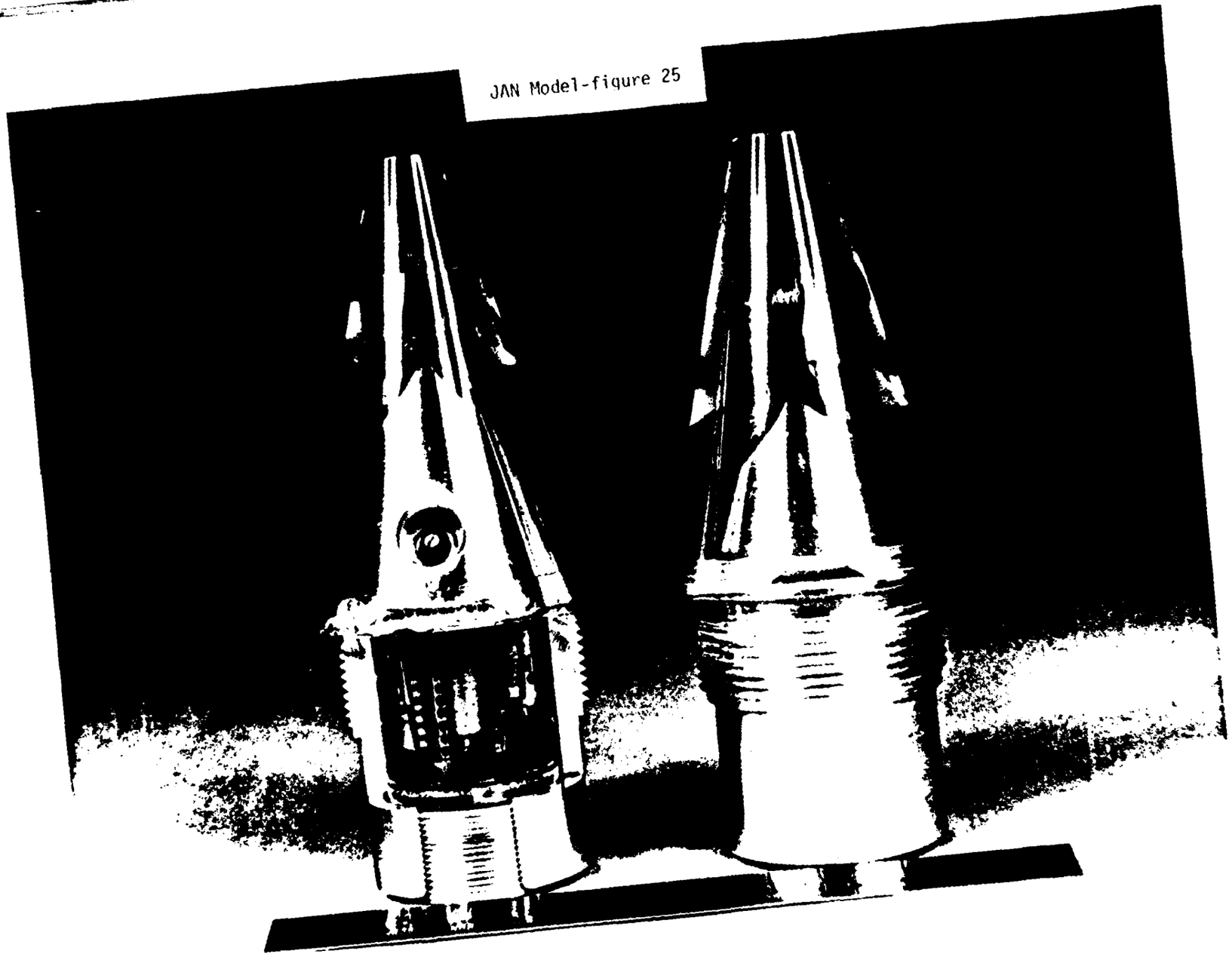

JAN Model-Figure 24

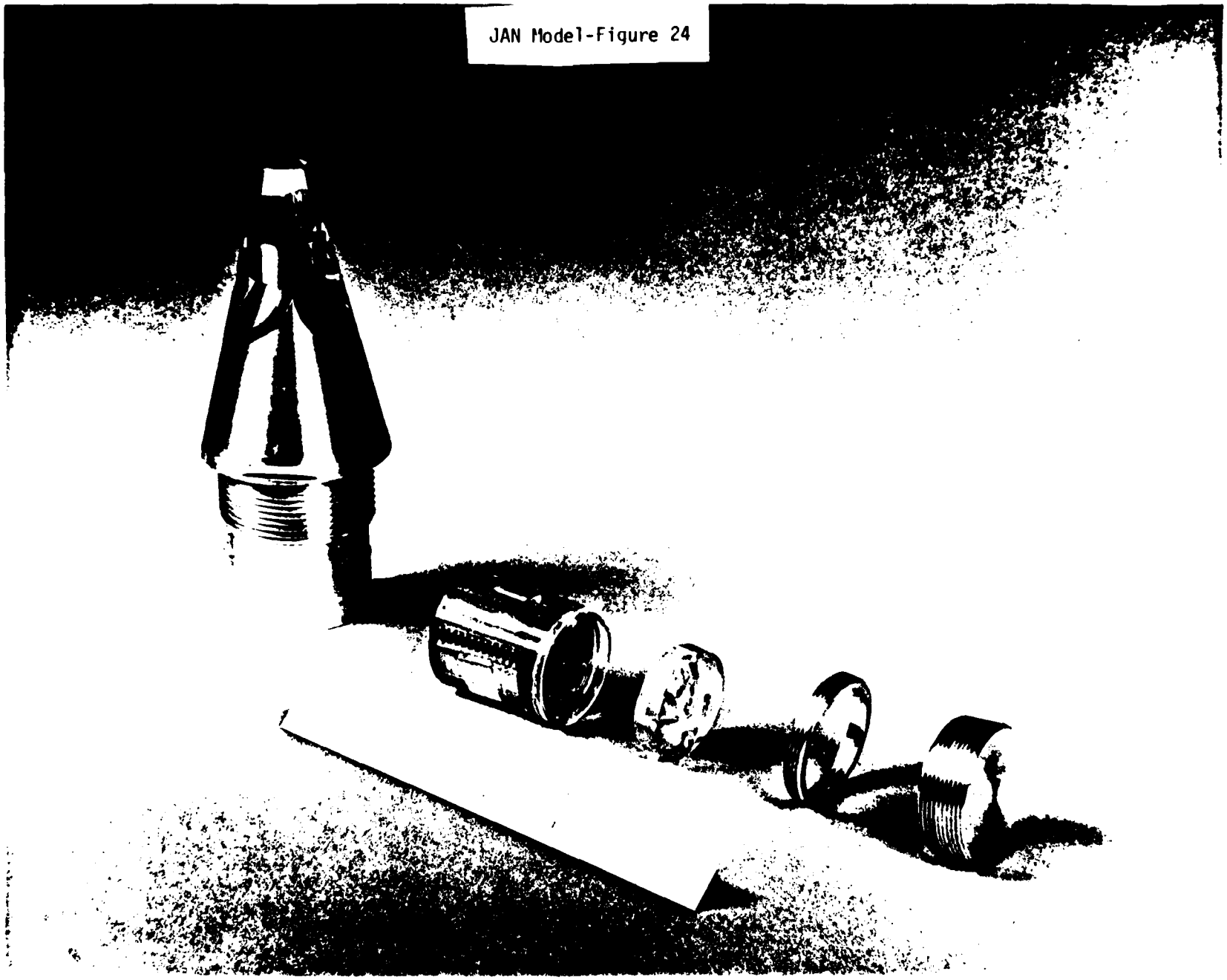

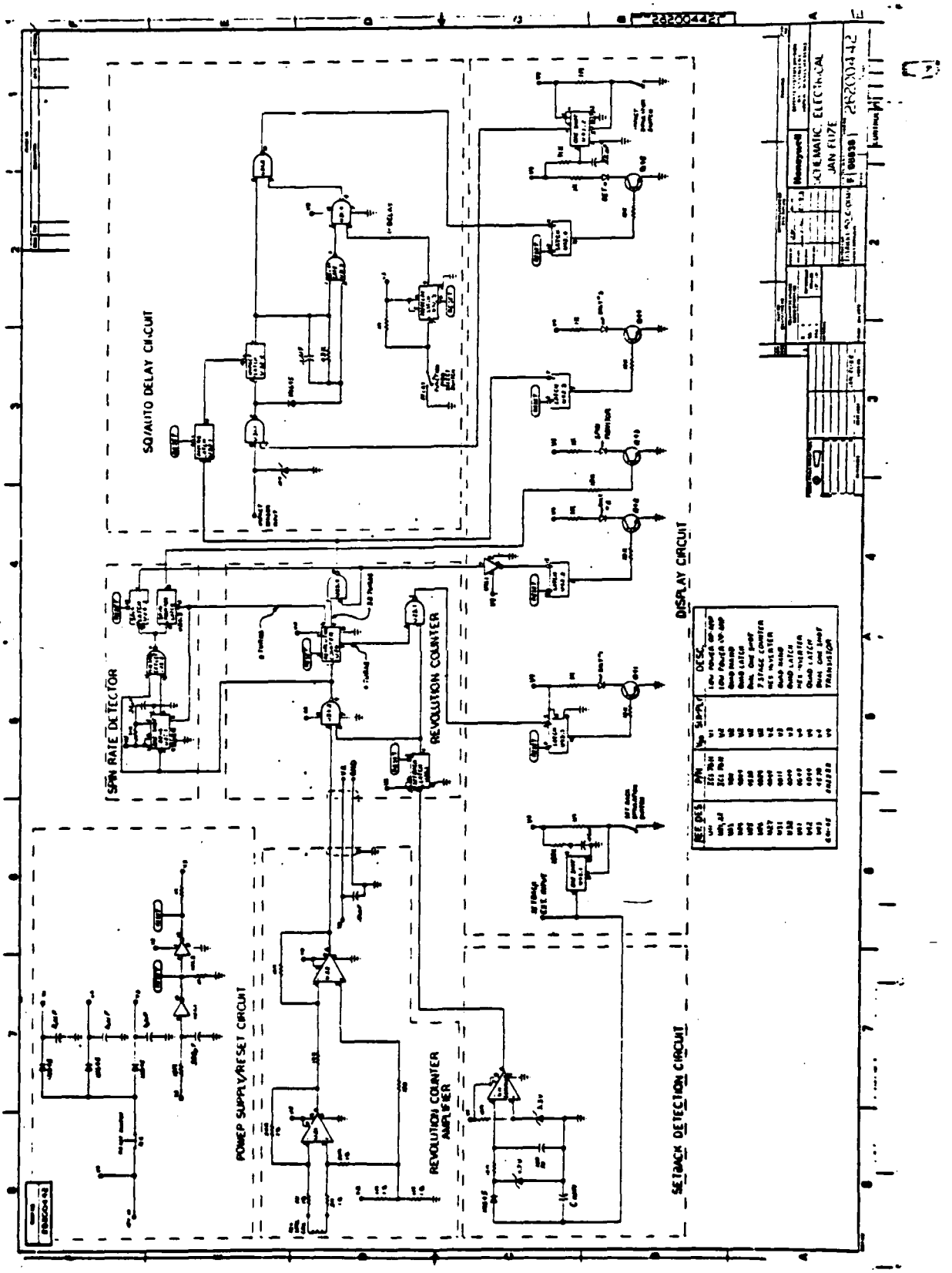
SQ/AUTO DELAY CIRCUIT
SPIN RATE DETECTOR
REVOLUTION COUNTER
DISPLAY CIRCUIT
POWER SUPPLY/RESET CIRCUIT
REVOLUTION COUNTER AMPLIFIER
SETBACK DETECTION CIRCUIT
SCHEMATIC, ELECTRICAL
JAN FUZE
Honeywell

FIGURE 26

impact or after void sensing plus a short delay, as determined by the function switch. Supply V4 is used to operate the LED's in the display circuit, but V4 in the tactical version will consist of four diode isolated capacitors used to fire the three EBM detonators and the main detonator.

The revolution counter is used to count revolutions and to sequence the EBM functioning. The outputs to the EBM are enabled by the revolution counter, which eliminates the possibility of simultaneous EBM bolt movement and thereby gives each bolt sufficient time to stabilize.

V. Reliability and Safety Analysis

A reliability prediction and a safety analysis were performed for the JAN fuze. The reliability study, Appendix D, yielded a .977 predicted reliability. This prediction was reached by evaluating the shock survival reliability and the operational reliability, and the primary conclusion was that the fuze will function if it survives setback.

The Safety Analysis, Appendix E, was conducted by comparing the fuze to MIL-STD-1316B (Safety Criteria for Fuze Design). The fuze design should comply with the intent of MIL-STD-1316B, and it should have a safety failure rate of less than one in a million.

VI. Conclusions and Recommendations

The major emphasis of this program was in the subsystem design and development. An Army and Navy penetrator was designed and run with the EPIC-2 computer simula-

tion program and the Navy version showed no housing deformation with 1/2" steel while the Army penetrator showed noticeable deformation with 4" of concrete. The revolution sensor was made to be sensitive to within $\pm 1^{0}$ of the earth's magnetic field while requiring only 20 micro Amps to function. The proposed piezoelectric spin rate sensor was tested, but good results were not observed, so an alternate spin rate sensor which utilizes the revolution sensor output was designed, tested, and proven.

A piezoelectric setback sensor was tested which yielded ambiguous results, while excellent results were achieved with setback discriminator testing. The Point Detonation/Void Sensing circuit was developed and successfully tested. The piezoelectric power supply was rejected due to insufficient energy output and the magnetic environmental power supply was chosen for the fuze. No testing was done with either the impact sensor or the EBM. The system control logic was developed and built into a demonstration unit which contains LED's to indicate the firing of the three EBM bolts and the main detonator. The reliability prediction is .977 and the estimated safety failure rate is less than one in a million.

Recommendations for further work include additional testing and subsystem development. Further setback sensor testing is needed and it would involve mounting a piezoelectric setback sensor, discriminator circuit, battery, and LED on the shock machine so acceptable pulses would be indicated by the LED. The backup delay for the void sensor should be added to the circuit and tested. Revolution sensor tests could be done where a study would be conducted to determine the minimum number of turns needed in the sensing coils to yield sufficient sensitivity. Further work can be done on the revolution amplifier and system logic to attempt to reduce power consumption and testing should be done to determine if

the system will run off of a typical magnetic supply energy output. Gun firing testing is needed to evaluate the fuze at a system level. A battery would be used to power the electronics for all gun firing tests, which could consist of a soft catch test to evaluate electronic setback survivability and functioning, and/or impact tests to evaluate penetrator performance and impact sensing. Modifications to the penetrator and subsystems would be made as needed, and retesting would be done as time and funding allow.

VII. Appendix A

Magnetoresistive Bridge Sensor

APPENDIX A - MAGNETORESISTIVE BRIDGE SENSOR

Sensor Configuration

The integrated magnetometer sensing element consists of four Nickel-Iron (NiFe) thin film magnetoresistors connected in a bridge configuration as shown in Figure A-1. The magnetoresistive response of the resistor elements is controlled such that R_1 and R_4 increase with an increase in applied H field, and R_2 and R_3 decrease with an increase in applied field. The resultant output signal V_o is proportional to the magnetically induced resistance changes, $(\frac{\Delta R}{R})$, and the bridge bias voltage V_B. Resistors R_1, R_2, R_3, and R_4 are sputter deposited films and have identical temperature, electrical and noise characteristics.

The Magnetoresistive Effect

The operation of the magnetometer is based on the fact that the resistance of a single thin film NiFe resistor is a function of an applied magnetic field. This magneto-resistive phenomena is explained by considering a simple element of thin film NiFe as shown in Figure A-2. The vector $\vec{M}$ represents the "easy axis" magnetization of the sample as established by the deposition process and the element geometry. The voltage, V, results in a current vector $\vec{I}$ that is parallel with $\vec{M}$. The magnitude of $\vec{I}$ is of course related to the resistance, R_o of the thin film element along the direction of $\vec{I}$. When an external magnetic field, $\vec{H}$, is applied normal to $\vec{I}$ and $\vec{M}$, the resultant magnetization vector $\vec{M}'$, is rotated from the current vector $\vec{I}$ by some angle θ. $\vec{M}'$ is a function of $\vec{H}$ and the demagneticizing forces within the element. The element resistance with the application of $\vec{H}$ is given by:

$$R = R_o + \Delta R$$

$$\text{and } \Delta R = \Delta R_m (1-\cos^2\theta)$$

where: R_o = resistance of element with H = 0

ΔR_m = maximum resistance change – typically 2-3 percent of R_o

The static transfer function of a typical element is shown in Figure A-3. The response is quite nonlinear near the origin and also near the saturation point at $\theta = \pm \pi/2$ radians.

The region from $\theta = \frac{\pi}{8}$ to $\frac{3\pi}{8}$ is nearly linear and also provides the area of greatest sensitivity. These desirable characteristics can be realized by magnetically biasing each magnetometer bridge element to operate about point A. The biasing scheme used in the integrated magnetometer is discussed below.

Biased Magnetometer

The quiescent operating point of the integrated magnetometer can be achieved by controlling the initial angle between $\vec{I}$ and $\vec{M}'$. This angle is achieved by placing a thin film permanent magnet over resistor elements that are oriented $\pi/4$ radians with respect to the bias field and the sensitive axis of the magnetometer as shown in Figure A-4. The resistor elements are processed with the magnetization vector $\vec{M}$ parallel with the resistor longitudinal body axis, which is in turn skewed $\pi/4$ radian with the bias field $\vec{H}_B$. The $\vec{H}_B$ is selected such that the resultant magnetization vector M' is $\pi/4$ radian with respect to $\vec{I}$, and normal to the device input axis. Magnetic fields along the input axis will cause $\vec{M}'$ to rotate away from $\vec{I}$, (increasing θ) causing element A to increase in resistance. The same signal will cause $\vec{M}'$ to rotate toward $\vec{I}$ (decreasing θ) in element B resulting in a decrease in resistance. The integrated biased magnetometer uses several series connected elements oriented such that R_1 and R_4 increase and R_2 and R_3 decrease with input signals. This configuration, shown in Figure A-5 provides a bridge that is biased at the optimum point for linearity and sensitivity and also makes all four resistors active. Sensitivities of 0.5 mV/oersted/volt are typical with this arrangement (3mV/oersted at 6.0 volts V_B).

The power consumption of the bridge can be controlled by the bridge insertion resistance R_i. R_i is in turn controlled by the thickness, length and width of the NiFe films. The limiting factor on large values of R_i is

due to the degradation of the magnetic properties of very thin, narrow elements. Values of R_i in the 100 K ohm range are feasible and are currently under evaluation at Honeywell.

Preliminary results indicate that the magnetoresistive bridge (MRB) will be able to meet the following specifications:

Linearity: 5 percent over 0.001 to 1.0 Orsteads

Temp. Sensitivity: ±2.5 percent over -40°C to +55°C

This represents significant improvement over existing magnetometers.

NOTE:

The above is taken from "Design and Fabrication of a Digital Magnetometer Compatible with the Improved CHOS Hybrid Microcomputer" Unclassifed Document No. 45551-1.

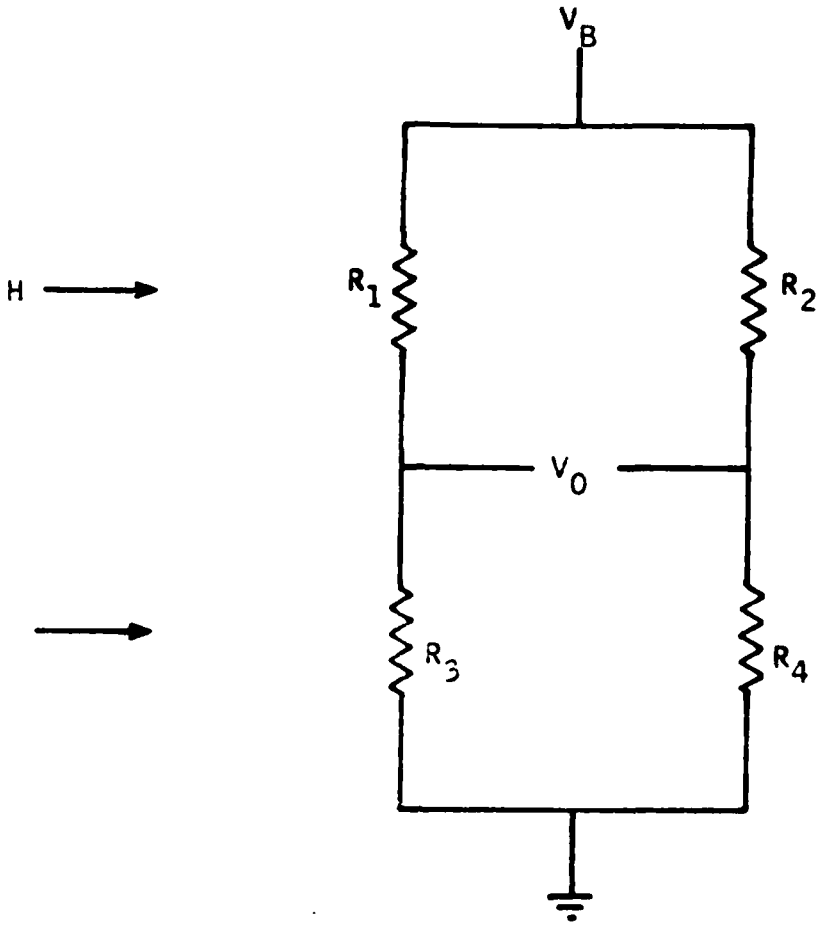

Figure A-1 Sensor Configuration

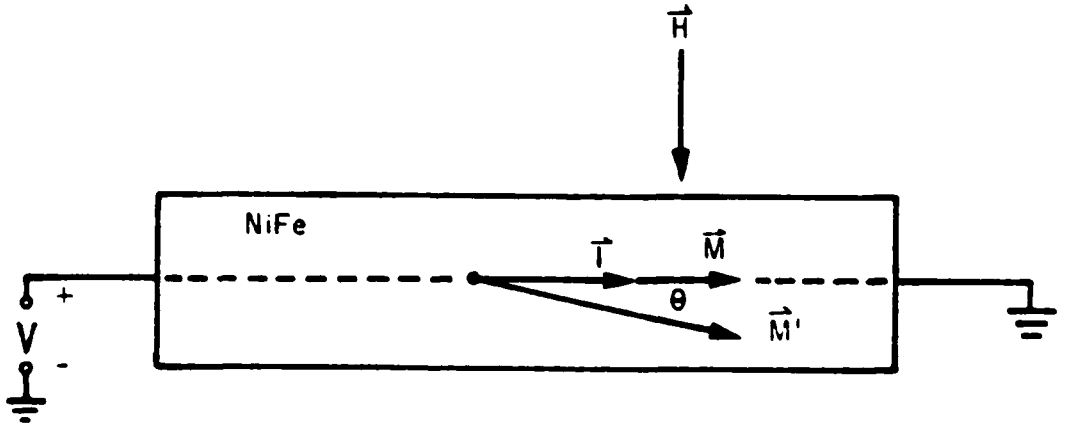

Figure A-2 Elementary NiFe Magnetoresistor Element

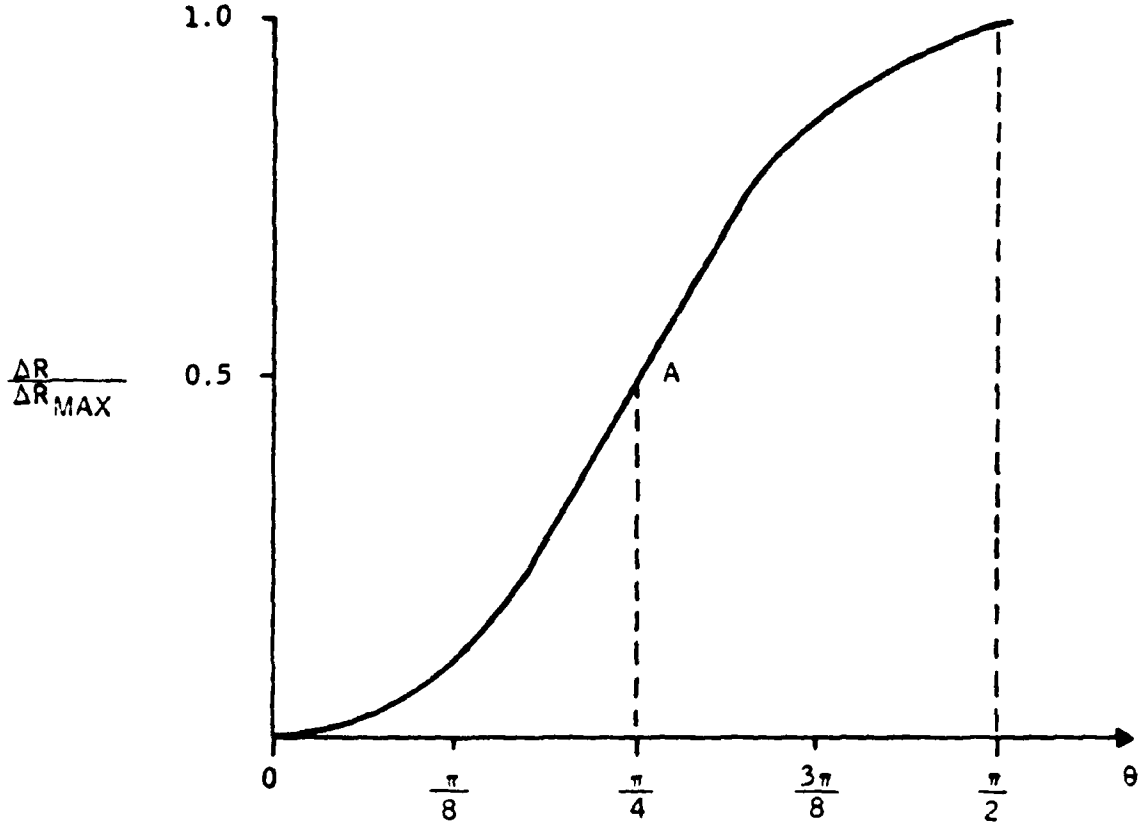

Figure A-3 Magnetoresistor Static Transfer Characteristic

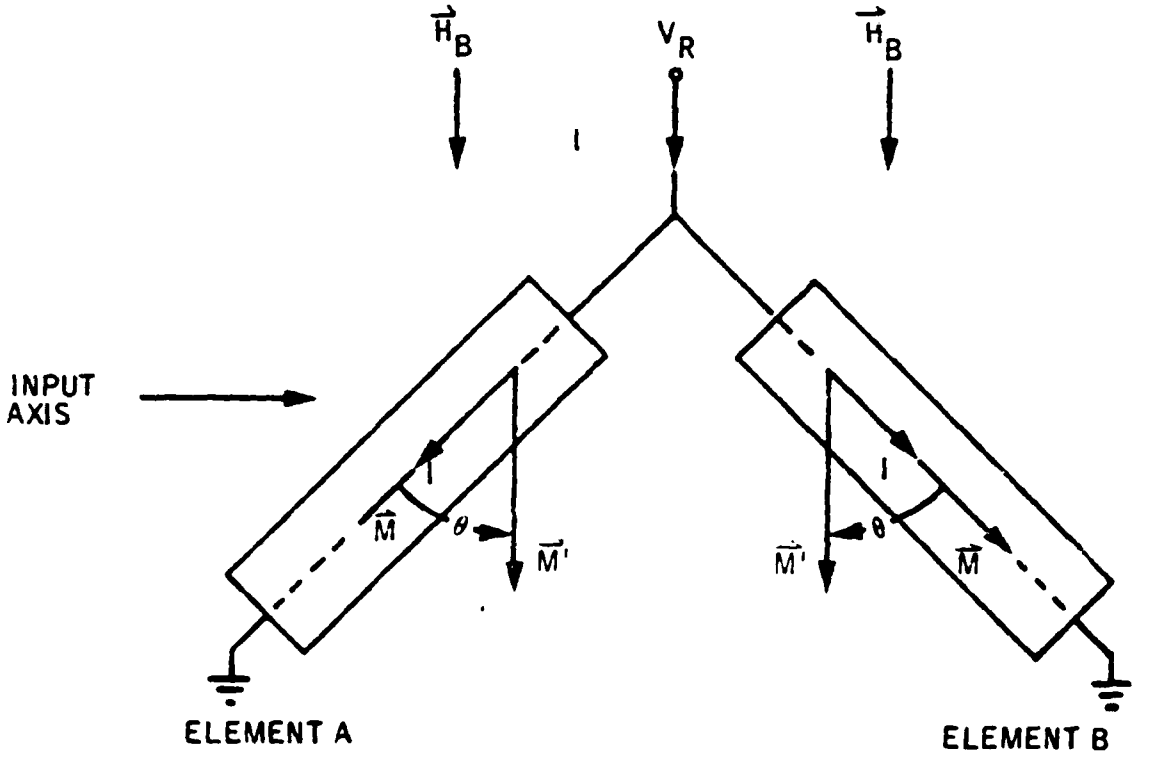

Figure A-4 Integrated Magnetometer Biased Configuration

VIII. Appendix B

Theoretical Studies

Properties of P.Z. Materials for Spin Sensing Applications

Spin Sensors

The proposed spin sensor consists of a mass (M) compressing a piezoelectric crystal to produce a voltage (V) proportional to the spin rate (X).

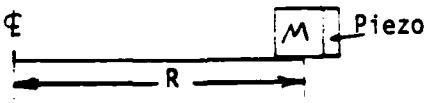

$$(1)\quad V\ (\text{volts}) = \frac{4\pi^2\ R\ (m)\ X^2\ (RPS)^2\ M\ (Kg)\ d_{33}\ (C/Nt)^*}{C_{piezo} + C_{external}\quad (F)}$$

The piezoelectric properties of the crystal are:

d_{33} in colombs/newtons $\quad \in$ in F/m or C/mV

$C_{piezo} = \in A/l$

The effective spin radius R will be at the center of the mass (M). It is assumed that for maximum output the piezo will always be mounted at 0.625 inches from spin center. This leads to:

$$(2)\quad R = .625 - l_{piezo} - l_{mass} / 2$$

The simplest assembly would consist of a mass and crystal of equal diameters epoxied together and mounted on the PW Board like a standard component. The reason for keeping the diameters equal is to prevent interference from the potting compound. Under this condition the radius factors cancel out, leaving the voltage at a particular RPM to be:

$$(3)\quad V = KR\ l_m\ l_x$$

K = Constant

R = Spin radius = $.625 - l_x - l_m /2$

l_x = Piezo length

l_m = Mass length

Evaluating this equation shows that for any length piezo (l_x), the maximum voltage will result at: $l_m = .625 - l_x$

and the optimum lengths are: l_m = 0.417 in.

l_x = 0.208 in.

For example: a piezo with the properties

d_{33} = 350 pC/Nt
ϵ = .0142 μ F/m
l_x = .208 in.

and a mass with the properties
M/Vol = 7530 Kg/m^3 (steel)
l_m = .417 in.

V(1700 RPM) = 1.7 volts
V(1100 RPM) = 0.73 volts

The voltage could be increased proportionally by using a denser mass like brass or lead.

Honeywell C-16 Army All Arm

1.7 00	=V
1. 03	=RPM
209.0-03	=RAD
0.0 00	=C-S
831.4-06	=ERG
100.0-03	=R-X
417.0-03	=L-M
208.0-03	=L-X

Army No Arm

731.5-03	=V
1.1 03	=RPM
209.0-03	=RAD
0.0 00	=C-S
145.7-06	=ERG
100.0-03	=R-X
417.0-03	=L-M
208.0-03	=L-X

For the Navy version a 330pF external capacitor can be added to compensate for the higher RPM levels

V(4500 RPM) = 1.7 volts
V(3000 RPM) = 0.77 volts

Navy All Arm

1.7 00	=V
4.5 03	=RPM
209.0-03	=RAD
330.0-12	=C-S
5.8-03	=ERG
100.0-03	=R-X
417.0-03	=L-M
208.0-03	=L-X

Navy No Arm

770.9-03	=V
3.0 03	=RPM
209.0-03	=RAD
330.0-12	=C-S
1.1-03	=ERG
100.0-03	=R-X
417.0-03	=L-M
208.0-03	=L-X

C-External

Radius-Xtal

DERIVATION OF SPIN SENSOR EQUATIONS

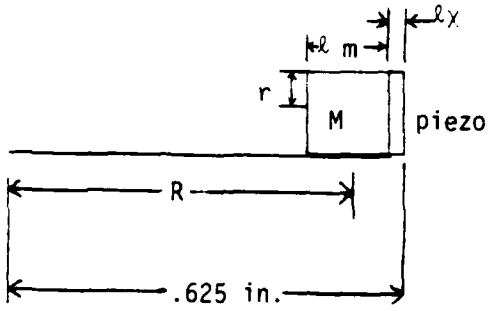

Piezoelectric Constants

d_{33} Coulombs/N_t

ε Farads/m^2

$$V_{out}\ (\text{Volts}) = \frac{Q}{C} = \frac{F\ (N_t)\ .d_{33}\ (C/Nt)}{C_{total}}$$

$$F = Ma = M\cdot\left[\frac{\text{Velocity}^2}{R}\right]\cdot\left[M\ \frac{(2\pi\ R(m)\ \overline{X}\ (RPS)\ )^2}{R\ (m)}\right]$$

$$C_{total} = C_{piezo} + C_{external} = \frac{\varepsilon\pi\ r^2}{\ell x} + C_{external}$$

$$(1)\quad V\ (\text{Volts}) = \frac{4\ \pi^2\ R\ (m)\ \overline{X}^2\ (RPS)^2\ M(Kg)\ d_{33}\ (C/Nt)}{C_{piezo}\ +\ C_{external}}$$

M = Vol . Density = $\pi r^2\ \ell_m$. 7530 (Kg/M^3) Steel

For $C_{external} = 0$

$$V = \frac{4\ \pi^2\ R\ \overline{X}^2\ (\pi r^2\ \ell m\ .\ 7530)\ d33}{\varepsilon\pi r^2/\ \ell\chi}$$

$$= \frac{(4\ \pi^2\ .\ 7530\ d33)}{\varepsilon}\cdot\ \overline{X}^2\ (R\ \ell m\ \ell\chi\ )$$

<u>For a given $\overline{X}$ (RPS):</u>

V = Constant . ($R\ \ell m\ \ell\chi$)

The effective Spin Radius (R) will be at the center of the mass (M)

$$(2)\quad R = .625 - \ell\chi\ -\ \ell m/2$$

$$(3)\quad V = K\cdot R\cdot \ell m\ \ell\chi\ = K\cdot\left[.625 - \ell\chi\ -\ \ell m\ /2\right]\cdot \ell m\ \ell\chi$$

$$= K\left[.625\ \ell m\ \ell\chi - \ell m\ \ell\chi^{\ 2} - \ell\chi\ \ell m^2/2\right]$$

To find the optimum ℓ m for a given ℓ_χ

$$\frac{dV}{dL_m} = .625\,\ell_\chi - \ell_\chi^2 - \ell_\chi\,\ell m = 0$$

$$.625 - \ell_\chi - \ell m = 0$$

$$\ell m = .625 - \ell_\chi$$

To find the optimum system let $\ell m = .625 - \ell_\chi$

$$V = K\,R\,\ell_m\,\ell_\chi = K\left(\ell m/2\right)\left(\ell_m\right)\left(.625 - \ell m\right)$$

$$= (K/2)\left(.625\,\ell_m^2 - \ell_m^3\right)$$

$$\frac{dv}{d\,\ell m} = K/2\left[1.25\,\ell m - 3\,\ell m^2\right] = 0$$

$$1.25\,\ell m = 3\,\ell m^2$$

$$\ell m = 1.25/3 = .417 \text{ in.}$$

$$\ell_\chi = .625 - \ell m = .208 \text{ in.}$$

POWER SUPPLY ANALYSIS

A) Power Supply Requirements

For a loss less system:

$E = 1/2\ A+^2\ C$

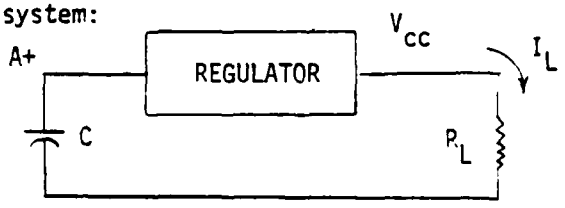

$e = V_{cc}\ I_L\ t$

The relationship between the energy (e) required by the circuit and the energy(E) that must be stored on the power supply capacitor (C) will be:

$$(1) \qquad \frac{e}{E} = 2\,\frac{V_{cc}}{A+}\left[\,1-\frac{V_{cc}}{A+}\right]$$

A trade-off of choices between A+ and C occurs since for a minimum E: $A+ = 2V_{cc}$, $E_{min} = 2e$ (2) but capacitance is inversely proportional to $A+ - V_{cc}$

$$C = \frac{e}{V_{cc}\,(A+ - V_{cc})} \qquad (3)$$

so for small values of A+, C becomes very large increasing both size and cost. The optimum value for A+ will depend on the amount of energy available from the power supply and the volume available for the capacitors. Until this can be determined a supply voltage of 50V will be used.

To get a first estimate of the system's power requirements the basic circuit diagram shown in Figure 1-1 will be used. For this estimate the current required by the logic gates will be assumed to be 10 times the typical room temperature performance quoted in Motorola's current CMOS data book. Under those assumptions with a regulated voltage (V_{cc}) of 5V and a supply voltage (A+) of 50V the minimum energy required (E) will be:

	E	C
Spin/Setback (20μA) (0.5 sec)	2.8 K ergs	.22μ F
Revolution Count (20.2μA) (1.5 sec)	8.4	.67
Impact/Delay (0.25μA) (120 sec)	8.3	.67
Firing Energy -4 Detonators	4.0	.32
	23.5 K ergs	1.88μ F

When account is taken for sequencing circuitry, regulator and capacitor losses, and part tolerances an additional 75% to 100% will probably be required bringing the totals to 40 to 46 K ergs and 3.2 to 3.7μ F.

B) Capacitor Leakage

For a capacitor (c) with a known leakage resistance (R_L) the energy remaing (E_F) after a length of time (t) will be:

$$(4)\ 5 \cdot \left[(A+)\, e^{-t/R_L c}\right]^2 \cdot C = E_F \text{ (ergs)} \qquad \begin{matrix} c \text{ in } \mu F \\ R_L \text{ in M} \end{matrix}$$

The energy for the final detonator must be sufficient to reliably detonate after a maximum flight time of 120 sec. Table 1 shows how increasing leakage current effects the total energy requirements based on the basic circuit previously analyzed.

The trade-off is that the lower I_L capacitors are larger and more expensive than the leakier parts. The problem with the leakier parts is, obviously, that they require more initial energy. From the tables it can be seen that very low leakage parts will be needed for the final detonator and the impact circuits. How much leakage can be tolerated in the other systems will depend on the total power available and the actual power requirements of the system.

FIGURE 1-1

BASIC JAN CIRCUIT WITHOUT CONSIDERATION OF

RESET OR SEQUENCING REQUIREMENTS

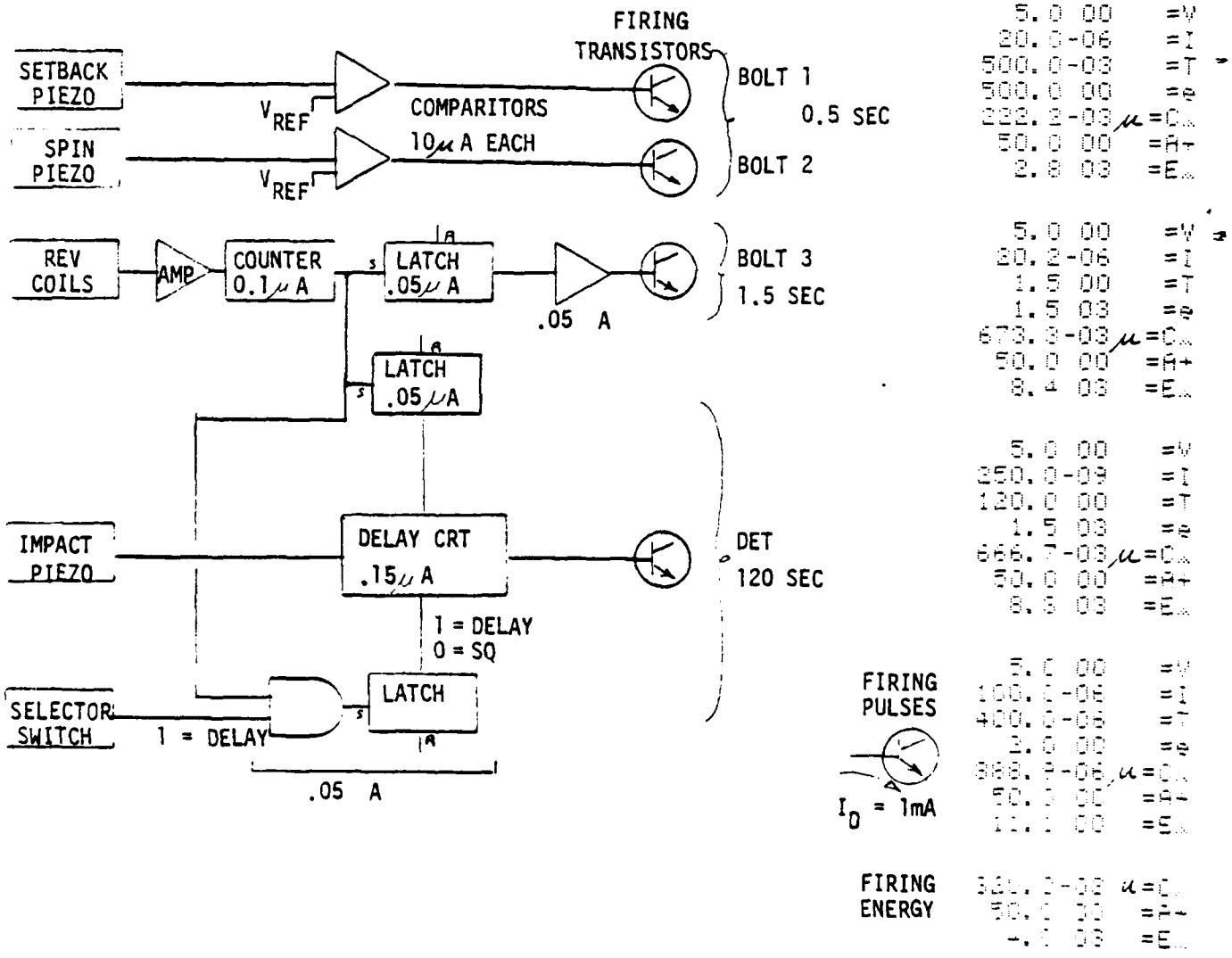

TABLE 1

ENERGY REQUIRED TO COMPENSATE FOR CAPACITOR LEAKAGE

	MIL-C- I_L at 100°C	POLY-CARBONATE 83421 5 n A	MYLAR 55514 100 n A	TANTILUM SOLID 5 μA	
BOLT 1 & 2	1000 ergs	1000	1000	1900	ergs
.5 sec.	.08 μF	.081	.083	.15	μF
BOLT 3	1000 ergs	1000	1100	3200	ergs
1.5 sec.	.08 μF	.081	.085	.26	μF
DETONATOR	1000 ergs	1300	4200	70,500	ergs
120 sec.	.08 μF	.11	.33	5.6	μF
IMPACT/DELAY CKT	10,000 ergs	10,300	15,000	120,000	ergs
120 sec.	.8 μF	.83	1.2	9.7	μF

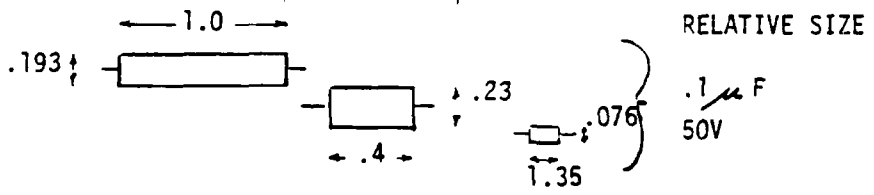

DERIVATION OF POWER SUPPLY EQUATIONS

$V_C(t=t') = V_{cc}$

$V_C(t=0) = A^+$

$E+\frac{1}{2}CA^{+2}$

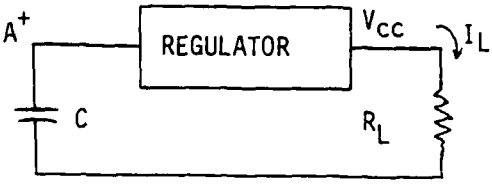

$e = V_{cc} I_L t'$

$$\frac{e}{E} = \frac{Vcc\ I_l\ t'}{\frac{1}{2}\ A^{+2}\ C} = \frac{Vcc\ \dfrac{C(A^+ - Vcc)\cdot t'}{t'}}{\frac{1}{2}\ A^{+2}\ C}$$

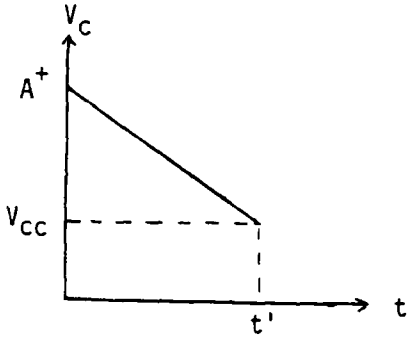

(1) $$\frac{e}{E} = \frac{2\ Vcc}{A^{+2}} \cdot (A^+ - Vcc) = \underline{\underline{2\ \frac{Vcc}{A^+}\ \left(1 - \frac{Vcc}{A^+}\right)}}$$

SOLVING FOR $\frac{e}{E}$ MAX:

$$\frac{d\ e/E}{d\ Vcc/A^+} = 2 - 4\ \frac{Vcc}{A^+} = 0$$

$$I_L = -C\ \frac{dV_C}{dt} = \frac{C(A^+ - V_{cc})}{t'}$$

(2) $$A^+ = 2\ Vcc$$

$$\underline{\underline{E\ min = 2e}}$$

SOLVING FOR C AS A FUNCTION OF e AND A+

$$e = VccI_L\ t' = Vcc\ \frac{C(A^+ - Vcc)}{t^+}\ t+$$

(3) $$C = \frac{e}{\underline{\underline{Vcc\ (A+ - Vcc)}}}$$

IX. Appendix C

ARRADCOM Magnetic Power Supply Computer Simulation

Subject:

Analysis of the M509A2 magnetic setback generator for use in the JAN PD Fuze.

Background:

A magnetic setback generator in one method being considered to generate the power required for the fuse. ARRADCOM was requested to run the computer model of the generator developed for the M509A2 fuze to ascertain if it will supply sufficient energy for the JAN PD fuze application. The capacitor loads requested were 2, 3 and 4 ufds. The 155 mm gun, zone 1, was used as a typical low g forcing function. Figure 1 shows a cross-sectional view of the M509A2 magnetic setback generator.

Laboratory Evaluation

The generator was tested in the laboratory by placing it in a fixture and driving the gap open by means of a hammer blow. The gap opening time was measured at approximately .24 milliseconds. The capacitor values tested were 2, 3 and 4 ufds and the voltage for each case was recorded on a storage oscilloscope. This condition was simulated in the computer model by using a table that linearly opens the gap in this time frame. Plot 1 shows the gap opening programmed. Plots 2, 3 and 4 show the predicted and recorded voltages for each case. As indicated, good correlation was obtained for all cases.

Gun Environment

Plot 13 shows the acceleration profile used as a forcing function in the computer model that calculates the gap opening. It was obtained from the "Heppner" report. The results of their model are shown on Plots 5A to E. The Plots are self-explanatory and the predicted output (Plot 5D) is approvimately 28 volts.

If a shear plate is added to the generator so that the gap would start to open at a higher acceleration level the gap would open faster and a higher voltage should result. A 1,000 g shear plate was added to the model simply by adding a 4.9 pound factor to the PFA term. The force was added in the form of a table that goes from 4.9 pounds to zero in approximately 20 usec. The results of this model are shown on Plate 6A to E. As indicated by the plate, the gap opens later in time and faster. The predicted voltage output (Plot 6D)

goes up to approximately 30 volts, an increase of about 2 volts. Plots 8 and 9 shows the output voltage for this model for a 3 and 2 ufd capacitor load.

Coil Modification

It was felt that more voltage would be obtained on these large values of capacitors if the coil resistance was lowered. Therefore the gun environment model, with shear plate, was modified to reflect a coil with 500 turns of NO. 35 wire. The out-put voltage for this model is shown on Plot 9 and indicates no increase in voltage. The model was rerun with a 1000 turns of NO. 38 wire coil. The results for a 4, 3, and 2 ufd capacitor load are shown on Plots 10, 11, and 12. As indicated an increase in voltage output did occur. A summary of the predicted output voltages for two coils and three capacitor load as well as the stored energy are shown of Plots 14 and 15.

Conclusions

For the larger values of capacitors required for the JAN PD Fuze more energy is supplied by the generator if the number of turns are reduced from 2,000, of number 41, to 1,000 turns of number 38 wire. The increase in voltage and stored energy are shown on Plots 14 and 15. The peak energy is 27.3 ergs (37 volts on a 4 ufd capacitor).

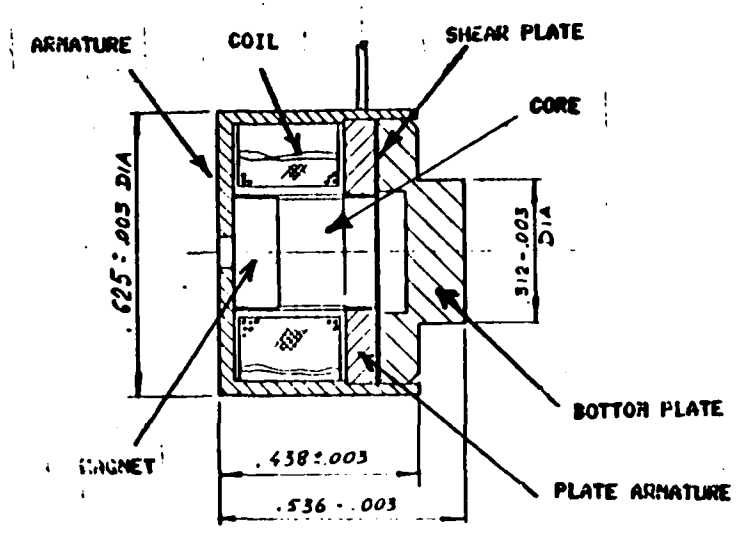

FIGURE 1 MAGNETIC SETBACK GENERATOR

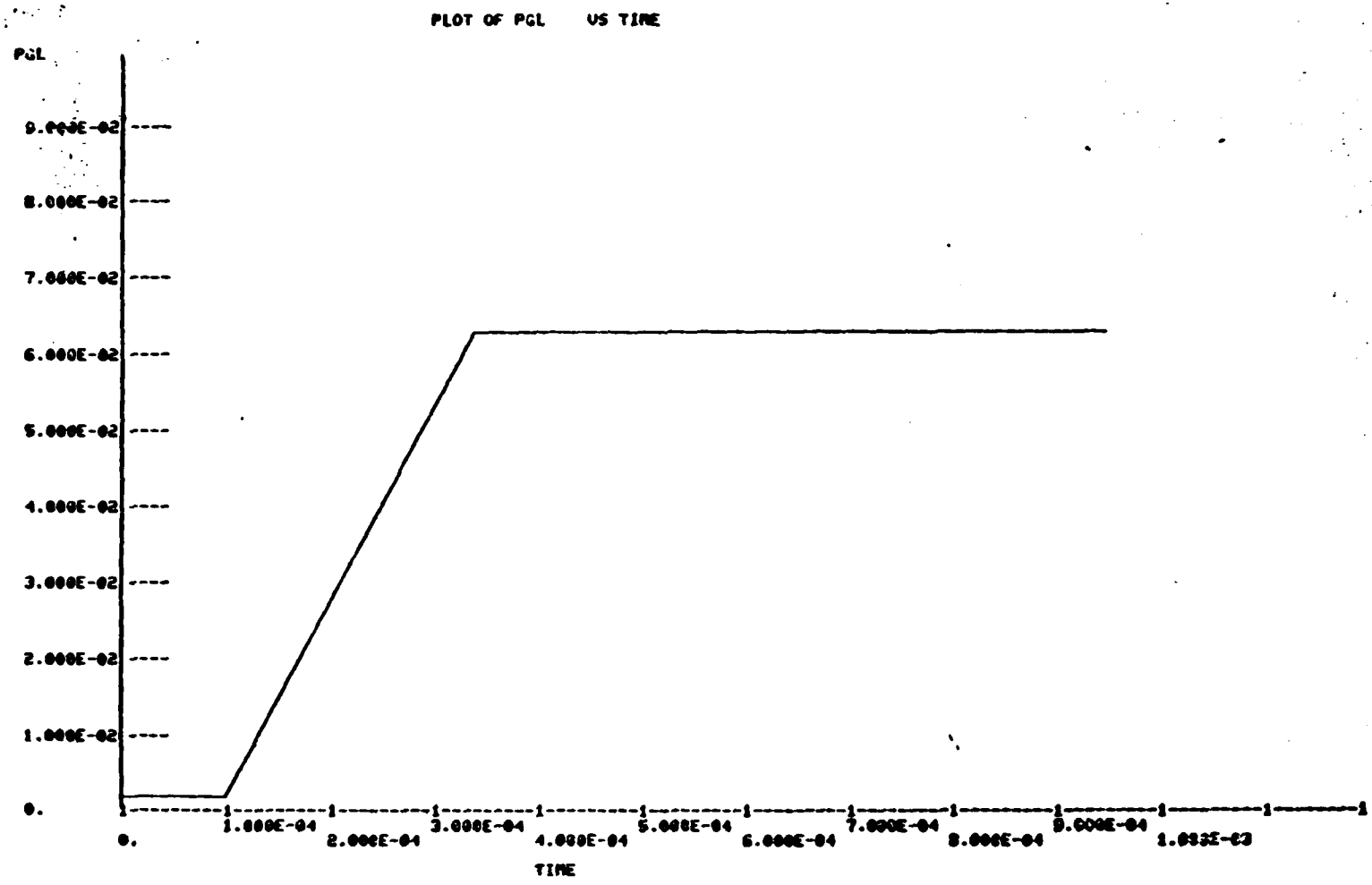

PLOT 1 LINEAR GAP OPENING

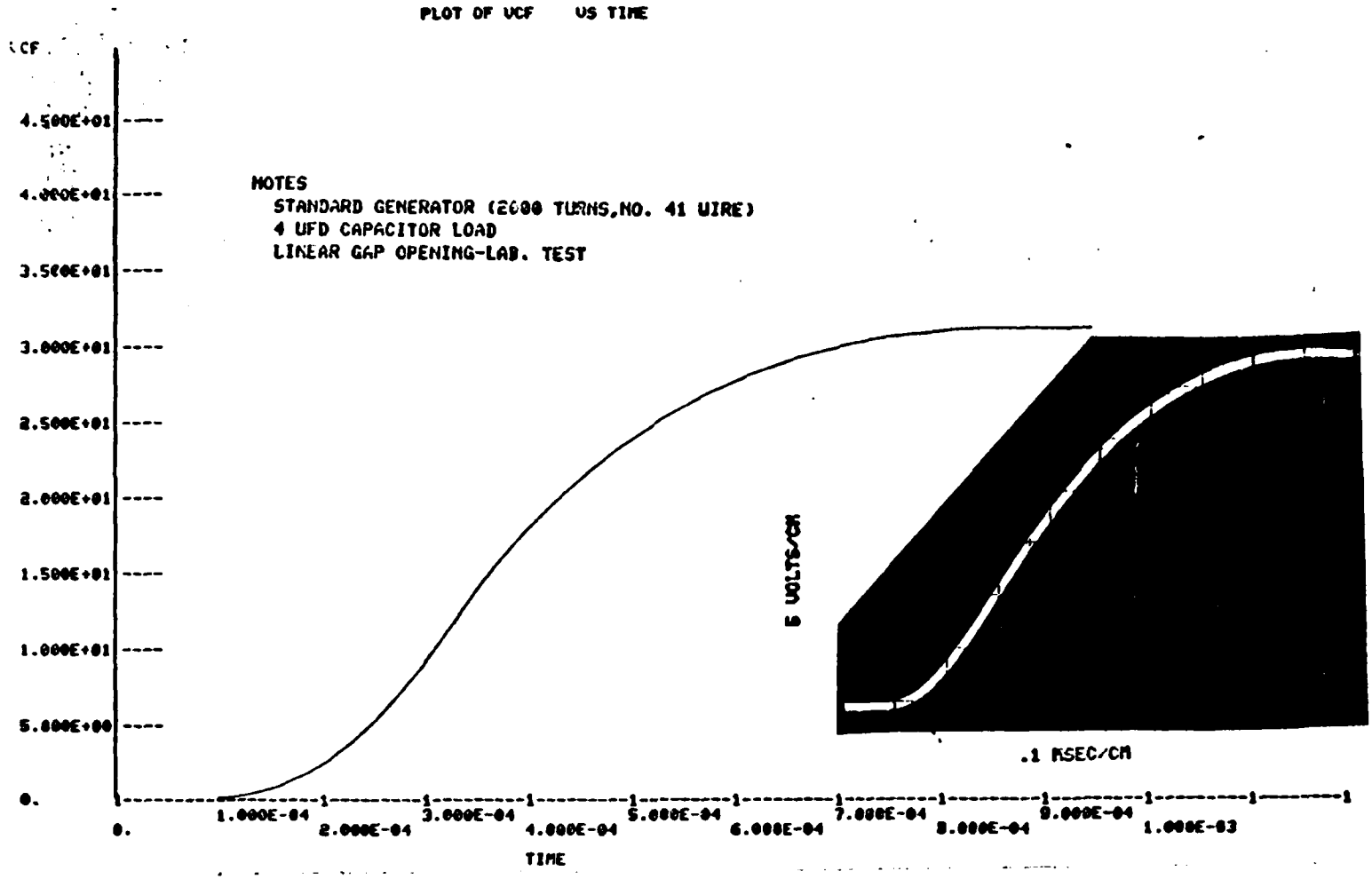

PLOT 2 VOLTAGE OUTPUT (VCF) VS. TIME

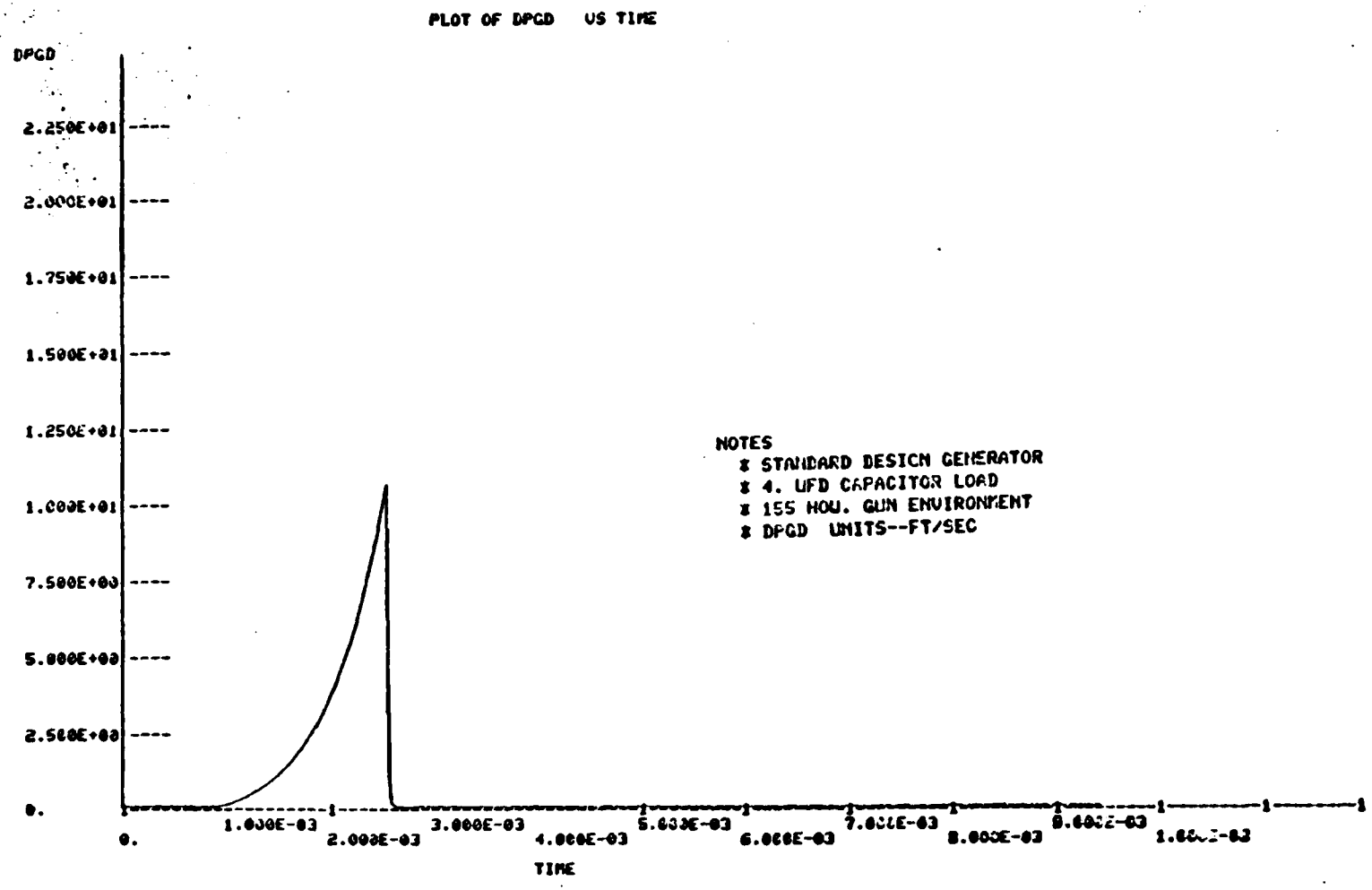

PLOT 5A CORE VELOCITY VS. TIME

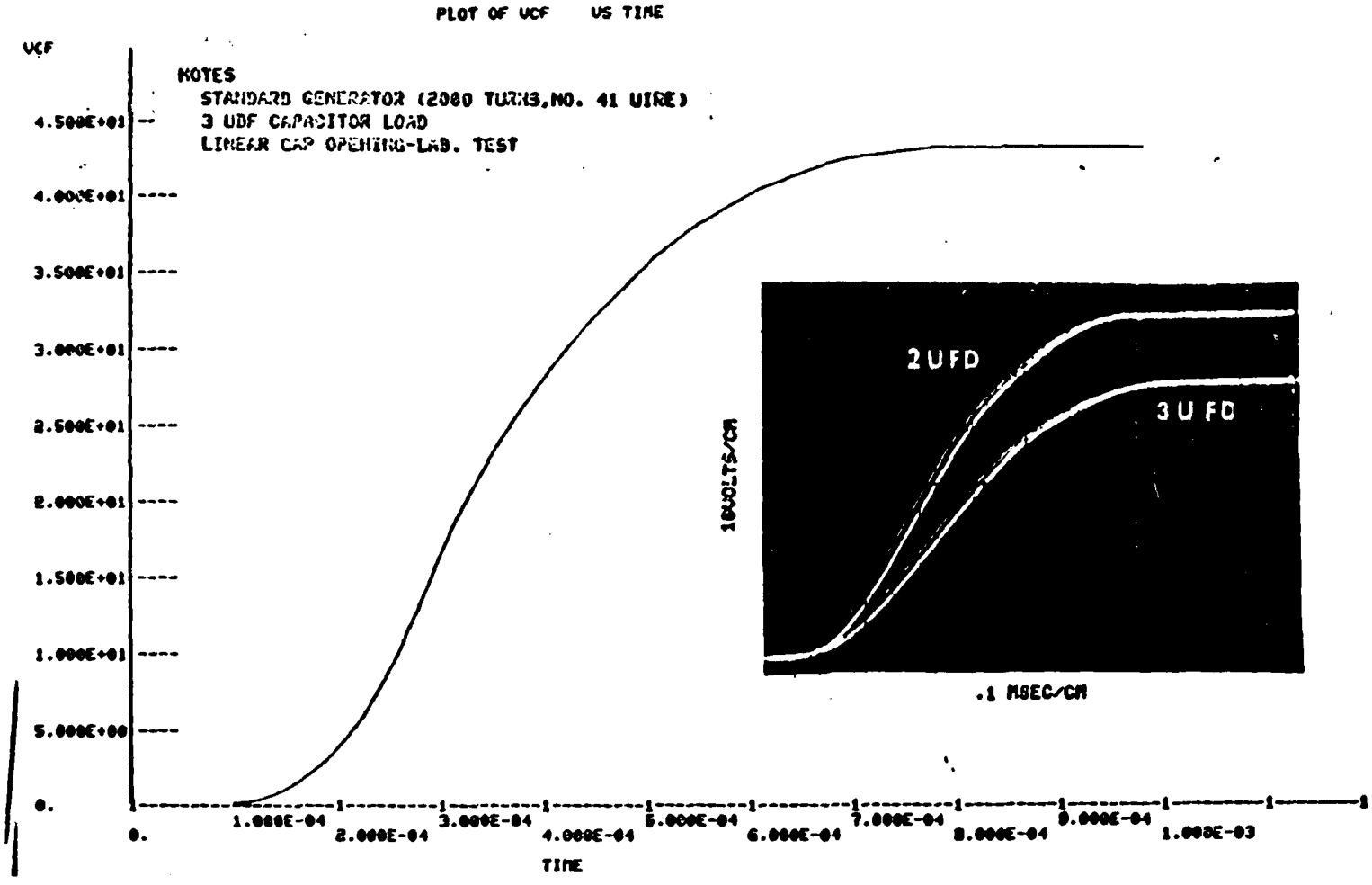

PLOT 3 VOLTAGE OUTPUT (VCF) VS. TIME

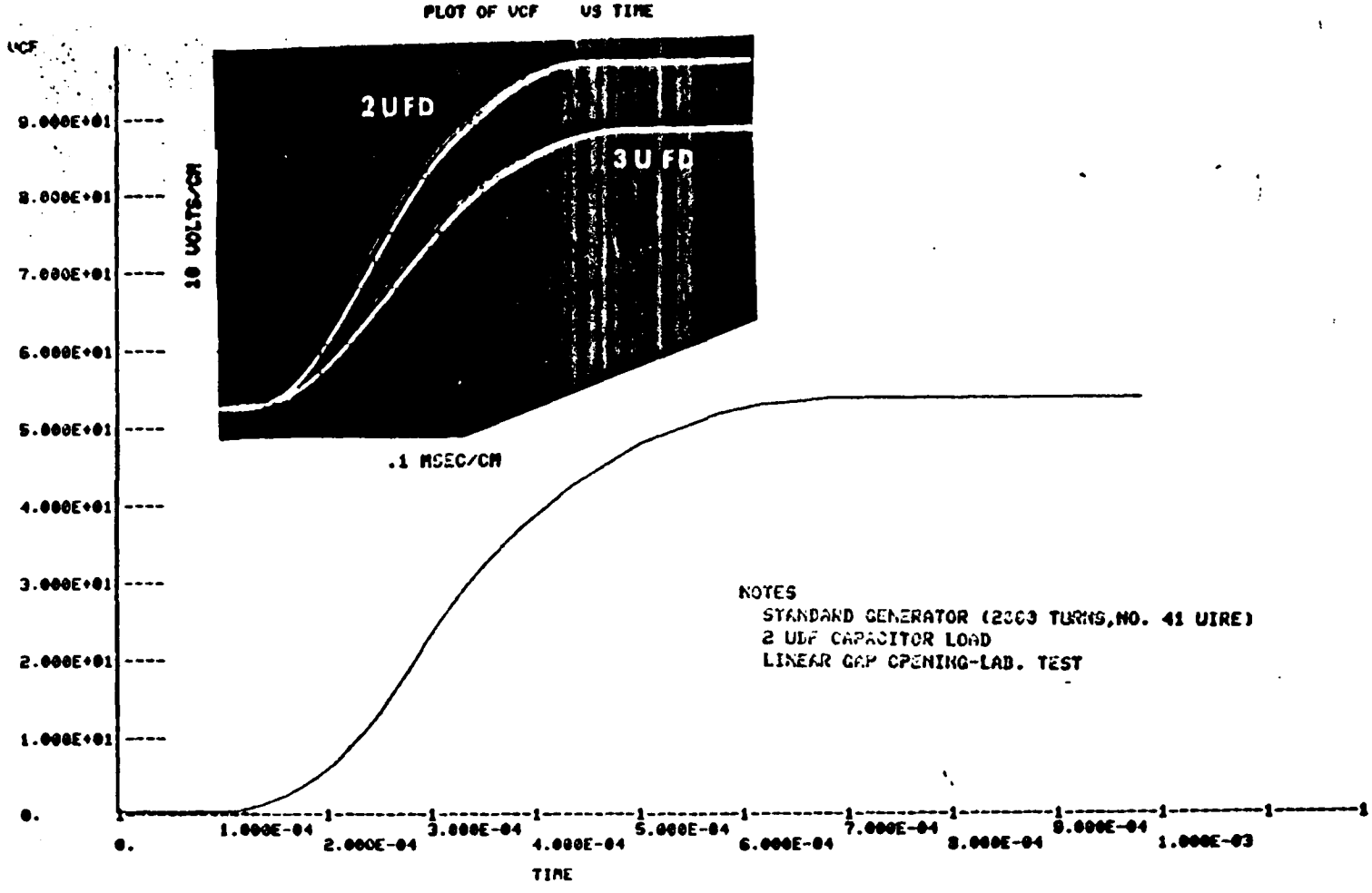

PLOT 4 VOLTAGE OUTPUT (VCF) VS. TIME

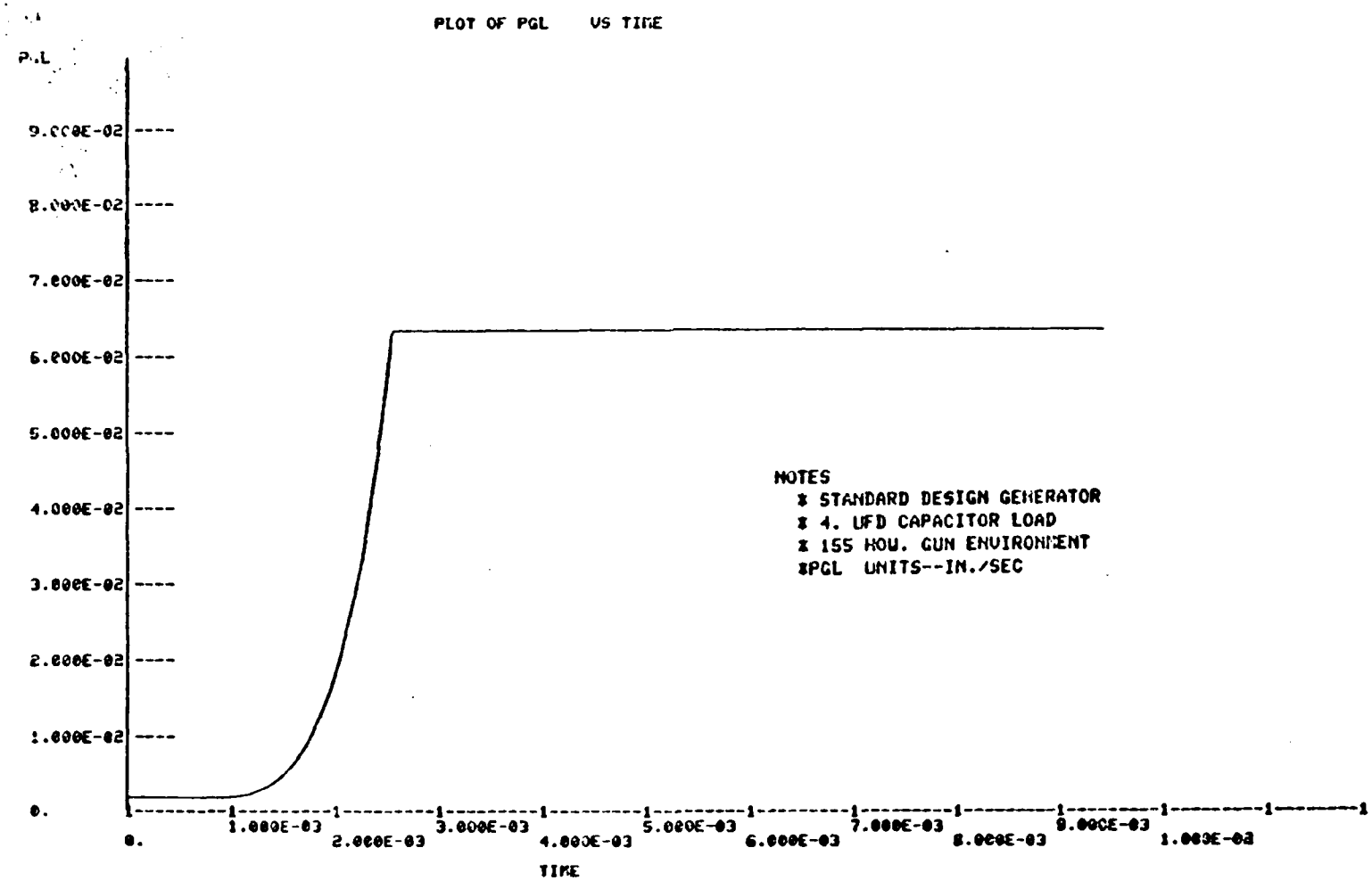

PLOT 5B GAP DISTANCE VS. TIME

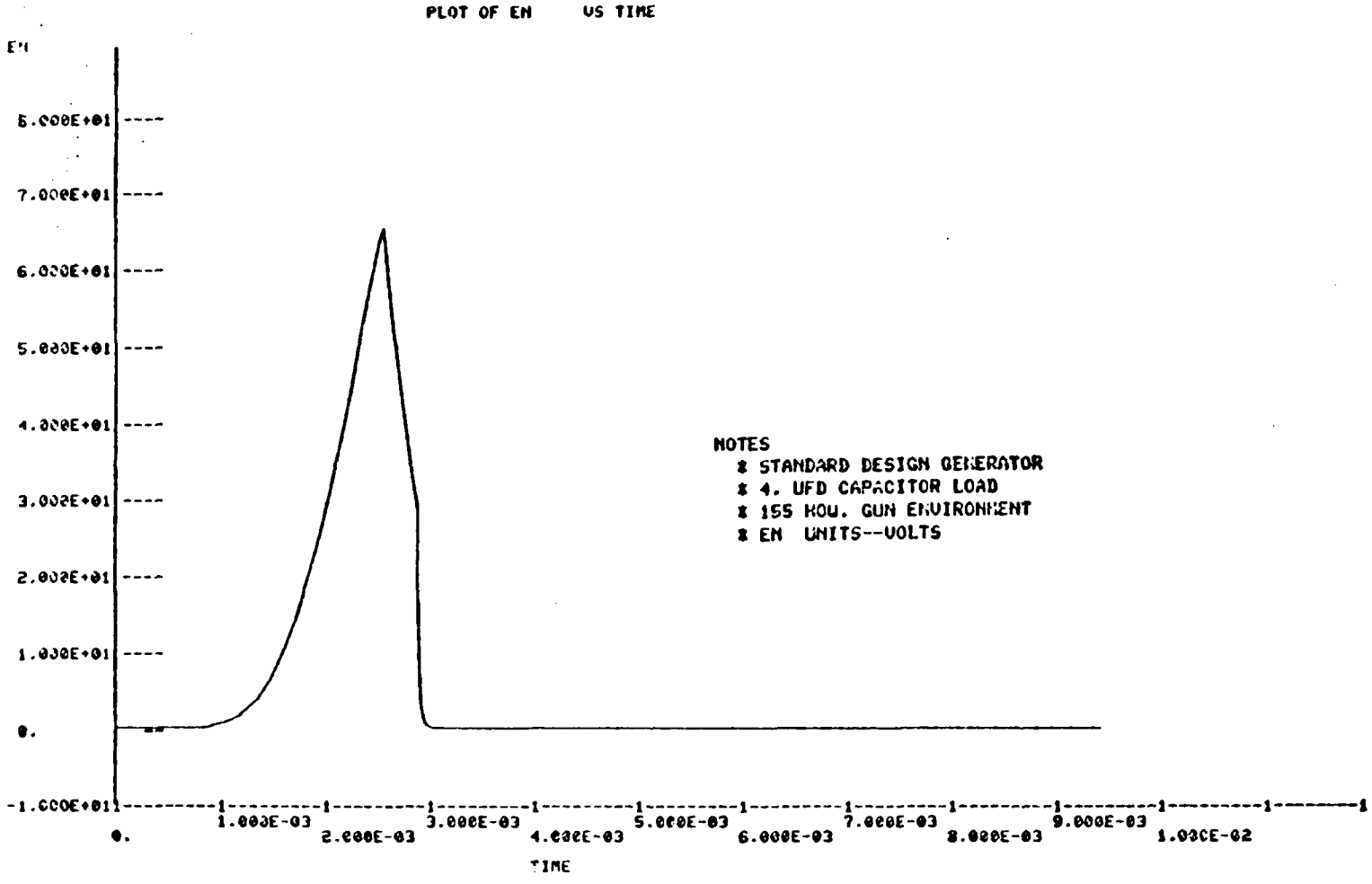

PLOT 5C VOLTAGE DERIVATIVE VS. TIME

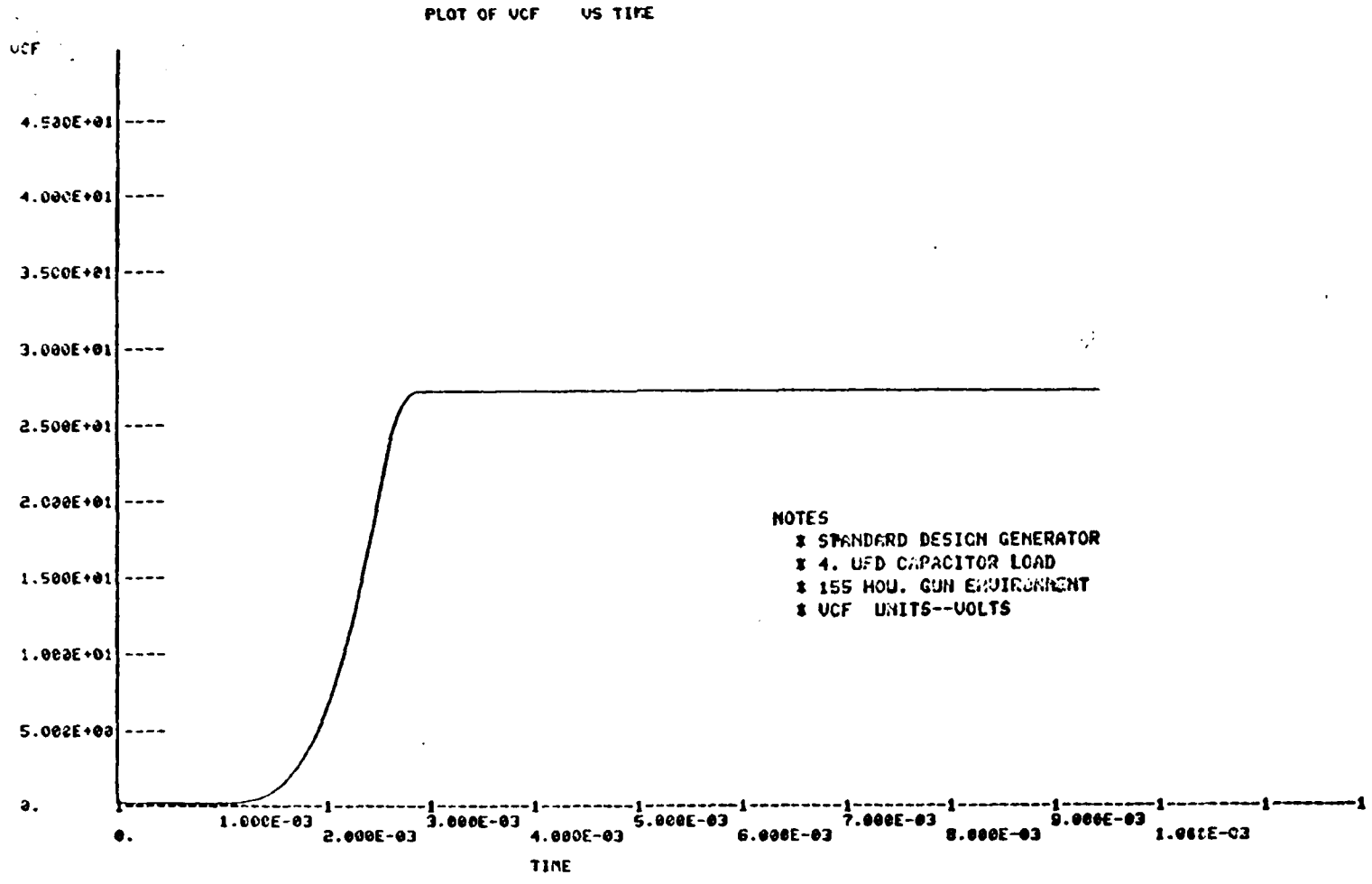

PLOT 50 VOLTAGE OUTPUT (VCF) VS. TIME

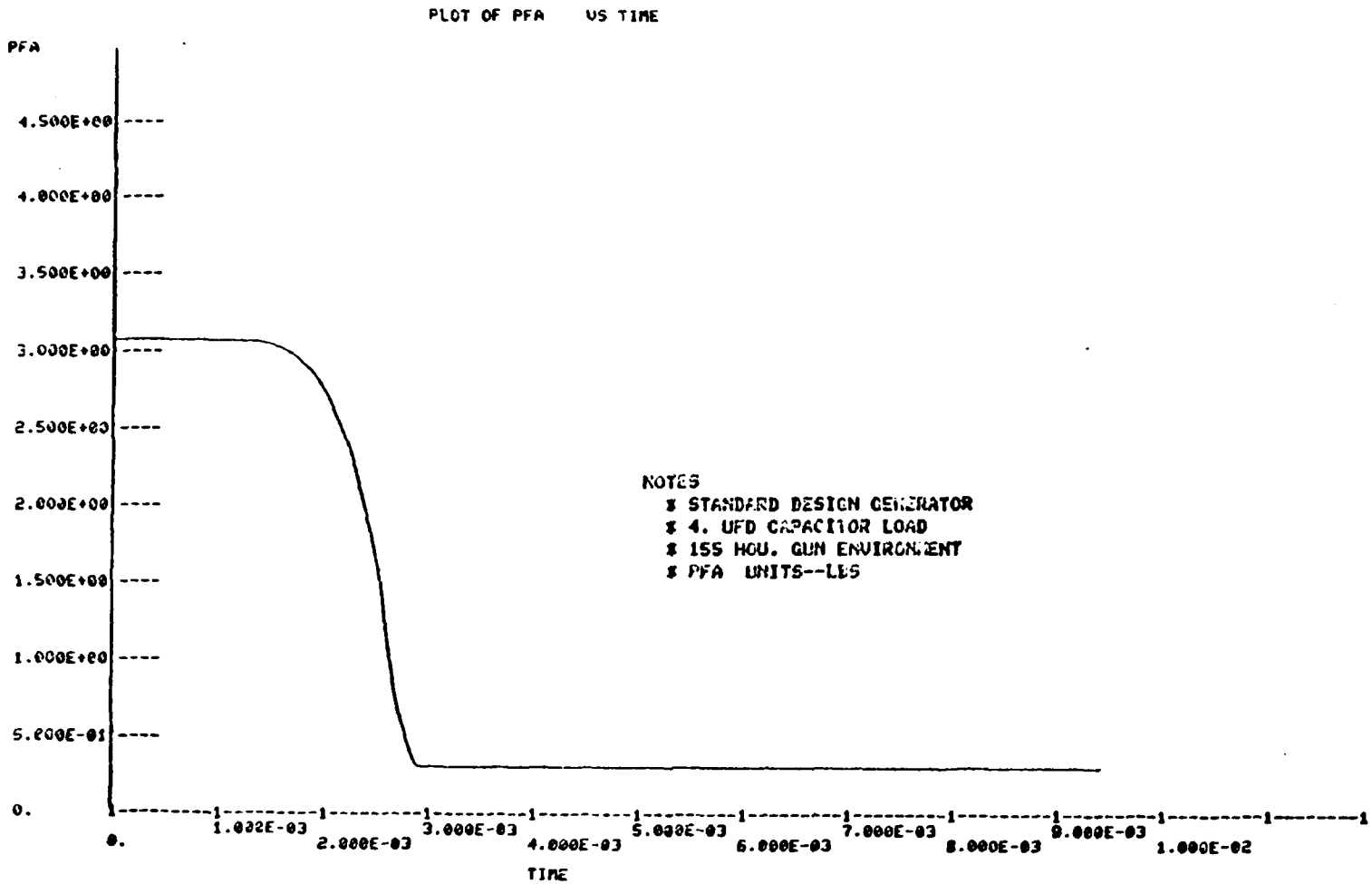

PLOT SE FORCE OF MATNETIC ATTRACTION VS. TIME

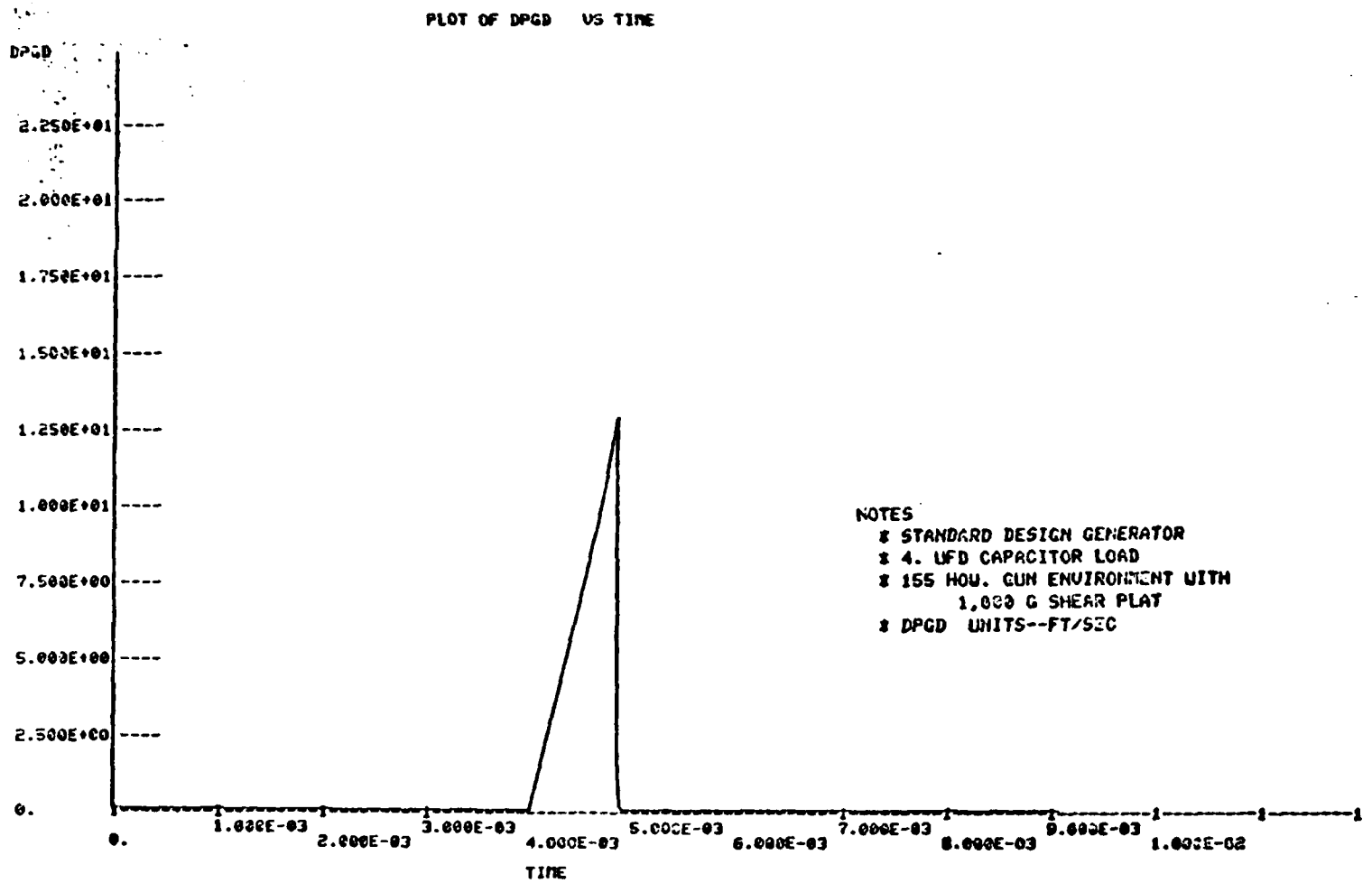

PLOT 6A CORE VELOCITY VS. TIME

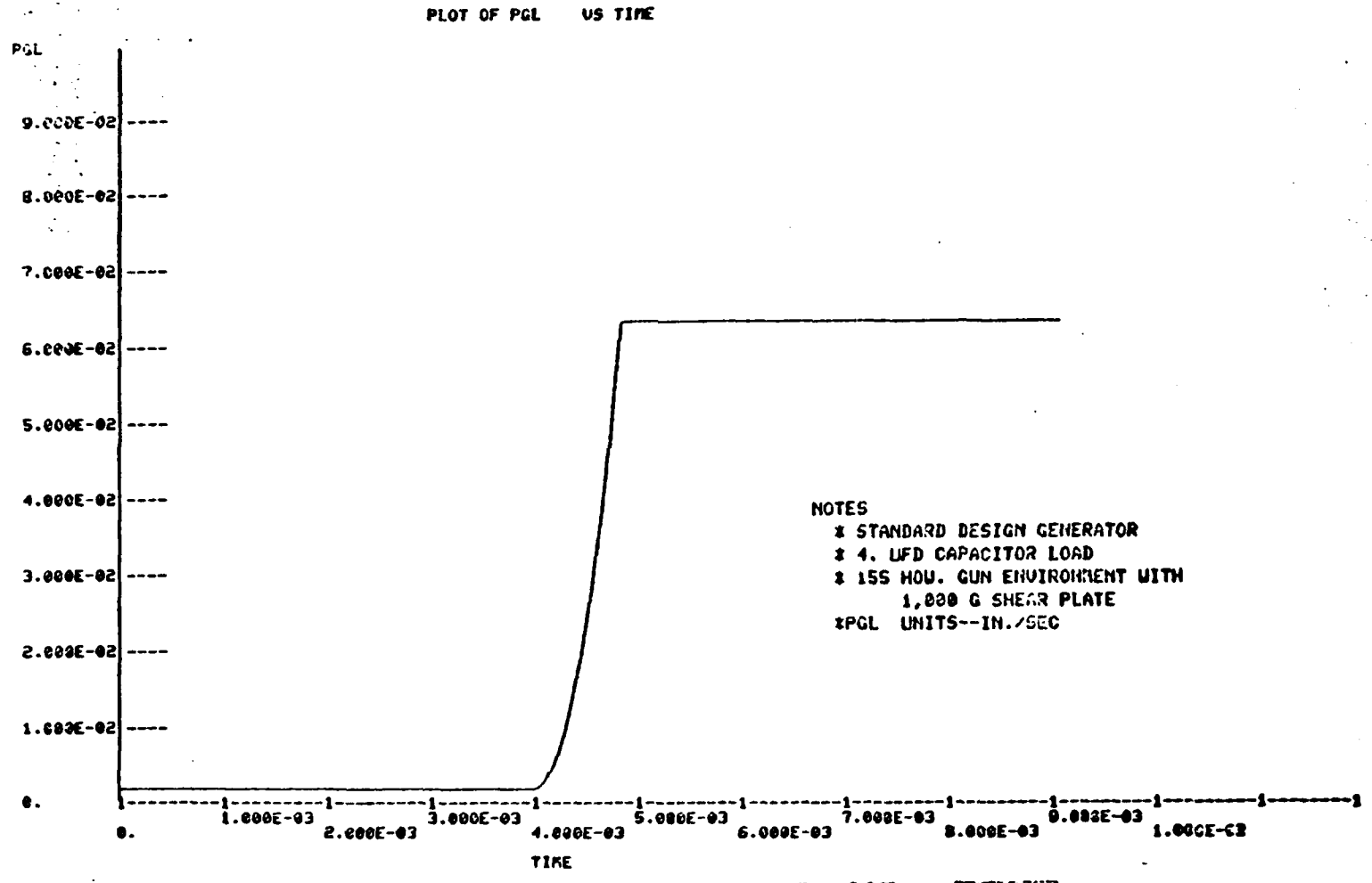

PLOT 68 GAP DISTANCE VS. TIME

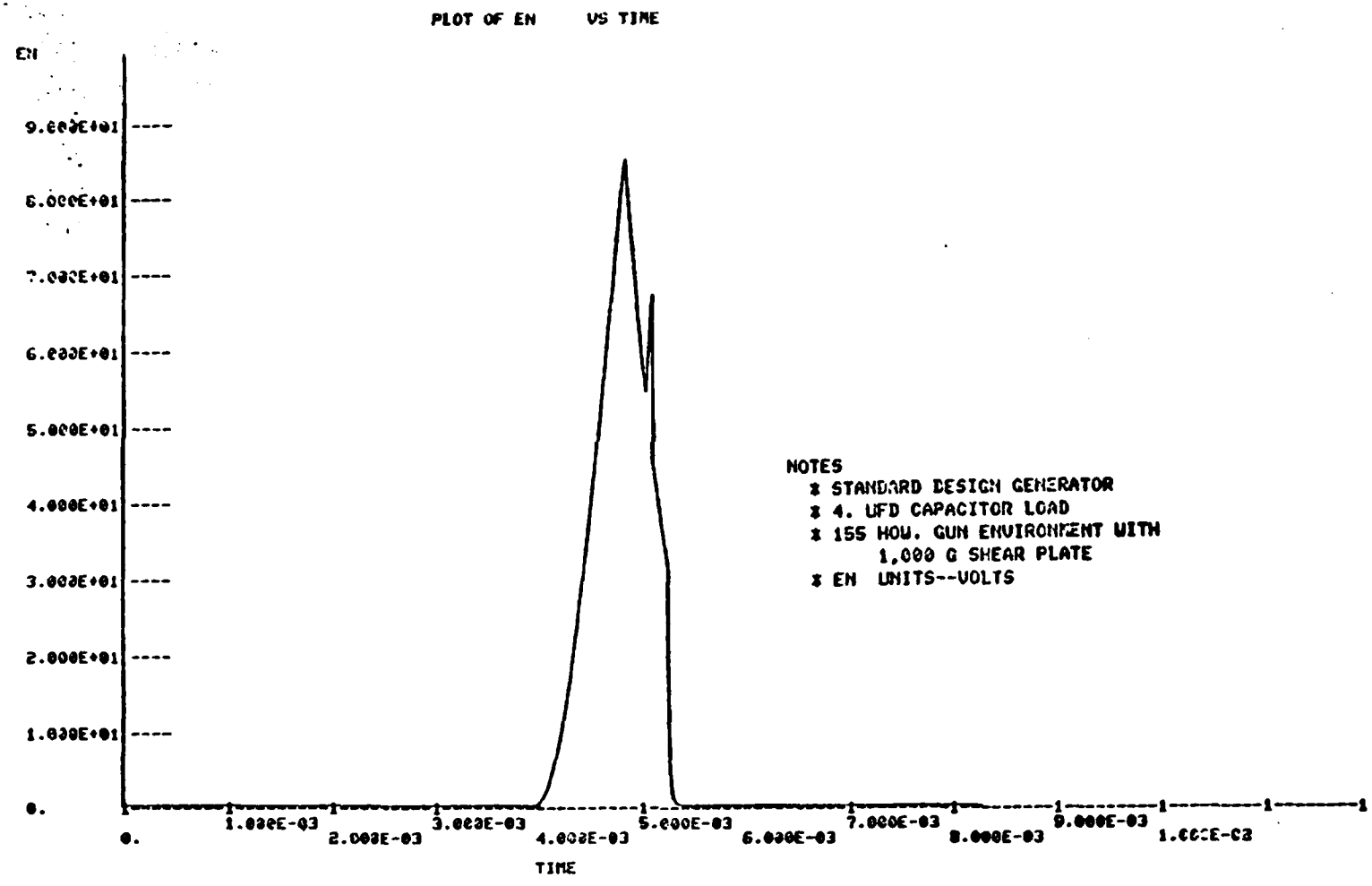

PLOT 6C VOLTAGE DERIVATIVE VS. TIME

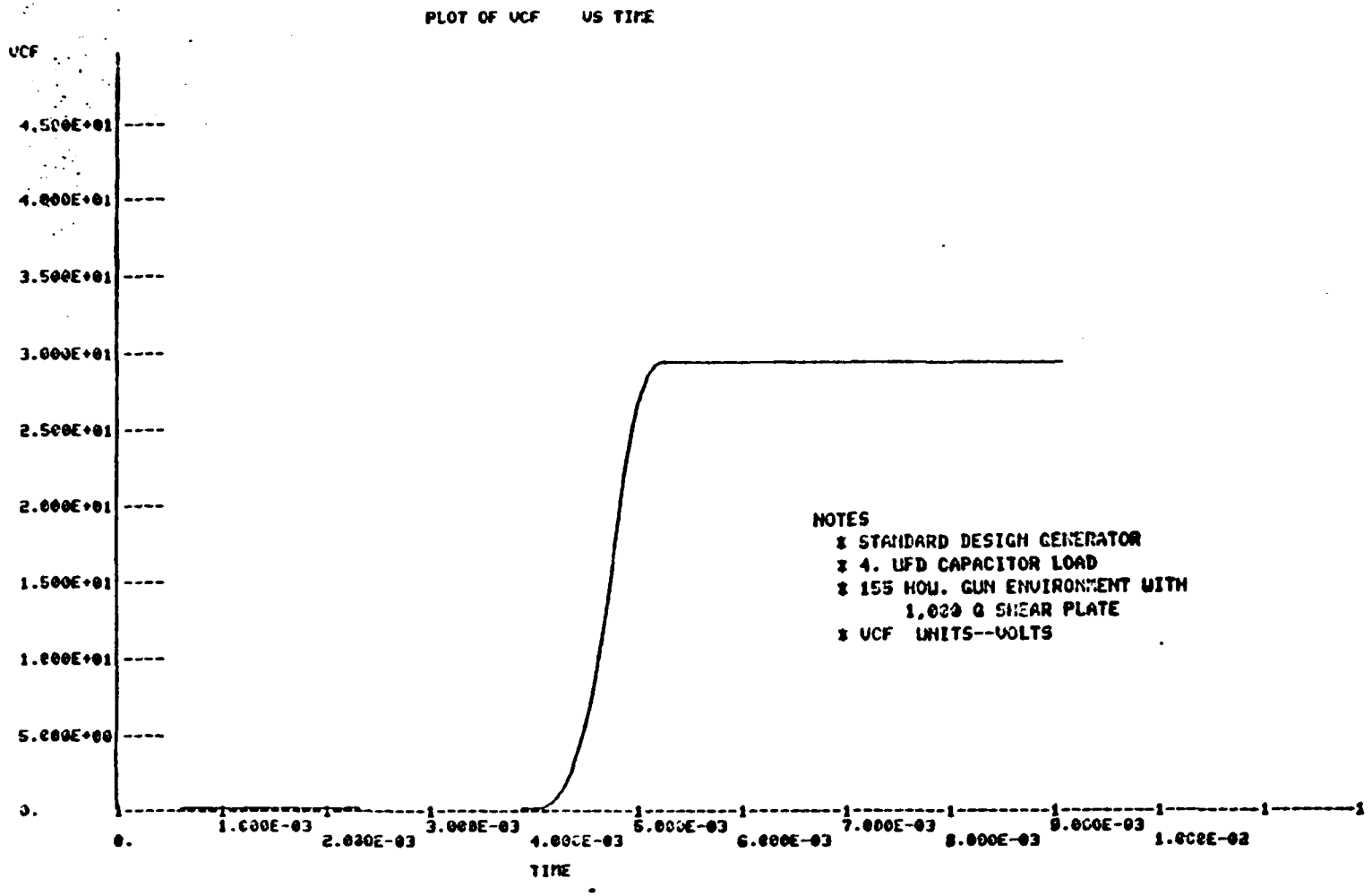

PLOT 6D VOLTAGE OUTPUT (VCF) VS. TIME

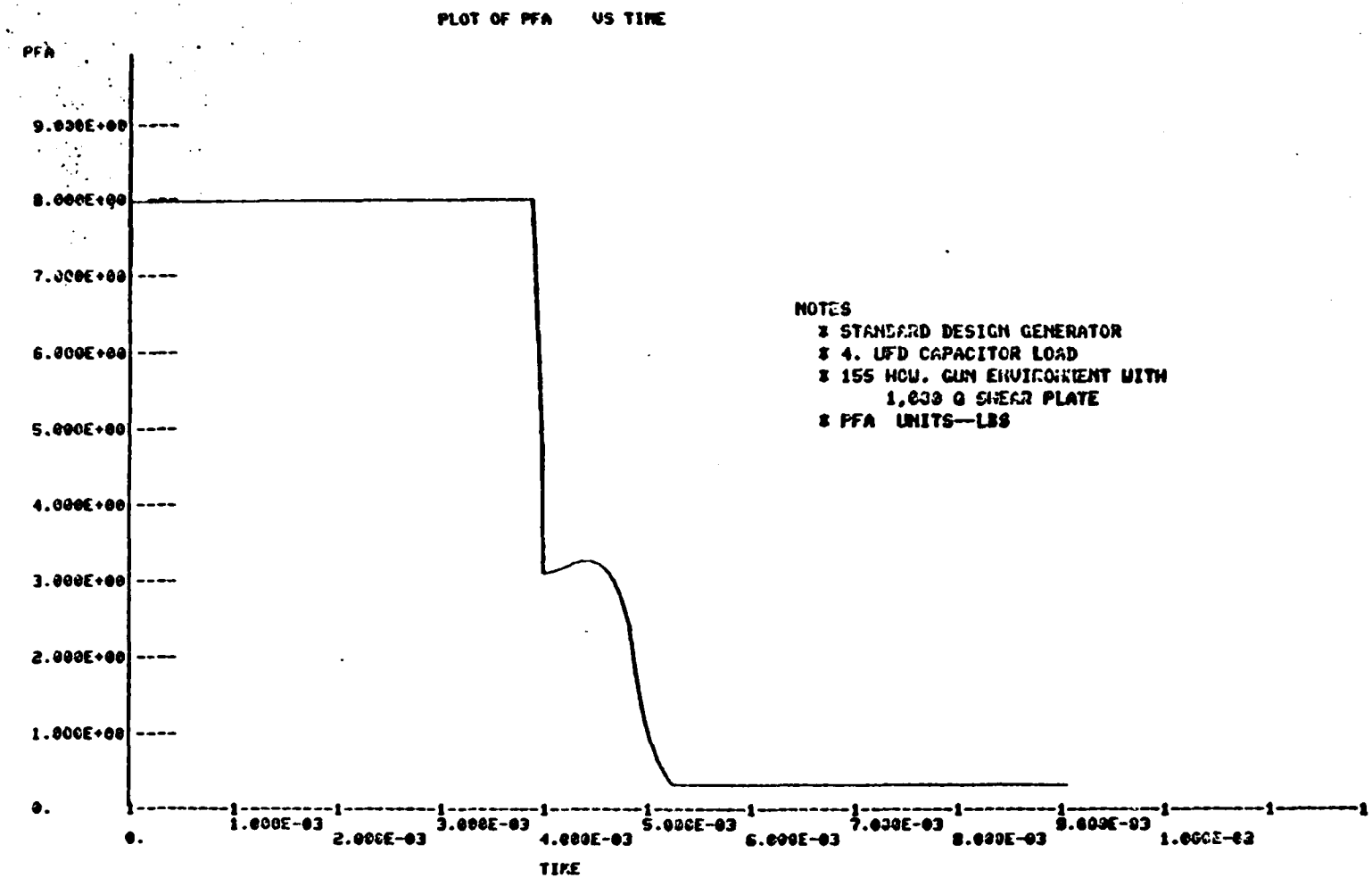

PLOT 6E FORCE OF MATNETIC ATTRACTION VS. TIME

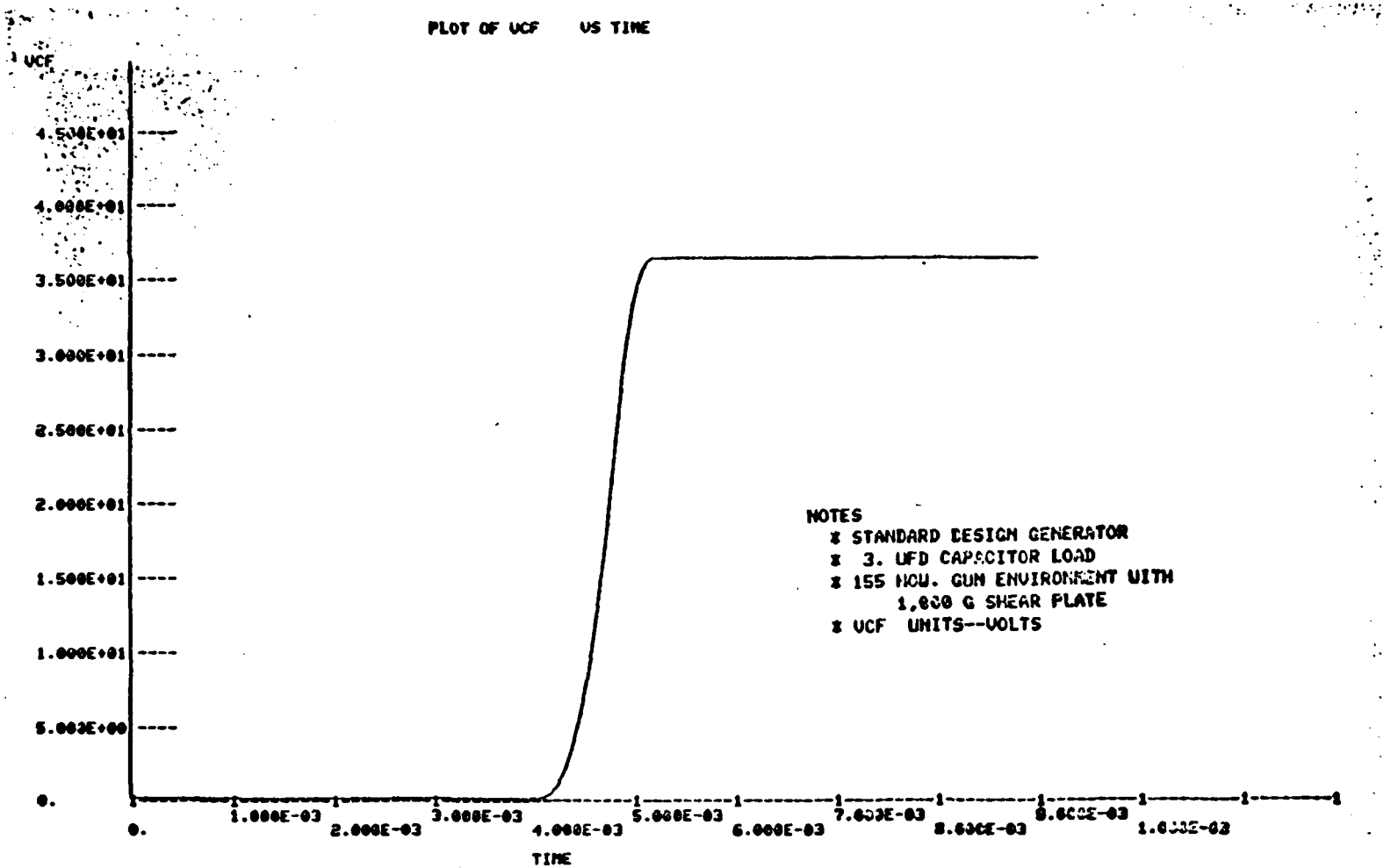

PLOT 7 VOLTAGE OUTPUT (VCF) VS. TIME

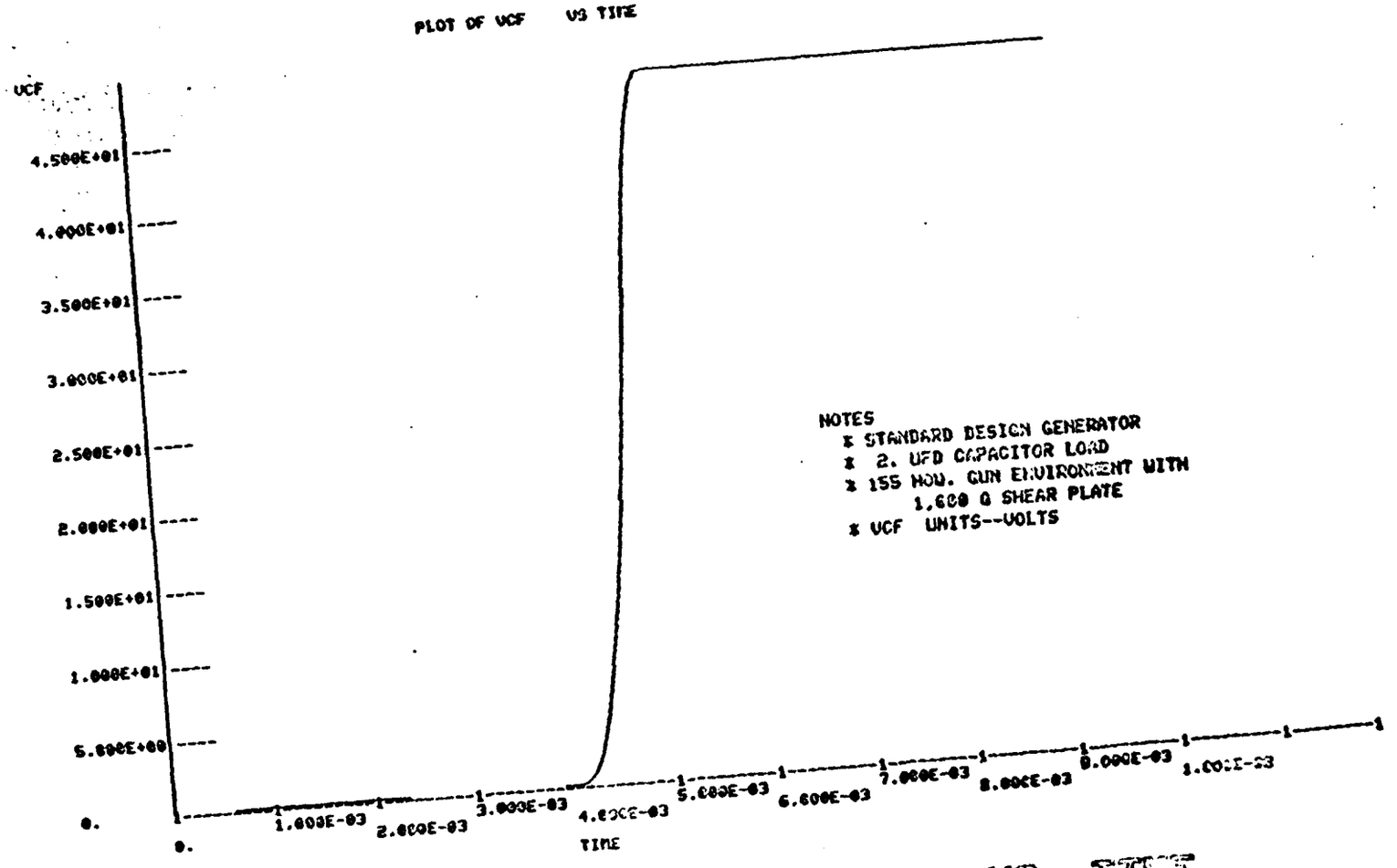

PLOT 8 VOLTAGE OUTPUT (VCF) VS. TIME

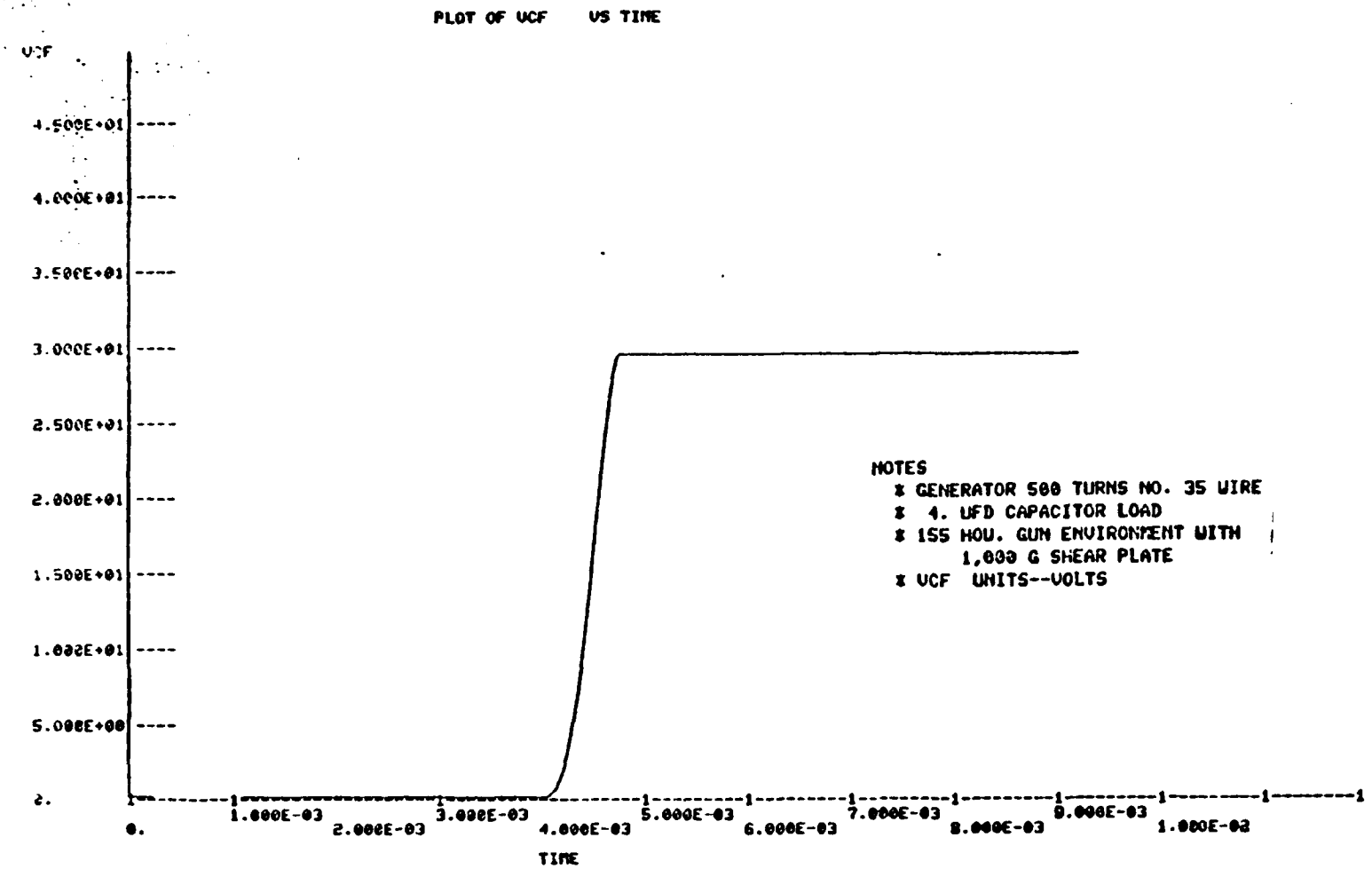

PLOT 9 VOLTAGE OUTPUT (VCF) VS. TIME

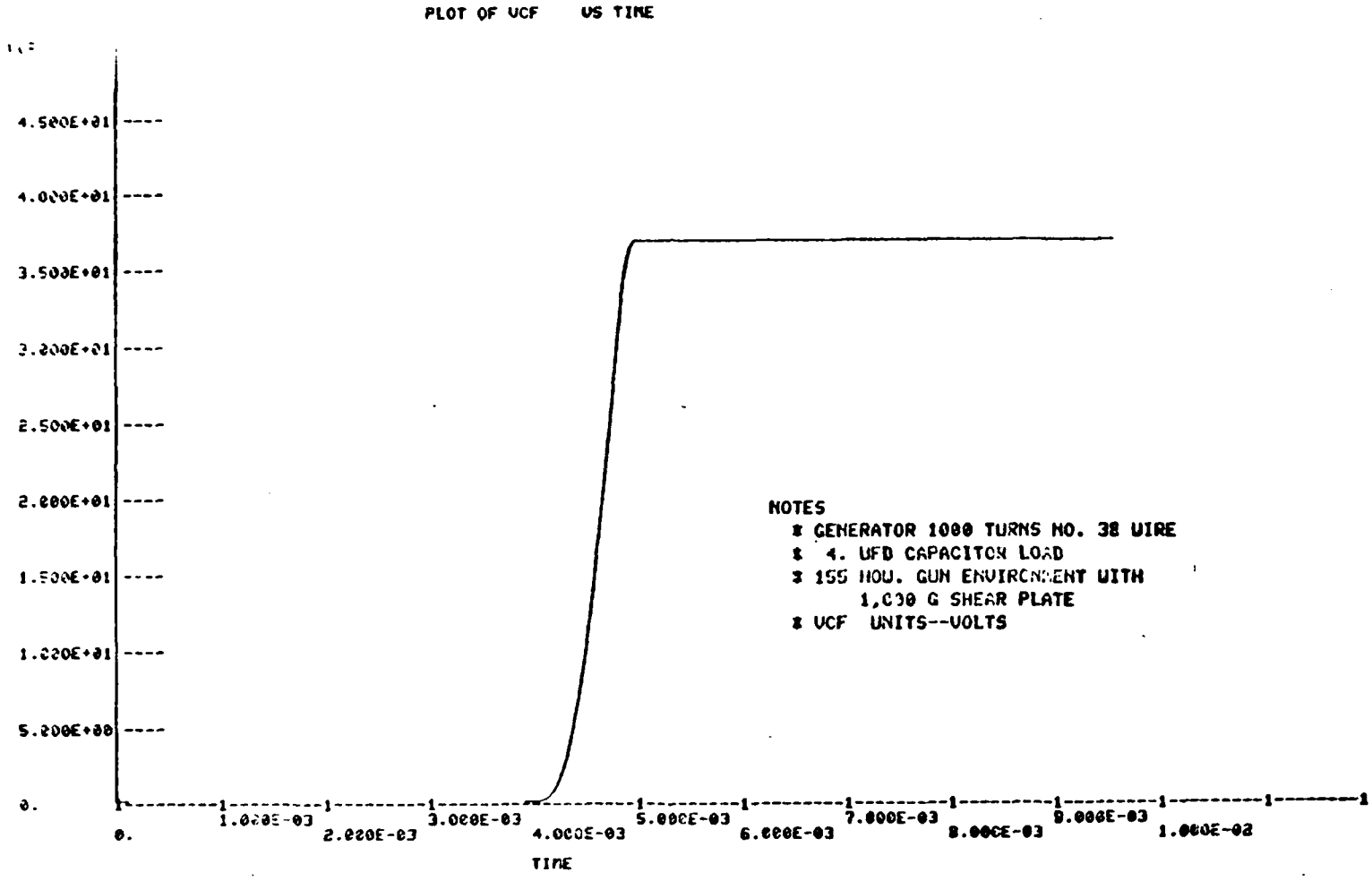

PLOT 10 VOLTAGE OUTPUT (VCF) VS. TIME

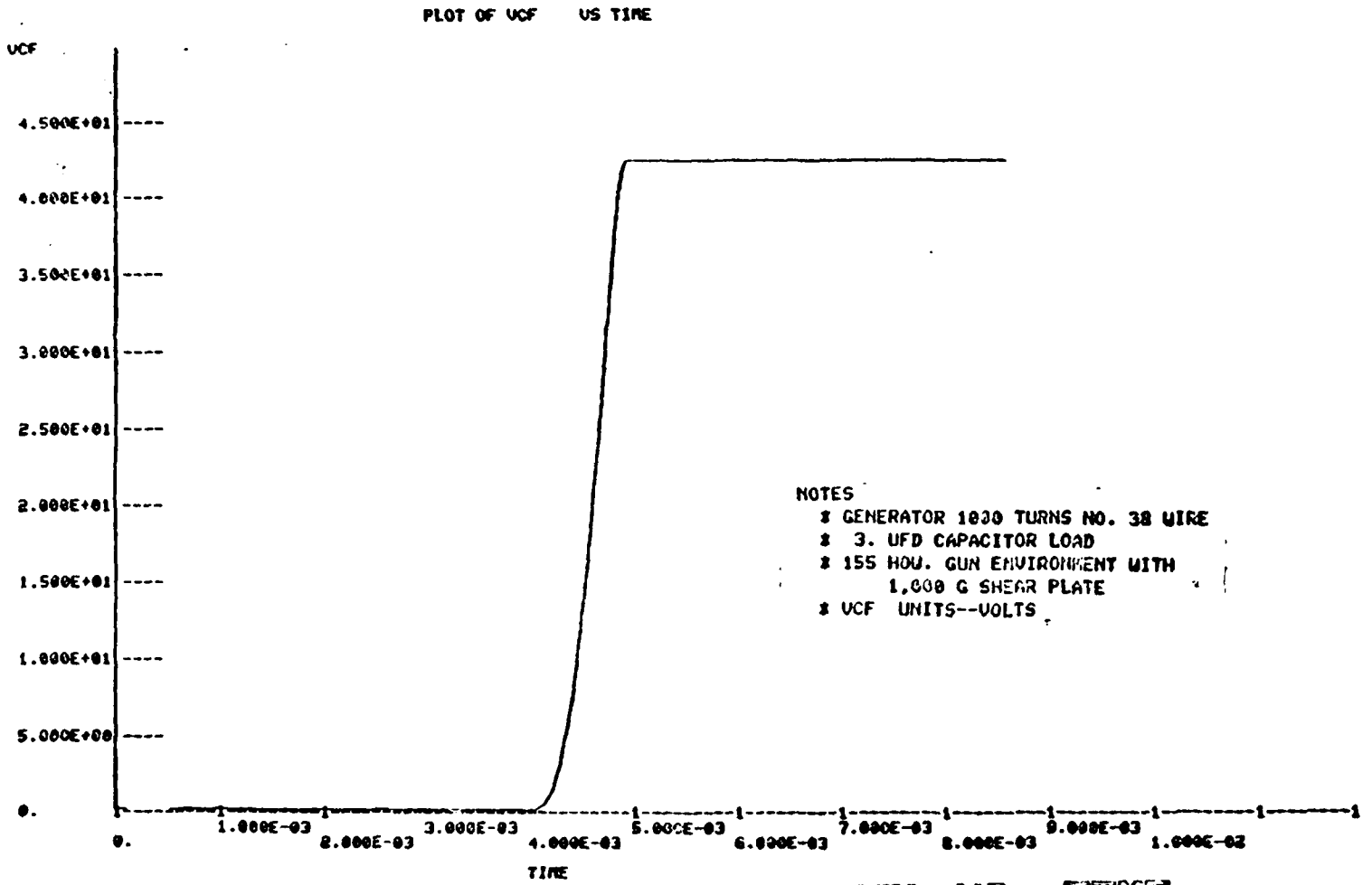

PLOT 11 VOLTAGE OUTPUT (VCF) VS. TIME

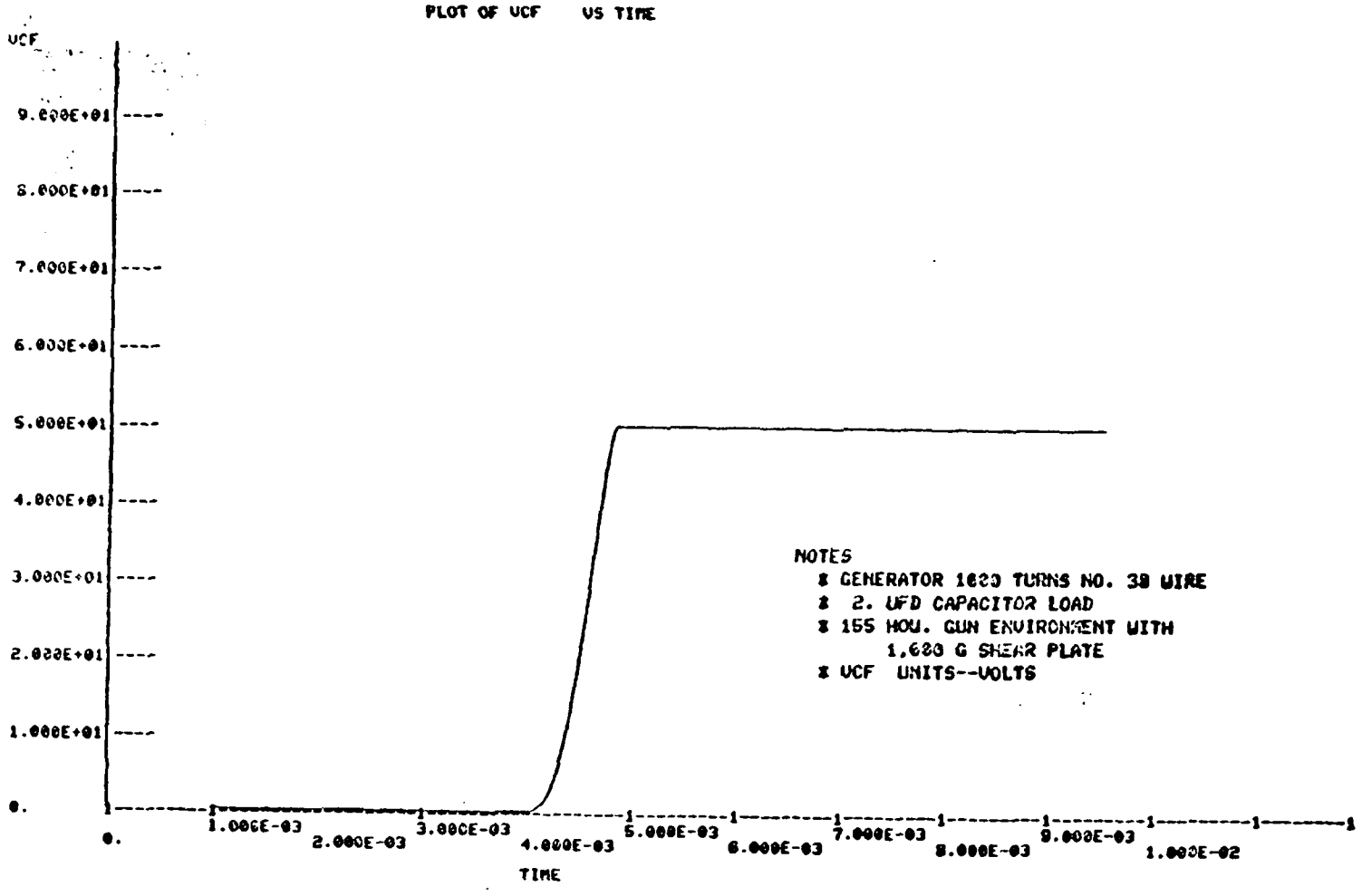

PLOT 12 VOLTAGE OUTPUT (VCF) VS. TIME

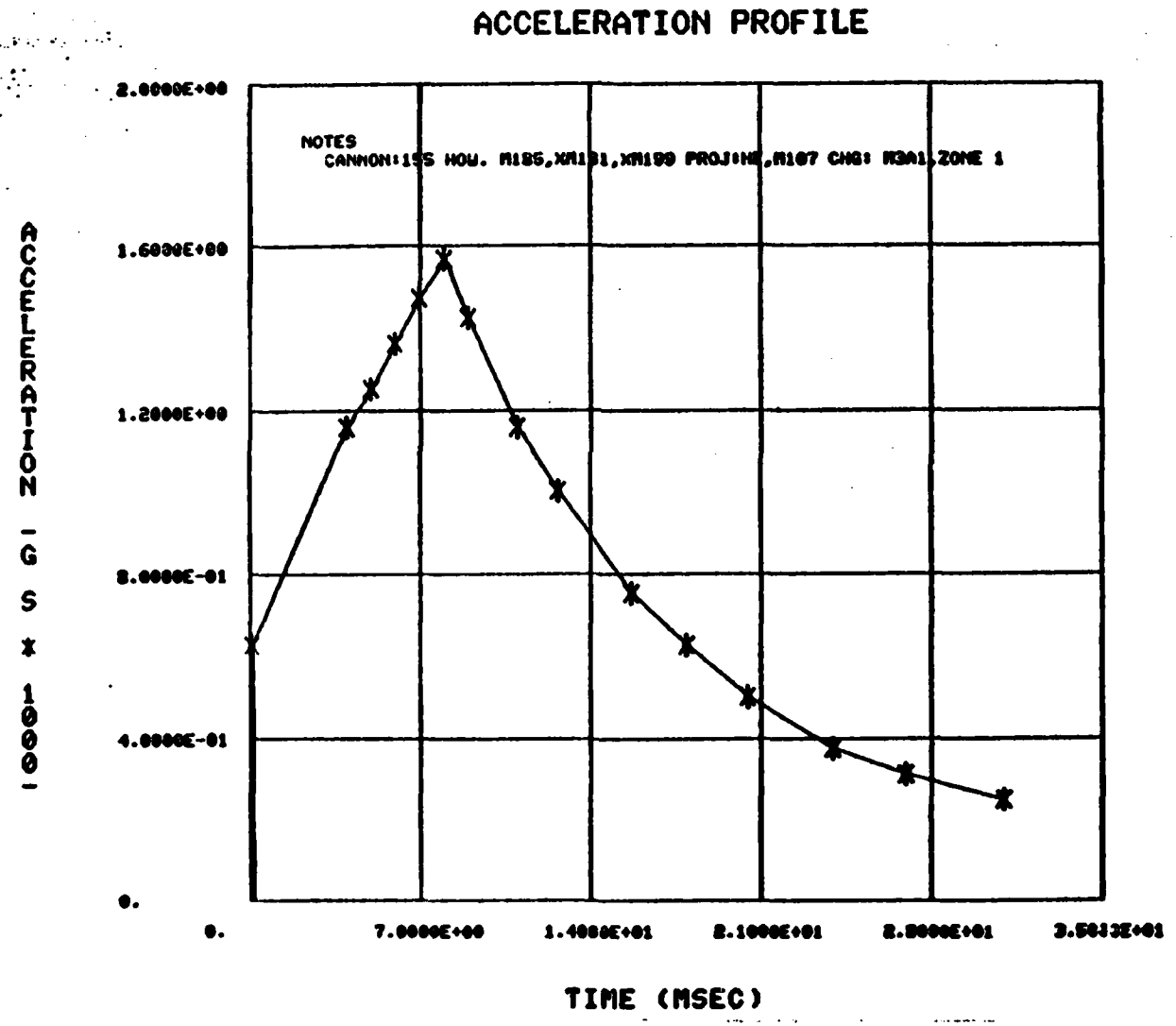

PLOT 13 ACCELERRATION PROFILE

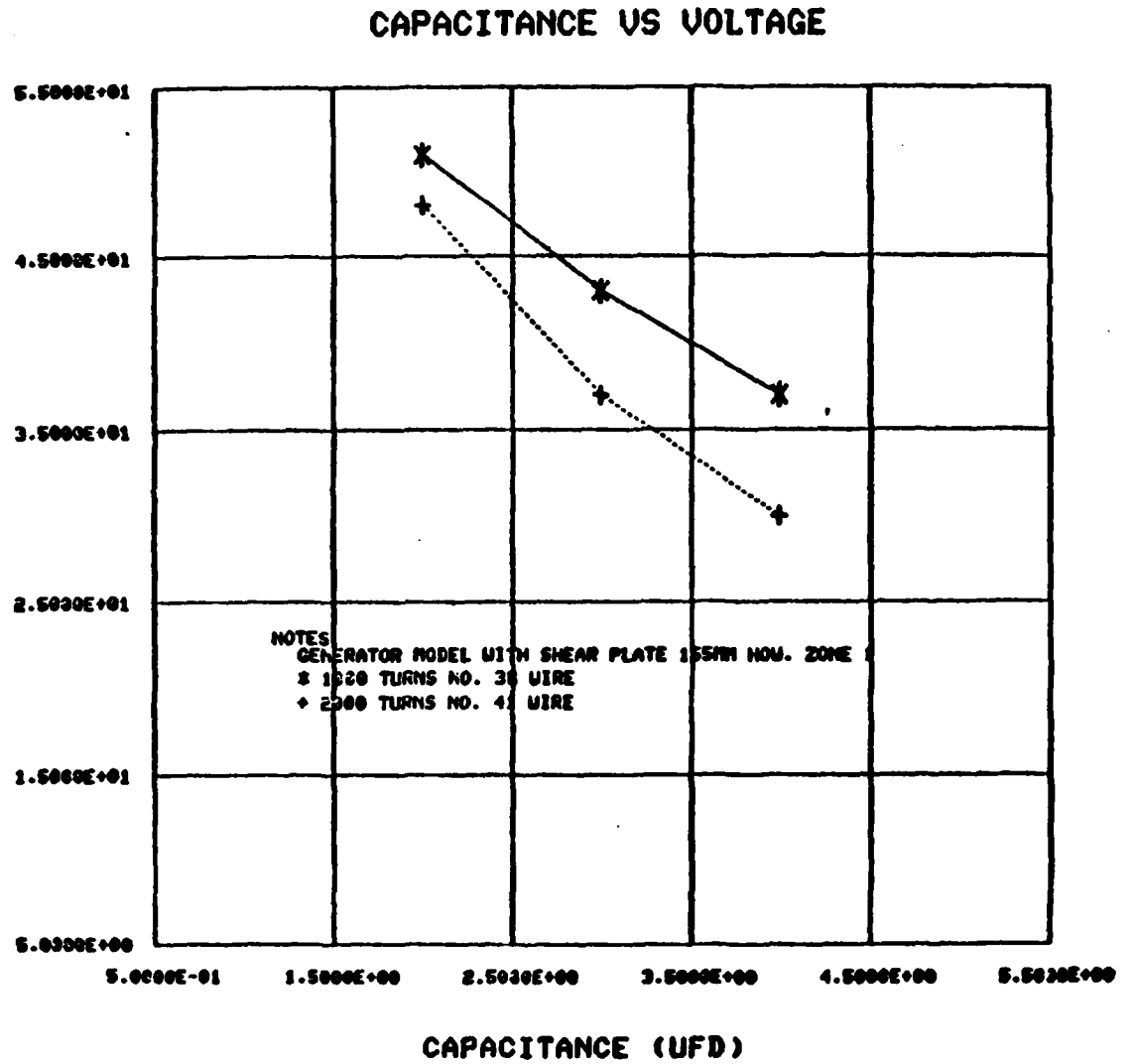

PLOT 14 CAPACITANCE VS. OUTPUT VOLTAGE

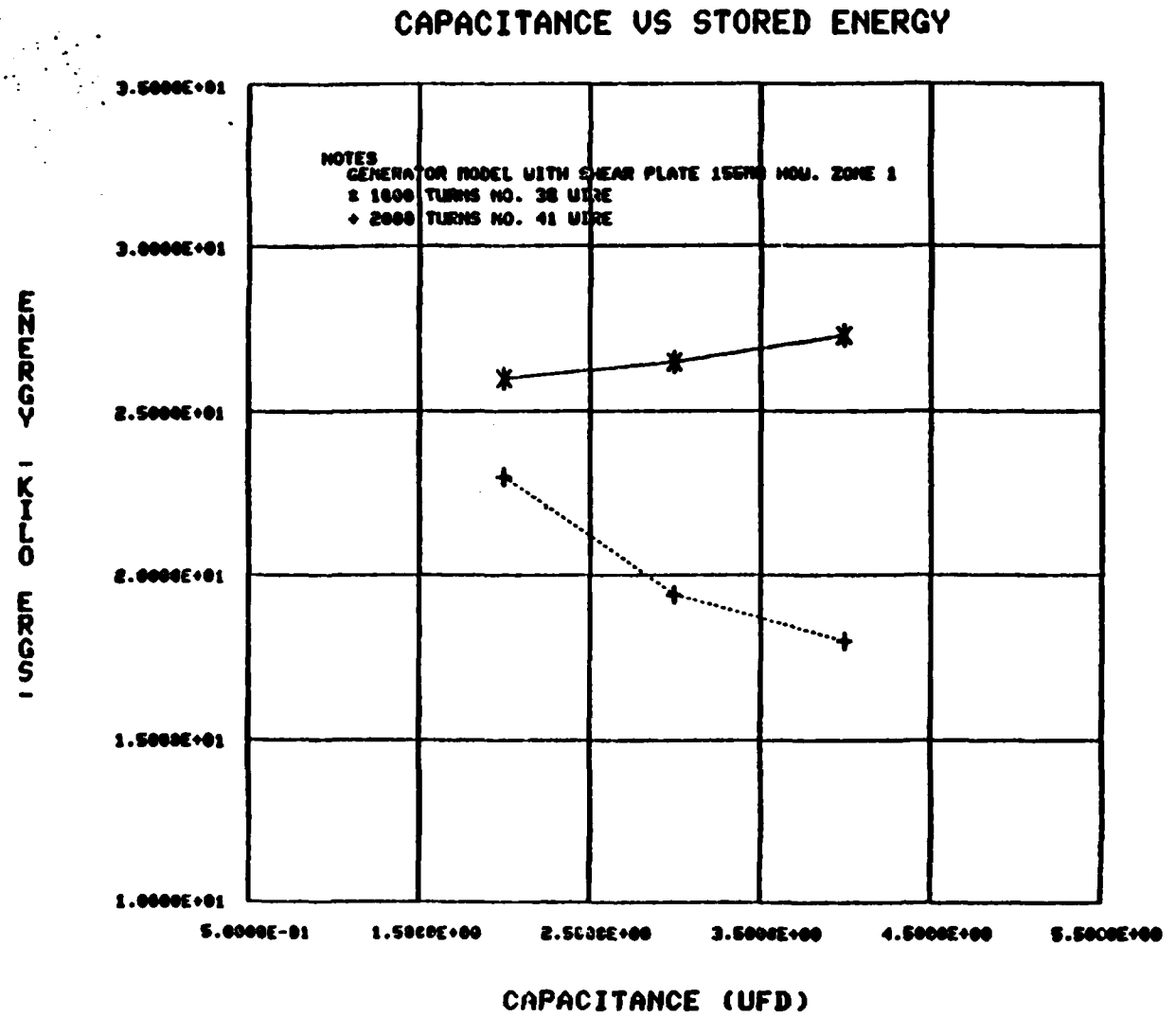

PLOT 15 CAPACITANCE VS. STORED ENERGY

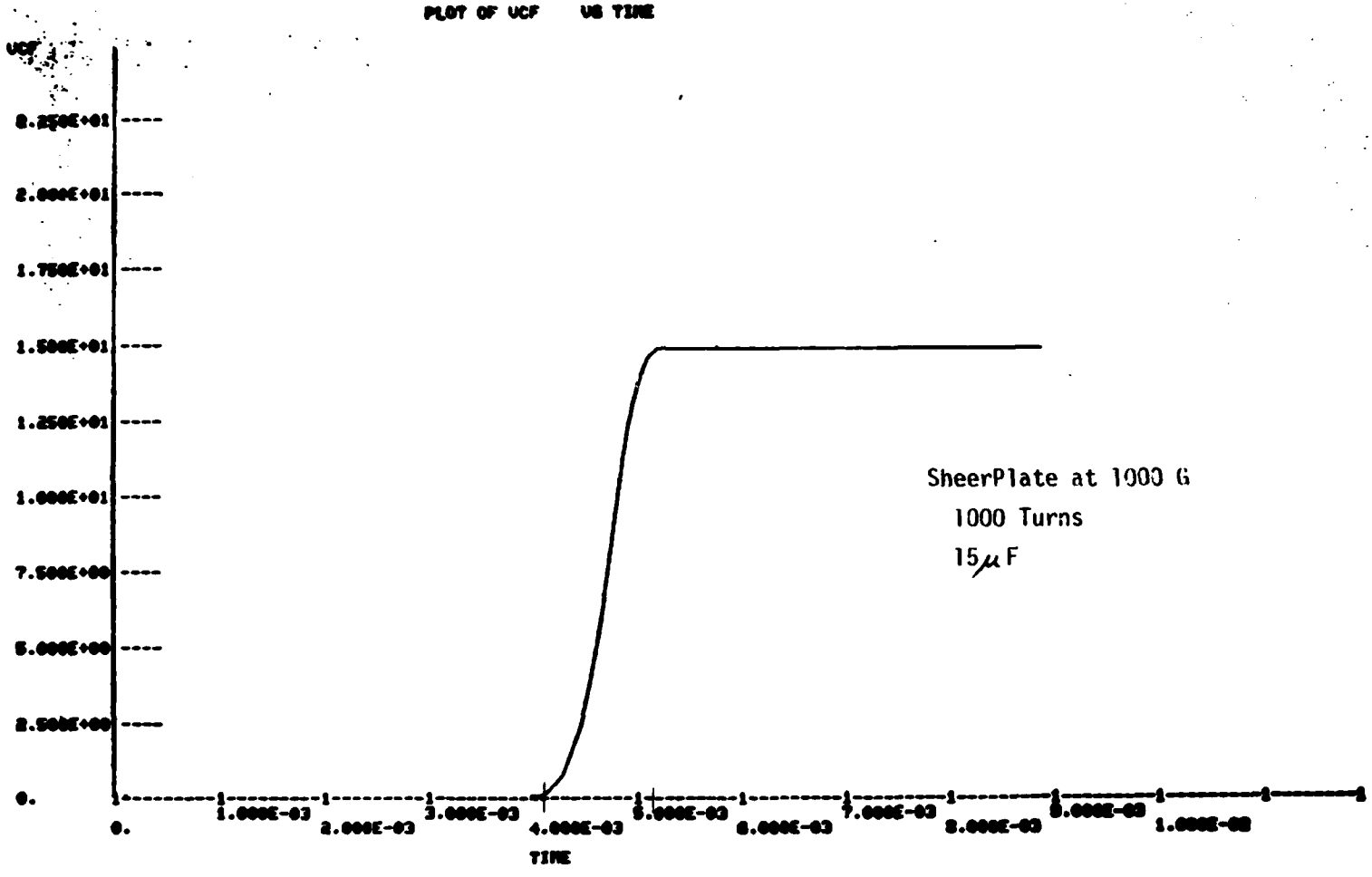
PLOT OF UCF VS TIME
UCF
8.250E+01
2.000E+01
1.750E+01
1.500E+01
1.250E+01
1.000E+01
7.500E+00
5.000E+00
2.500E+00
0.
0.
1.000E-03
2.000E-03
3.000E-03
4.000E-03
5.000E-03
6.000E-03
7.000E-03
8.000E-03
9.000E-03
1.000E-02
TIME
SheerPlate at 1000 G
1000 Turns
15μF

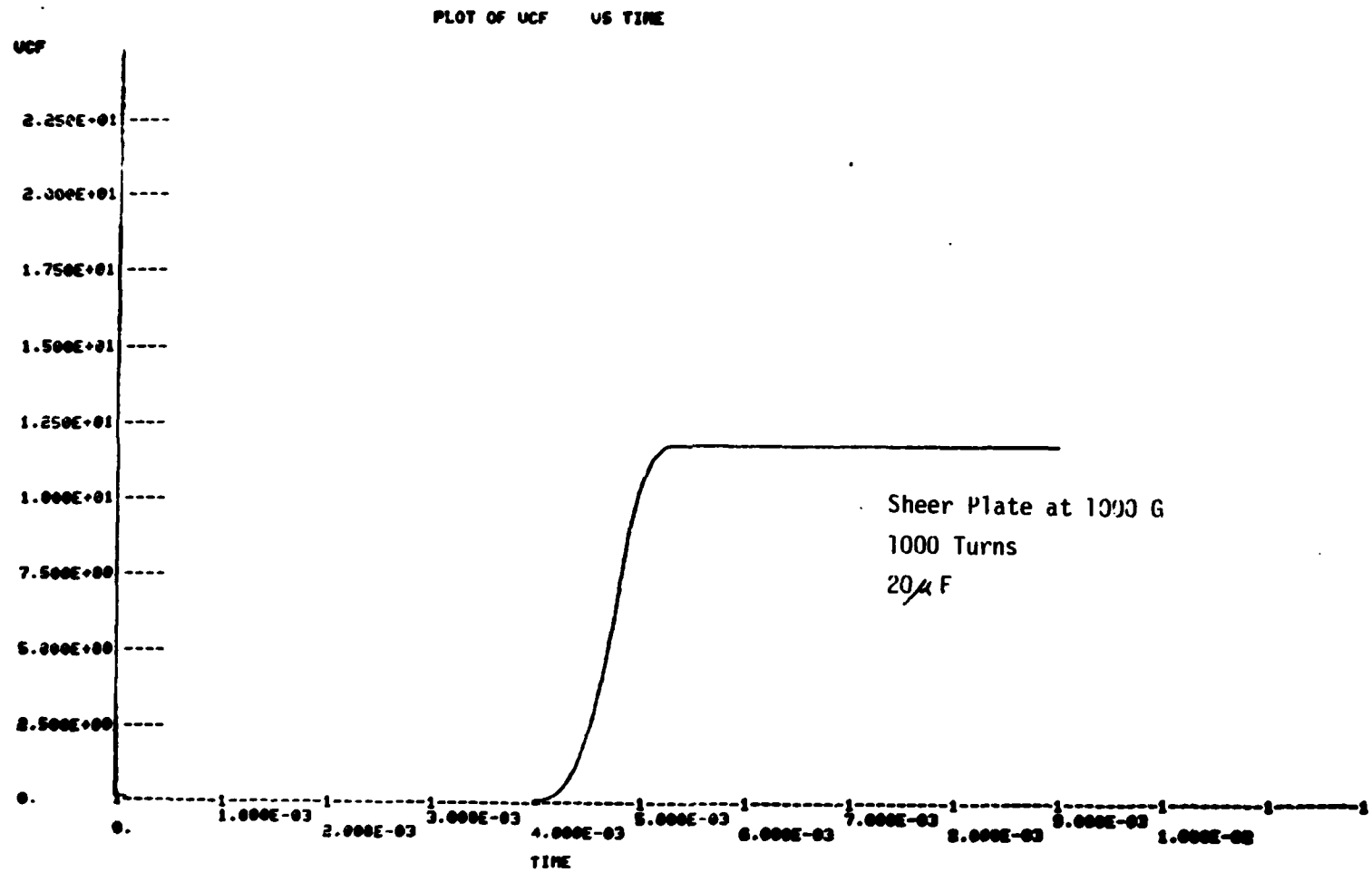

PAGE NUMBER = 15 TOTAL PAGES OF OUTPUT = 21

PAGE = (RIGHT JUSTIFIED)

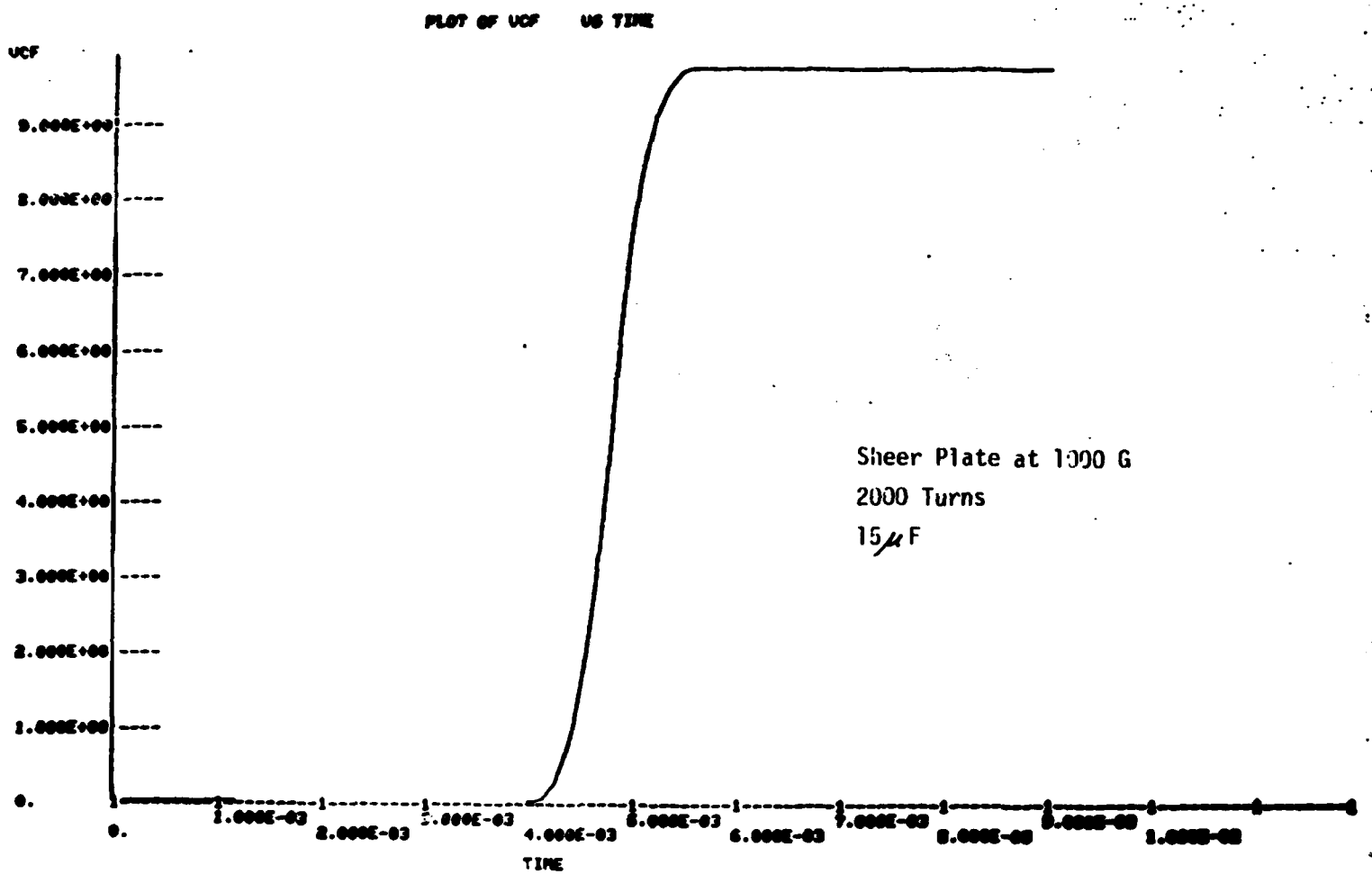

Sheer Plate at 1000 G
2000 Turns
15 μF

PAGE NUMBER = 15 TOTAL PAGES OF OUTPUT = 21
PAGE = (RIGHT JUSTIFIED)

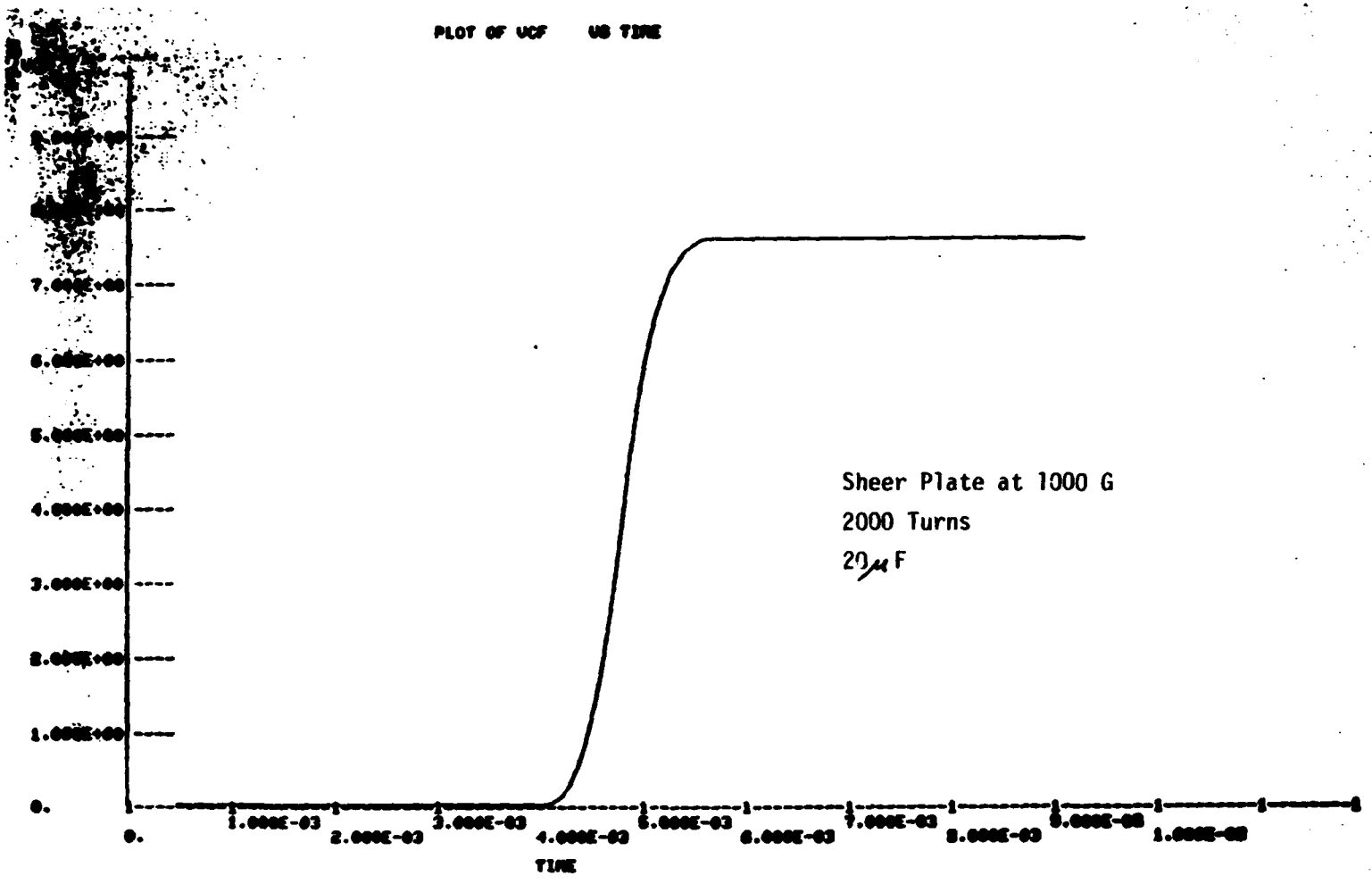

PAGE NUMBER = 18 TOTAL PAGES OF OUTPUT = 21

PAGE = (RIGHT JUSTIFIED)

X. Appendix D

JAN Fuze Reliability Prediction

SUMMARY

The predicted reliability for the JAN Fuze is 97.7 percent. The fuze reliability diagram is shown in Figure 1. The prediction was made in two parts, a shock survival reliability and an operational reliability. The reliabilities are shown in Table 1.

BACKGROUND

The JAN Fuze reliability prediction was made using MIL-HDBK-217C for the electronics operational failure rates, a Honeywell shock survival factor for the electronics, Honeywell defect rates for the mechanical S&A, and Honeywell reliabilities for the explosive components. An operating temperature of $30^{o}C$ and a one minute operating time were assumed for the prediction; however, as seen via Table 1, the operating time and temperature do not significantly effect the predicted reliability. The primary conclusion is that the fuze will function reliably for its intended mission if it survives the gun launch. The probability of surviving the gun launch is 98.0 percent.

The details of the prediction will be retained on file at Honeywell for reference, and review by DOD representatives when appropriate.

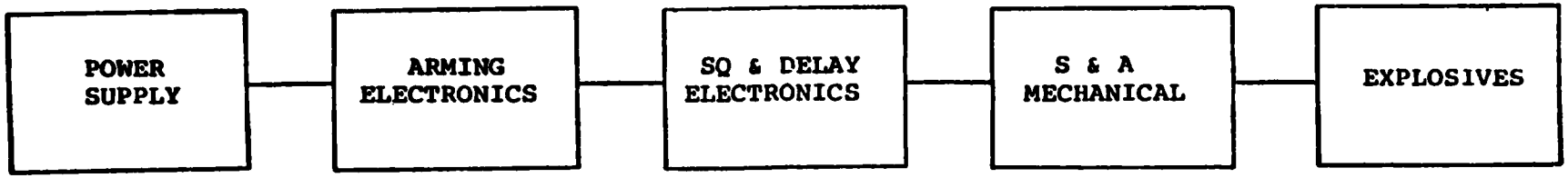

$$R_{FUZE} = R_{PS} \times R_{AE} \times R_{SDE} \times R_{SM} \times R_E$$

$$= .9966 \times .9877 \times .9955 \times .9996 \times .9982 = .977$$

FIGURE 1. RELIABILITY DIAGRAM - JAN FUZE

TABLE 1. RELIABILITY PREDICTION SUMMARY

FUZE SECTION	SHOCK SURVIVAL RELIABILITY	OPERATING RELIABILITY	TOTAL RELIABILITY
Power Supply	.9966	.99999995	.9966
Arming Electronics	.9877	.9999997	.9877
SQ & Delay Electronics	.9955	.9999999	.9955
S&A Mechanical	-----	.9996	.9996
Explosives	-----	.9982	.9982
Fuze	-----	-----	.977

XI. Appendix E

JAN Fuze Safety Analysis

SUMMARY

A JAN Fuze design comparison with MIL-STD-1316B (Safety Criteria for Fuze Design) is presented in evaluation of the design safety of the fuze. There are seventeen applicable requirements, and the fuze design complies with eight, is expected to comply with seven more, partially complies with one, and does not comply with one requirement.

BACKGROUND

The comparison analysis presented in this section was performed using the present electrical JAN Fuze design. The design is expected to comply with all MIL-STD-1316B requirements except safe/arm condition indications. There is a safe/arm window visible before final fuze assembly, but it does not have an alpha designator - it relies strictly on color coding. Once the fuze is completely assembled, it is not possible to determine whether or not it is armed either before or after assembly into the munition. However, based on the type of ammunition, and past experience with similar fuzes, this fuze design is expected to comply with the intent of MIL-STD-1316B, and have a safety failure rate of less than one in a million. Further safety analyses should be performed as fuze development progresses.

JAN FUZE COMPARISON ANALYSIS

MIL-STD-Criteria	Compliance	Remarks
4. REQUIREMENTS		
4.1 General. The features, procedures or controls listed in this section shall be used in the design of fuzes included in the scope of this document.		
4.2 Fuze Safety System		
4.2.1 Safety Redundancy. The safety system of fuzes shall comprise of at least two independent safety features, each of which shall prevent unintentional arming of the fuze and unintentional detonation of the ammunition due to the fuze. The forces enabling a minimum of two safety features shall be derived from different environments. An action taken to initiate launch may be considered an environment if the signal generated by the action irreversibly commits the ammunition to complete the launch cycle. Operation of at least one of these safety features shall depend on sensing an environment after first motion in the launch cycle or on sensing a post launch environment to unlock or arm the interrupted explosive train.	Yes	The fuze has two barriers preventing the detonator from moving to the in-line position. The barriers must sense unique launch environments in the proper sequence in order to arm the fuze. First, the fuze must experience setback, then it must experience a spin environment, and when the fuze reaches its safe separation distance, arming is achieved.
4.2.2 Arming Delay. A safety feature of the fuze shall provide an arming delay. Arming delay when used as the criteria for safety shall assure a safe separation distance can be achieved for all defined geometries of operational weapon use.	Yes	Arming delay is achieved by the revolution sensor being used as a clock to assure a safe separation before arming.

JAN FUZE COMPARISON ANALYSIS

MIL-STD-Criteria	Compliance	Remarks
4.2.3 Manual Arming. An assembled fuze shall not be capable of being armed manually.	Yes	Once assembled, the fuze may not be manually armed-arming requires setback and spin.
4.3 Explosive Trains		
4.3.1 Explosive Train Interruption. At least one interruptor (barrier, shutter, slider, rotor) directly locked mechanically in the safe position by at least two independent safety features shall separate the explosive element which initiates the explosive train from the lead and booster until the arming sequence begins. If the initiating explosive material is housed in the interrupter, a single interrupter locked by the two independent safety features is acceptable. If the sensitive element is positioned such that safety is completely dependent upon the presence of an interruptor, the design shall include positive means to prevent the fuze from being assembled without the interruptor. The effectiveness of interruption shall be determined by techniques described in MIL-STD-331, Test 115, Section 6, during design evaluation.	Yes	The explosive barrier module separates the detonator from an in-line position with the booster explosives. The module remains stationary - the detonator moves in-line upon arming, and is locked in a safe position by two independent barriers.
4.3.2 Explosive Sensitivity (lead and booster explosives). Only explosives subjected to the tests of OD-44811, Chapters 3 and 4 and specifically approved by the associated safety evaluation board of 7.3 for each application are permitted in a position leading to the initiation of a high explosive main charge without interruption, when the fuze is in the safe condition. Table 1 contains a list of currently approved explosives.	Yes	The booster explosives will be PBXN-5.

MIL-STD-Criteria	Compliance	Remarks

TABLE 1. Approved Explosives for all Services

Explosive	Specification
Comp A3	MIL-C-440
Comp A4	MIL-C-440
Comp A5	MIL-E-14970
Comp CH6	MIL-C-21723
PBXN-5	MIL-E-81111
PBXN-6	WS-12604
DIPAM	WS-4660
HNS Type 1 or Type 2 GR A	MIL-T-339
*Tetryl	MIL-P-46464-
*Tetryl Pellets	

*No longer manufactured. Not for use in new developments.

4.4 Safe and Armed Condition

4.4.1 Safe-Arm Options. One or more of the following options shall be selected or combined in the fuze design.	No	None of the options are utilized in the JAN Fuze. The EBM has a safe-arm indicator window which is visible before final assembly into the fuze and will indicate the condition of the fuze. However, once the fuze is completely assembled, it is impossible to determine if it is safe or armed visually. The safe/arm condition could be determined by x-ray.

JAN FUZE COMPARISON ANALYSIS

MIL-STD-Criteria	Compliance	Remarks
4.4.1.1 A feature which assures a positive means of determining the safe condition at the time of fuze installation into the munition; for example by visual observation.	-	
4.4.1.2 A feature which prevents installation of an armed, assembled fuze into the munition.	-	
4.4.1.3 A feature which prevents assembling the fuze in the armed or partially armed condition. This single option may be selected only if the fuze contains at least one arming mechanism which requires an environmental force for operation which precludes accidental or inadvertent arming from handling prior to launch. (Also see 4.4.3).	-	
4.4.1.4 Safe-Arm Indication for Bomb Fuzes. A bomb fuze must possess a feature(s) which assures a positive means of determining the safe condition of the fuze before and after installation into the bomb.	N/A	
4.4.2 Visual Indication. If visual indication of the safe-armed condition is to be employed in the fuze, visible indicators shall be color coded (see 7.1) to reflect the fuze condition as follows: a. Safe condition. Fluorescent green background with the letter S or word SAFE superimposed thereon in white or silver. b. Armed condition. Fluorescent red background with the letter A or word ARMED superimposed thereon in white or silver.	Partially	Visual indication of the safe/arm condition is utilized in the EBM and will be properly color coded but will not have the alpha designation.
4.4.3 Arming and Reset. If arming and reset of the assembled fuze in tests is a normal procedure in manufacturing, inspection, or at any time prior to fuze installation, option 4.4.1.3 is not sufficient and the provision of 4.4.1.1 and 4.4.1.2 shall be met.	N/A	

JAN FUZE COMPARISON ANALYSIS

MIL-STD-Criteria	Compliance	Remarks
4.5 Safety System Failure Rate. The safety system failure rate of a fuze shall be calculated by performing a safety analysis (see 6.3) and shall be verified to the extent practicable by test and analysis during fuze evaluation. As a minimum requirement, the safety system failure rate shall not exceed one failure in one million prior to intentional initiation of the arming sequence. A minimum quantitative requirement is not specified for the proper arming delay since it will be dependent upon the particular weapon and its use. Fuze malfunctions which occur after the proper arming delay shall not be included in the fuze safety system failure rate.	Expected	Safety analyses of this type should be conducted in later program phases.
4.6 Documentation. The evaluation program used as the basis of the safety assessment which is prepared by the developing agency shall be documented in both detail and summary form.	Yes	A summary of this comparison analysis is included in this document.
4.7 Design for Quality Control and Inspection		
4.7.1 Fuzes shall be designed and documented to facilitate application of effective quality control and inspection procedures. Design characteristics critical to fuze safety shall be identified to assure that the designed safety is maintained.	Expected	Representatives from Production and Quality Engineering are expected to integral members of the development team. The design should be monitored throughout its development to insure adequate safety consideration.
4.7.2 The design of the fuze shall facilitate the use of inspection and test equipment for all critical design characteristics identified.	Expected	Inspection and test equipment for verification of critical design characteristics will be utilized and developed as appropriate.

JAN FUZE COMPARISON ANALYSIS

MIL-STD-Criteria	Compliance	Remarks
5. OBJECTIVES		
5.1 General. The features, procedures, or controls listed as objectives in this section are to be accepted as requirements in the design of fuzes covered by the scope of this document when achievement is within the state-of-the-art of fuze development and is feasible within the scope of the development. Necessity for deviations from these objectives shall be documented, showing that compliance is not feasible.		
5.2 Design Features		
5.2.1 Stored Energy. The fuze safety system should not incorporate a stored energy mechanism which is used to remove an interrupter of the fuze explosive train unless no adequate environmental force is available to remove the interruption.	Yes	No adequate environmental force is available to remove the barriers in the EBM and the module serves as the detonator interrupter.
5.2.2 Fail-Safe Features. Fuze systems should incorporate fail-safe features based on their applicability to system requirements.	Yes	If either environment is not sensed, the fuze will not arm. If the sensing coils do not sense the proper field, or if there is a delay, the fuze will not arm, or will delay arming.

JAN FUZE COMPARISON ANALYSIS

MIL-STD-Criteria	Compliance	Remarks
5.2.3 Explosive Ordnance Disposal. Fuzes should incorporate Explosive Ordnance Disposal (EOD) features based on the applicability of EOD to operational system requirements. (See AFR 136-8).	Expected	JAN Fuzes should be disposed in accordance with an approved EOD procedure in a manner applicable to large caliber ammunition fuzes.
5.2.4 Inspection and Test. The design of the fuze should facilitate the use of inspection and test equipment for visual, physical, or electronic monitoring of all characteristics which assure the safety and intended functioning of the fuze at all appropriate stages. The fuze design should facilitate the use of automatic inspection equipment. Design considerations should include possible connections with the weapon in-flight telemetry test devices.	Expected	Critical characteristics are expected to be inspected during fuze assembly.
6. DESIGN GUIDES		
6.1 General. Design guides are defined as concepts, logic, background, examples, statements of good practices or rules, time-proven concepts or features, any of which can be used as reminders to aid the thought process of the designer or design agency in an effort to obtain optimum safety through design. The references listed in this section should be used when applicable during the development of fuzes covered by the scope of this document.		
6.2 System Safety Program. Requirements for a system safety program are given in MIL-STD-882. Applicable portions of this standard should be applied throughout the development and life cycle of fuzes.	Expected	MIL-STD-882 has been used as a guide in this analysis.

JAN FUZE COMPARISON ANALYSIS

MIL-STD-Criteria	Compliance	Remarks
6.3 Analyses. Analyses are performed to identify hazardous conditions for the purpose of their elimination or control. MIL-STD-882 recommends the performance of Preliminary Hazard Analysis, Subsystem or System Hazard Analysis and Operating Hazard Analysis. A Preliminary Analysis (Pre-design Analysis of Potential Hazards) should be conducted to identify the hazards of abnormal environments, conditions and personnel actions which may occur in the phases before safe separation, and this analysis should be used as a guide to the preparation of design requirements. A system hazard analysis (Failure Modes and Effects Analysis, Fault Tree Analysis, etc.) should be conducted to evaluate safety of the fuze design, and if quantified, to estimate the safety system failure rate. Techniques for conducting hazard analyses are described in the literature. Examples are given in NAVORD OD 44942 and AFSC Design Handbook DH-16.	Expected	These analyses should be performed during further development of the fuze.